

DISK RAY THEORY IN TRANSVERSELY ISOTROPIC MEDIA

by

Mathew Jacob Yedlin

B.Sc.(Hons.), University of Alberta, 1971

M.Sc., University of Toronto, 1973

A THESIS SUBMITTED IN PARTIAL FULFILMENT OF  
THE REQUIREMENTS FOR THE DEGREE OF  
DOCTOR OF PHILOSOPHY

in

THE FACULTY OF GRADUATE STUDIES  
(Department of Geophysics and Astronomy)

We accept this thesis as conforming to the required standard

The University Of British Columbia

April, 1978



Mathew Jacob Yedlin, 1978

In presenting this thesis in partial fulfilment of the requirements for an advanced degree at the University of British Columbia, I agree that the Library shall make it freely available for reference and study. I further agree that permission for extensive copying of this thesis for scholarly purposes may be granted by the Head of my Department or by his representatives. It is understood that copying or publication of this thesis for financial gain shall not be allowed without my written permission.

Department of GEOFYSICS AND ASTRONOMY

The University of British Columbia  
2075 Wesbrook Place  
Vancouver, Canada  
V6T 1W5

Date APRIL 28, 1978

### Abstract

The first motion approximation has been used to calculate synthetic seismograms in transversely isotropic, linear, elastic media. To achieve this end the equations of motion have been solved in a geometrical optics regime. Formally, this has been accomplished by the use of asymptotic propagator matrices. This formalism is important, since the phase of the JWKB reflection coefficient can be easily calculated by consideration of the radiation condition. Calculation of this reflection coefficient has shown that the turning point behaviour is identical to that obtained for an isotropic medium. The similarity of the turning point behaviour is a direct consequence of the physical result that at a turning point the phase and group velocities are in the same direction.

To understand the results of the first motion approximation applied to a simple upper mantle model, it is first necessary to understand the basic physics of transversely isotropic media. This has been achieved by examination of the dispersion relation arising from Newton's Laws for an elastic solid. From the dispersion relation, it has been demonstrated how the Green's Function can be constructed using elementary projective geometry. Subsequently, the nature of the Green's Function has been analyzed. The analysis of the Green's Function (wave

surface) is important because it facilitates comprehension of any dynamical results.

The synthetic seismograms were calculated using ray parameter versus distance curves. These curves were obtained by integration of the ray equations derived from the dispersion relations. A Gaussian-Kantorovich method was utilized to perform the required integration. This hybrid integration technique proved to be extremely fast and accurate. When the resulting p-delta curve was used to calculate the synthetic seismogram, the main effect of the anisotropic model considered was a kinematic one - the main arrivals were earlier than those for an isotropic model.

## Table of Contents

Abstract .....	ii
Table of Contents .....	iv
List of Figures .....	v
Forward .....	viii
Acknowledgements .....	xi
Chapter I .....	1
Chapter II .....	13
Introduction .....	13
Section 1. Foundations For The Equations Of Motion .....	14
Section 2. Solutions Of The Equations Of Motion .....	27
Chapter III .....	52
Introduction .....	52
Section 1. Ray Theory Part I .....	54
Section 2. Ray Theory Part II .....	64
Chapter IV .....	85
Introduction .....	85
Section 1. Development Of The Equations Of Motion .....	87
Section 2. Details Of The Source .....	99
Section 3. Solution For The Homogeneous System Using Airy Functions .....	107
Chapter V .....	136
Introduction .....	136
Section 1. Intuitive Development Of Disk Ray Theory .....	138
Section 2. Equal Phase Method-JWKB .....	148
Reflection Coefficient .....	148
Section 3. Equal Phase Method- Implementation .....	155
Section 4. Simple Seismic Calculations .....	168
Conclusions .....	198
Bibliography .....	200

## List Of Figures

Figure		Page
1.1	Model for olivine orientation near a ridge	6
2.1	Geometric construction of wave surface from the slowness surface	34
2.2	Slowness and wave surface for a transversely isotropic medium	35
2.3	Illustration of the definition of pole and polar	36
2.4	Construction of the polar reciprocal	38
2.5	Points on the slowness surface sharing a common tangent	40
2.6	Differing group velocity magnitudes in the neighborhood of points sharing a common tangent	41
2.7	Illustration of wave surface with singularities	42
2.8	Parametric representation of the slowness surface	46
5.1	Suite of rays leaving a shot	139
5.2	Acoustic plane waves in a quartz crystal	141
5.3	Disk intercepting the surface in an anisotropic medium	142
5.4	Simple p-delta curve	145
5.5	P-delta curve for compressional waves-no anisotropy	173
5.6	P-delta curve for quasi-compressional waves-10% anisotropy	174
5.7	P-delta curve for quasi-compressional waves-30% anisotropy	175
5.8	Directivity function (compressional waves) horizontal displacement-no anisotropy	176

5.9	Directivity function (quasi-compressional waves) horizontal displacement- 10% anisotropy	177
5.10	Directivity function (quasi-compressional waves) horizontal displacement- 30% anisotropy	178
5.11	Directivity function (compressional waves) vertical displacement-no anisotropy	179
5.12	Directivity function (quasi-compressional waves) vertical displacement-10% anisotropy	180
5.13	Directivity function (quasi-compressional waves) vertical displacement-30% anisotropy	181
5.14	Synthetic seismogram of horizontal displacement for compressional waves calculated using p-delta curve shown in figure 5.5	182
5.15	Synthetic seismogram of horizontal displacement for quasi-compressional waves calculated using p-delta curve shown in figure 5.6 10% anisotropy	183
5.16	Synthetic seismogram of horizontal displacement for quasi-compressional waves calculated using p-delta curve shown in figure 5.7 30% anisotropy	184
5.17	Synthetic seismogram of vertical displacement for compressional waves calculated using p-delta curve shown in figure 5.5	185
5.18	Synthetic seismogram of vertical displacement for quasi-compressional waves calculated using p-delta curve shown in figure 5.6 10% anisotropy	186
5.19	Synthetic seismogram of vertical displacement for quasi-compressional waves calculated using p-delta curve shown in figure 5.6 30% anisotropy	187
5.20	P-delta curve for quasi-shear waves- 10% anisotropy	188
5.21	P-delta curve for quasi-shear waves- 30% anisotropy	189

5.22	Directivity function (quasi-shear waves) horizontal displacement-10% anisotropy	190
5.23	Directivity function (quasi-shear waves) vertical displacement-10% anisotropy	191
5.24	Directivity function (quasi-shear waves) horizontal displacement-30% anisotropy	192
5.25	Directivity function (quasi-shear waves) vertical displacement-30% anisotropy	193
5.26	Synthetic seismogram of horizontal displacement for quasi-shear waves, calculated using p-delta curve shown in figure 5.20-10% anisotropy	194
5.27	Synthetic seismogram of vertical displacement for quasi-shear waves, calculated using p- delta curve shown in figure 5.20-10% anisotropy	195
5.28	Synthetic seismogram of horizontal displacement for quasi-shear waves, calculated using p-delta curve shown in figure 5.21-30% anisotropy	196
5.29	Synthetic seismogram of vertical displacement for quasi-shear waves, calculated using p- delta curve shown in figure 5.21-30% anisotropy	197



Forward: Aims, Objectives, And Originality

The main thrust of the thesis will be the analytic derivation (using geometrical optics) and numerical calculation of simple disk ray seismograms in transversely isotropic, vertically inhomogeneous elastic media. In Chapter I the main emphasis is the motivation for the study of anisotropy. This is followed in Chapter II by the presentation of the basic physics of anisotropic media. The objective in this chapter is the development of an understanding of the wave surface, the Green's Function for the elastodynamic equations driven by a point source. This objective is achieved by describing in detail the geometric constructions, based on projective geometry. The nature of the singularities of the wave surface are then analyzed algebraically.

Chapter III uses the physical results of Chapter II to develop the relevant ray equations. Two different approaches are used to obtain these equations. The objective in presenting these methods is to compare them algebraically, and use the final result in the construction of an efficient, accurate, ray tracing technique. The purpose in developing a good ray-tracing technique is that  $p$ - $\delta$  curves may be constructed, and from these, the main

objective of the thesis may be realized.

Chapter IV is concerned with the the development of a uniformly valid solution to the equations of motion. This objective is achieved by using classic asymptotic techniques, and the turning point problem is solved using the Langer transformation.

In Chapter V, the main objective of the thesis is realized. An intuitive derivation of disk ray theory is presented. This is followed by an evaluation of the JWKB reflection coefficient, which is then used to obtain the analytic form for the disk ray theory seismogram. This analytic form is used to compute seismograms for simple earth models. In order to delineate the author's contribution from that existing in the literature, a list of original results is listed below:

- 1) A clear elucidation of the wave surface slowness surface correspondence has been demonstrated.
- 2) A differential geometric proof has been developed to illustrate how inflection points on the slowness surface cause cusps on the wave surface;
- 3) Gaussian integration has been applied to the tau function;
- 4) The method of Kantorovich has been combined with the Gaussian integration method to produce an accurate, fast ray-integral calculator;
- 5) The source term method of Takeuchi and Saito (1972) has been cast into the up and downgoing wave formalism;
- 6) The method of asymptotic propagators (Chapman 1974b; Woodhouse 1978) has been extended to transversely isotropic

media, and, the JWKB reflection coefficients have been calculated for such media;

7) An intuitive derivation for disk ray theory in anisotropic media has been presented;

8) An analytic derivation of the disk ray theory seismogram, including source effects has been obtained;

9) Seismograms have been calculated for vertical and horizontal displacements for quasi-shear and quasi-compressional waves, in the case of a point explosion.

## Acknowledgements

Due to the unusual nature of the supervision for this thesis, the author interacted with many individuals, and received helpful suggestions in the course of countless discussions. In particular, I would like to acknowledge the contribution of Ralph Wiggins, who suggested the project, and explained some of the intuitive aspects of d.r.t. John Woodhouse introduced me to his ideas on asymptotic propagators, and discussions with him on the intuitive basis for d.r.t. in anisotropic media also proved helpful. Chris Chapman was kind to send preprints of his soon-to-be published 1978 synthetic seismogram papers, and also to explain some of the subtleties of the JWKB method. Jim Varah helped set the stage for the hybrid method of integration developed, by introducing the "method of the subtraction of the singularity" in its simplest form.

Throughout the thesis work, Brian Seymour provided encouragement and weekly advice on all aspects of the work. To him I offer my deepest thanks. Mick Mortell participated in many of these weekly discussions. I am very grateful for his suggestions. George McMechan also offered encouragement, and I had many helpful discussions with him,

particularly the daily discussions during the two Augusts spent at University of Victoria. Thank you very much George.

To the members of the Geophysics Department, Bob Ellis, Ron Clowes, Garry Clarke, Don Russell, and my supervisor, Tad Ulrych, thank you not only for the helpful discussions about diverse thesis topics, but also thanks for introducing me to geophysics, and seismology in particular. A special mention of gratitude goes to John Gilliland, for helpful suggestions when the project was in its infancy. Also a word of thanks to my fellow students in the department, for their comments and interesting discussions.

I should like to express gratitude and acknowledge some enlightening discussions with John Orcutt, George Backus, and Stuart Crampin concerning wave propagation in anisotropic media.

\* \* \* \* \*

In an acknowledgement section of a thesis, it is always in order to thank the typist. There was no typist for this thesis. Rather, the author was fortunate to have the assistance of the boys at St. Andrew's Hall in typing and producing this thesis. The work production deadline could not have been met without the help of John Wester, who

drafted the equations, and helped in production matters, and members of the Hall (Steffan Wegner, John Skinner, Perry Williams, Randy Watson, Greg Jaron, Paul James, Ken Rush, Bob Cowin, Dave Simmons, Martin Connolly, Peter Cary, Shlomo Levy, and Millo Shaw). Sincerest thanks also to Ralph Pudritz, who aided and encouraged the final production of the thesis.

The author gratefully acknowledges the financial support given by the National Research Council of Canada and financial assistance of the International Nickel Company of Canada. To one and all, my sincerest merci beaucoup.

## Chapter I

Since earliest times, man has been interested in the study of anisotropy. As Musgrave (1970) remarks:

"Presumably, Stone age man observed and very probably studied, the phenomenon of cleavage--mechanical as well as anatomical!"

Impetus for the study of anisotropy in geophysics, and in particular seismology, stems not from any romantic impulse, but rather from petrology. Only 18 years ago, Birch (1960) published his measurements of the velocity of compressional waves in rocks at a pressure of 10 Kbars, using pulsed travel time techniques. An associate, Verma (1960), used pulse-interference methods to measure the acoustic wave velocity in high density crystals. In particular, he found that for olivine, the compressional wave velocities were as follows:

Direction	Velocity (km/sec.)
x axis [100]	9.87
y axis [010]	7.73
z axis [001]	8.65

His results were important, in that a conclusive demonstration was provided that some of the minerals comprising the earth were anisotropic, insofar as their acoustic wave velocities were concerned. Further stimulus to investigate was supplied by the first of many ocean refraction experiments performed by Raitt (1963) and his co-workers. Raitt's initial data were used by Hess (1964) to derive the first of many models of the oceanic upper mantle.

Hess (1964) combined the results of Raitt and Verma and arrived at a preliminary model. The sub-Moho compressional wave velocity, obtained by Raitt, was determined by shooting along different azimuths in the neighbourhood of Mendocino fracture zone. The maximum velocity (8.7 km/sec.) was measured parallel to the fracture zone and the minimum velocity (8.0 km/sec.) was perpendicular to the fracture zone. Hess reasoned, using Verma's data, that the b-axis of olivine (which defines the (0,1,0) plane) should align perpendicular to the fracture zone, and the a-axis should align parallel to it. This would be achieved by the (0,1,0) plane gliding along the plane of shear. For such a model the compressional velocity parallel to the fracture zone would be 9.87 km/sec. and perpendicular to it 7.73 km/sec. Although the physics of Hess's model appears correct, the numerical values are considerably off (Fuchs 1977).

A year later Backus (1965) again looked at Raitt's data and very elegantly derived an equation relating Pn velocity



to the azimuth of the refraction profile. The equation,

$$v_p^2 = A + C \cos 2\phi + D \sin 2\phi + E \cos 4\phi + F \sin 4\phi \quad (1.1-1)$$

$\phi$  = azimuthal angle  
 $v_p$  = p-wave velocity

was derived by application of formal perturbation theory to the elastodynamic wave equation, when the medium was "mildly anisotropic" (less than 10%). The perturbation to the wave velocity was then expressed as a Fourier series in the azimuth angle. As Backus demonstrated, (1.1-1) proved to be very useful in fitting the measured velocity as a function of the azimuth angle to obtain 5 elastic parameters. Backus also obtained correction terms to (1.1-1) in the case that the curvature of the upper mantle was significant. In conclusion, he pointed out that Hess's model based on alignment of olivine crystals could have an alternative, that is, the anisotropy could be due to a static stress pattern in an isotropic material.

Three years later, Christensen and Crosson (1968) postulated that an olivine-rich upper mantle material moving vertically in the presence of fracture zones, would be transversely isotropic, with the axis of symmetry inclined to the vertical. From a study of ultramafic rocks, the preferred orientation of the b-axis of olivine was perpendicular to schistosity or banding. Dunite (90%

olivine), in the above orientation, was found to behave like a transversely isotropic medium for compressional waves. As well, it was expected that in the case of a transversely isotropic medium, the maximum compressional wave velocity should be perpendicular to the symmetry axis.

The year 1969 provided a further wealth of information about the oceanic upper mantle. Raitt and Shor (1969) obtained more data in the northeast Pacific. For interpretation, a modified time term method was used to include azimuthal anisotropy. This was achieved by incorporating Backus' equation (1.1-1) in the time term method of Berry and West (1966). They found that the difference in velocity (0.3 km/sec.) parallel and perpendicular to fracture zones was not as large as that predicted by Hess.

Francis (1969) used the results of Raitt and Shor to offer an alternative to the model of Hess. His principal objection to Hess's model was that translational gliding of the (0,1,0) face of the crystals was, firstly, impossible, since the creep of ultramafics should be insignificant away from the ridge, and secondly, inconceivable, since the deformational strain required would have to extend a large distance away from the ridge. Further, Francis, citing Rayleigh (1968), stated that for olivine, the predominant glide mechanism was (0,k,l) [1,0,0], not necessarily (0,1,0) [1,0,0]. As a result, the model arrived at to

explain the data of Raitt was that velocity shear, greatest under the ridge due to convection currents, would cause slip with  $(0,k,1)$   $[1,0,0]$  the major mechanism. In the simplest case, the velocity shear orients the olivine so that  $(0,1,0)$  plane lies in the plane of flow and the direction of flow is the  $(1,0,0)$  direction. Such a model (illustrated in Fig. 1) explains the low compressional wave velocity parallel to the ridge and the high compressional wave velocity perpendicular to the ridge, although the anisotropy factor is too large, 20% (Fuchs 1977).

Finally, another model for the oceanic upper mantle was developed by Crosson and Christensen (1969) who used Backus' (1965) formulation postulating the existence of a tilted, transversely isotropic upper mantle. The data of Raitt (1963) fitted previously by Backus were refitted using the tilted transversely isotropic model. The fits obtained using the transversely isotropic model are in excellent agreement with Backus' fit using general anisotropy.

Since 1969, a number of refraction surveys have been undertaken with a view to check and reinforce the initial discovery of Raitt. Keen and Tramontini (1970), found that in the Atlantic Ocean, the  $P_n$  velocity was 7.9 km/sec, with an anisotropy factor of 8%. Again the formula of Backus was used to fit the data, but also the possibility that curvature or lateral variations affected the result was examined. It was found that neither of these effects could

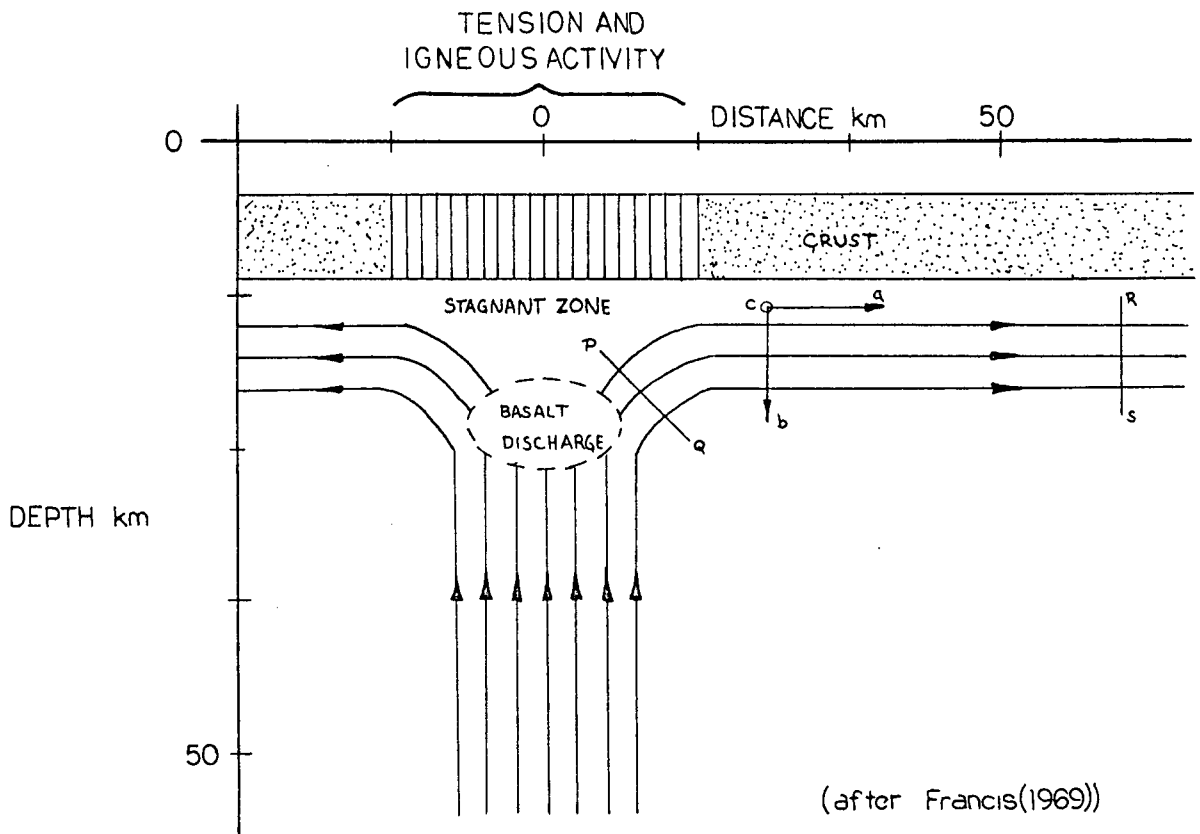


Figure 1.1 Model for olivine orientation near the ridge with the a-axis, which defines the direction of the fastest p-wave velocity perpendicular to the ridge strike. After Francis(1969).

explain the observed anisotropy since it was not possible that in the area of the survey, a lateral variation of 16% could occur. For curvature to affect the results, it was necessary that a variation of 7 km in the depth of the Moho

discontinuity exist in the region of the survey. Following this survey, Keen and Barrett (1971) estimated oceanic upper mantle anisotropy in the Pacific, and found that the direction of maximum compressional wave velocity at an azimuth of  $107^{\circ}$ , was not exactly the direction of strike of the nearest fracture zone, but only approximately so. Again, a value of 8% anisotropy was obtained, with a mean value of the compressional wave velocity computed as 8.07 km/sec. Most recently a seismic refraction profile parallel to and perpendicular to the Explorer Ridge has been completed. The Pn velocities derived by Clowes and Malecek (1976) were 7.3 km/sec. parallel to the ridge and 7.85 km/sec. perpendicular to the ridge with an anisotropy of 7%.

Upon consideration of the data presented above, it appears that for the oceanic upper mantle, an intrinsic anisotropy of 7% to 8% is obtained, with the direction of maximum velocity parallel to the fracture zones. However, why should the anisotropy be restricted to oceanic upper mantle? As Fuchs (1977) points out, the temperatures (800 to  $1000^{\circ}\text{C}$ ) and pressures (10 kbar.) are higher at the continental crust-mantle boundary than at the oceanic crust-mantle boundary. Therefore, the higher temperatures and pressures are more likely to generate the preferred orientation of olivine, held responsible for the azimuthal anisotropy observed.

The existence of anisotropy in the continental

lithosphere had been suggested as early as 1966 by Crampin. However, it was not until the work of Bamford (1973, 1976) that the existence of large scale continental anisotropy was observed. Bamford used data from the Federal Republic of Germany refraction profiles, and used a modified time term method to interpret the data. From the latest analysis (1977), which included results from the 1972 Rhinegraben experiment, Bamford obtained an anisotropy of 6% to 7%, with the direction of maximum Pn velocity N20° E. What is interesting about the result is that the magnitude of the anisotropy is equal to that deduced from oceanic upper mantle investigations. However, the direction of maximum crustal Pn velocity differs by 20° from the oceanic results, indicating a slight variation in the possible anisotropies of the oceanic upper mantle and the crustal upper mantle.

## Petrological Evidence for Anisotropy

The implication of the seismic experiments described in the previous section is that the sub-Moho is anisotropic. To reinforce the seismological evidence for the existence of anisotropy it is essential to consider petrological work which supports the seismic results.

After Verma's (1960) measurement of the compressional and shear wave velocities in olivine, the next significant work on the subject was by Raleigh (1968), who studied the mechanisms of plastic deformation of olivine. His analysis of the slip system for olivine  $(0,k,1)$   $[1,0,0]$  was later used by Francis (1969) in constructing his model of oceanic upper mantle. More petrological results on the deformation of olivine were obtained by Ave'Lallement and Carter (1970). They recrystallized olivine at temperatures greater than  $1050^{\circ}\text{C}$ , at pressures of 3 kbar, for a strain rate of  $10^{-3}/\text{sec}$ . Extrapolation of the results to strain rates and temperatures typical of oceanic lithosphere ( $10^{-14}/\text{sec}$ . and  $500^{\circ}\text{C}$ ) showed that the b axis  $(0,1,0)$  of the new crystals aligned in the direction of maximum compressive stress. Thus, Ave L'allement and carter deduced that the above mechanism accounts for the orientation of olivine crystals in oceanic lithosphere. However, as Fuchs (1977) has pointed out, the proposed mechanism could not explain the

seismic results for two reasons:

- A) The azimuthal velocity dependence would occur only near the ridge axis where the temperature is high ( $500^{\circ}\text{C}$ );
- B) The b axis would not align perpendicular to the plane of shear as suggested, since the principal axis is at  $45^{\circ}$  to the plane of shear.

The results of Ave'Lallement and Carter however, have been used by some authors (Christensen, 1971) to explain the orientation of the olivine fabric in the rocks from the Twin Sisters in Washington.

Further petrologic studies have been carried out by Peselnick et al (1974) in the Ivrea zone of the Italian Alps. This zone is of particular interest, since it may be the boundary of the mantle and deep crust. Again the olivine was found to have a preferred orientation. The measured velocity anisotropy was 7%, and was independent of pressure. The direction of minimum velocity was found to be perpendicular to the foliation plane, and the direction of maximum velocity was parallel to the foliation plane. Peselnick et al favored Francis' (1969) interpretation for the generation of ocean upper mantle anisotropy, with the principal slip mechanism, as described by Raleigh, being responsible for preferred orientation of olivine.

Within the last year, two articles have appeared which emphatically require intrinsic anisotropy of the upper mantle to explain the seismic results. Since the velocity



and anisotropy of eclogite is too small to account for that observed, Bottinga and Allegre (1976) have deduced that peridotite, not eclogite, must be the main constituent for sub-Moho anisotropy. Green and Liebermann (1976) state the following: "It appears to us unlikely that uncertainties in knowledge or error in prediction of the elastic properties of minerals and their P,T derivatives are sufficient to permit values of  $V_p \geq 8.5$  km/sec in petrologically reasonable rock types under upper mantle conditions, without appeal to seismic anisotropy".

## Other Forms of Anisotropy

The previous sections were concerned with the role of intrinsic anisotropy in the constituents of the upper mantle. However, there are other types of anisotropy which have significance in other strata of the earth. Such anisotropy can be generated in two ways: 1) pre-strain static strain field; and 2) thin layers.

Many geophysicists have been concerned with the thin layer problem which is important in exploration seismology. As early as 1950, Thomson investigated the periodic, isotropic two layered medium, consisting of fine layers, using the now- famous propagator matrices. Uhrig and Van Melle (1955) noted that fine stratifications of alternating bands of limestone and shale, or sand and shale could be regarded as smoothly anisotropic if the dominant wavelength was much greater than the bed thickness. Potsma (1955) quantified the above intuitive results by calculation of the effective elastic constants of a periodic isotropic two-layered medium. However, the results are specific only for periodic variations of the layer properties. Backus (1962) has given a more general treatment of the finely layered isotropic medium, which can be modelled as a smooth, transversely isotropic medium.

## CHAPTER II

### Introduction

In this chapter the basic elastodynamics of anisotropic elastic media will be presented. By examination of symmetry properties of the media, the most general equations of motion can be reduced to simpler and simpler forms. By substitution of plane wave solutions into the elastodynamic wave equations, dispersion relations may be derived. These dispersion relations can be used to construct the Green's function for the particular elastic material under consideration. This method of construction is based on principles of elementary projective geometry, which was at its peak in the 19th century. (Klein 1939; Poncelet 1822; Briot & Bouquet 1896)

The geometric results of this chapter are important, since they form the physical basis for the derivation of the ray equations to be considered Chapter III. These ray equations provide the basis for the construction of p-delta curves, which may then be used for the calculation of synthetic seismograms.

## Section 1 Foundations for the Equations of Motion.

The equations of motion are derived on the assumption that the elastic material is Hookean (Love 1945). That is, the free energy about an equilibrium configuration is expressed as a Taylor's expansion in the strain (Musgrave 1970; Landau-Lifschitz 1959) as follows:

$$F_{\text{DEFORMED}} = F(0) + \left[ \frac{\partial F}{\partial e_{ij}} \right]_0 e_{ij} + \frac{1}{2} \left[ \frac{\partial^2 F}{\partial e_{ij} \partial e_{kl}} \right]_0 e_{ij} e_{kl} \quad (2.1-1)$$

$$\Delta F = \frac{1}{2} \left[ \frac{\partial^2 F}{\partial e_{ij} \partial e_{kl}} \right]_0 e_{ij} e_{kl}$$

where  $\Delta F$  = free internal energy due to an elastic deformation,  $e_{ij}$  is the strain tensor and 0 refers to the undeformed state of the solid. Since work must be done to deform the system  $\Delta F > 0$ , and the right hand side of (2.1-1) must be a positive definite quadratic form. The work done in deforming an elastic body, equal to the change in free energy, is:

$$W = \frac{1}{2} \sigma_{ij} e_{ij} \quad (2.1-2)$$

By comparison of (2.1-1) and (2.1-2) it is evident that:

$$\sigma_{ij} = \left[ \frac{\partial^2 F}{\partial e_{ij} \partial e_{kl}} \right] e_{kl} \quad (2.1-3)$$

where  $\sigma_{ij}$  is the stress tensor. Equation (2.1-3) is a constitutive one relating stress to strain in a linear elastic medium. That is,

$$\sigma_{ij} = C_{ijkl} e_{kl} \quad (2.1-4)$$

The quantity  $C_{ijkl}$  is the fourth order stiffness tensor with 81 components. Since  $\sigma_{ij} = \sigma_{ji}$  and  $e_{kl} = e_{lk}$ , and

$$\left[ \frac{\partial^2 F}{\partial e_{ij} \partial e_{kl}} \right]_0 = \left[ \frac{\partial^2 F}{\partial e_{kl} \partial e_{ij}} \right]_0 \quad (2.1-5)$$

the following symmetry conditions are valid:

$$\begin{aligned} C_{ijkl} &= C_{jikl} \\ C_{ijkl} &= C_{ijlk} \\ C_{ijkl} &= C_{klij} \end{aligned} \quad (2.1-6)$$

Hence,  $C_{ijkl}$  the fourth order stiffness tensor with 81 components can be reduced to 21 independent components. Further reduction of the number of components is achieved by consideration of greater symmetries for the particular medium involved.

Newton's laws for an elastic solid in the absence of body forces become

$$\rho \frac{\partial^2 u_i}{\partial t^2} = \frac{\partial}{\partial x_j} \left( c_{ijkl} \frac{\partial u_k}{\partial x_l} \right) \quad (2.1-7)$$

Equation (2.1-7) relates the mass times acceleration (in Cartesian co-ordinates) to the divergence of the stress tensor. That the acceleration is related to the divergence of the stress tensor is derived by many authors (Love 1945; Bullen 1965; Jeffreys 1959).

The study of equation (2.1-7) will be the focal point in this chapter. Of course source terms will have to be included in any transient pulse propagation problem (Takeuchi & Saito 1972).

In most seismological problems it is neither essential nor possible to consider all 21 components of  $C_{ijkl}$ . Media usually under consideration have some degree of symmetry. This symmetry may be exploited and the number of components of the elastic tensor reduced. These manipulations are simplified if the basic concepts of group theory are introduced.

A group  $G$  is defined to consist of a set of elements  $A, B, C, \dots$  with an operation of computation (multiplication) such that the following axioms are satisfied:

- 1) Closure- For any A,B, members of G, AB, is also a member of G;
- 2) Associative Rule - For any A,B,C, members of G  
 $(AB)C = A(BC) = ABC$ ;
- 3) Identity - There exists an element of G known as I so that for all A, members of G,  $AI = IA = A$ .
- 4) Inverse - For every element A of G there exists an inverse  $A^{-1}$ , also in G, such that  $A^{-1}A = AA^{-1} = I$ .

To demonstrate the utility of the above abstract paradigm, consider the elements of the Group associated with the counterclockwise rotation of a square. Rotations of 0, 90, 180, 270 degrees, can be represented as complex numbers  $e^{i\pi/2}$ ,  $e^{i\pi}$ ,  $e^{3i\pi/2}$ . The group multiplication table is given below.

	1	$e^{i\pi/2}$	$e^{i\pi}$	$e^{3i\pi/2}$
1	1	$e^{i\pi/2}$	$e^{i\pi}$	$e^{3i\pi/2}$
$e^{i\pi/2}$	$e^{i\pi/2}$	$e^{i\pi}$	$e^{3i\pi/2}$	1
$e^{i\pi}$	$e^{i\pi}$	$e^{3i\pi/2}$	1	$e^{i\pi/2}$
$e^{3i\pi/2}$	$e^{3i\pi/2}$	1	$e^{i\pi/2}$	$e^{i\pi}$

(2.1-8)

Here the identity element is 1, and the inverse elements are obvious from the table. An interesting point to note is that for the given multiplication rule, the element of G,  $\exp(i\pi/2)$ , can generate the other elements of the group. It is known as the generator of the group. Since any group can be defined in terms of its set of generators, it is sufficient to consider group operations involving only these generators.



In the study of the various symmetries of the elastic tensor the particular transformation of interest is known as a point transformation. These transformations leave at least one point of the elastic medium fixed, and consist of rotations and reflections. The complete description of all the symmetries of a particular elastic medium can be represented by this group, whose elements define the particular symmetry operations which are allowed. As shown above for the simple case of the rotation of the square, not all the elements of the group need be considered. Only the generators of the group need be involved in any co-ordinate manipulation.

Application of the above methodology is best illustrated by an example. First,  $C_{ijkl}$  can be rewritten as a second order tensor if the following indexing scheme is used (Daley & Hron 1977; Musgrave 1970):

Old Index Pair	New Single Index
11	1
22	2
33	3
23, 32	4
31, 13	5
12, 21	6

In this scheme the new stress- strain relation would be

rewritten as:

$$\underline{\sigma} = [c] \underline{e} \quad (2.1-9)$$

with the stress

$$\underline{\sigma} = \begin{pmatrix} \sigma_{11} \\ \sigma_{22} \\ \sigma_{33} \\ \sigma_{13} \\ \sigma_{13} \\ \sigma_{12} \end{pmatrix} \quad (2.1-10)$$

and the strain

$$\underline{e} = \begin{pmatrix} e_{11} \\ e_{22} \\ e_{33} \\ e_{13} \\ e_{13} \\ e_{12} \end{pmatrix} \quad (2.1-11)$$

Now for a particular symmetry, the application of a particular point transformation to generate a new elastic tensor may be written as (Auld 1973)

$$C_{ij} = m_{ik} C_{kl} p_{lj} \quad (2.1-12)$$

where

$$p_{lj} = (m_{jl})^T \quad (2.1-13)$$

As the transformation has at least one fixed point, (2.1-12) must hold identically. For a nontrivial example, consider an elastic medium with monoclinic symmetry. The simple reflection matrix which represents the generator of this point group is

$$\begin{pmatrix} 1 & 0 & 0 \\ 0 & 1 & 0 \\ 0 & 0 & -1 \end{pmatrix} \quad (2.1-14)$$

For this mirror reflection, the matrix used in (2.1-12) is

$$\begin{pmatrix} 1 & & & & \\ & 1 & & & \\ & & 1 & & \\ & & & 0 & \\ 0 & & & & -1 \\ & & & & & -1 \end{pmatrix} \quad (2.1-15)$$

Applying the symmetry condition (Auld 1973), it is found that

$$\begin{pmatrix} c_{11} & c_{12} & c_{13} & c_{14} & c_{15} & c_{16} \\ c_{21} & c_{22} & c_{23} & c_{24} & c_{25} & c_{26} \\ c_{31} & c_{32} & c_{33} & c_{34} & c_{35} & c_{36} \\ c_{41} & c_{42} & c_{43} & c_{44} & c_{45} & c_{46} \\ c_{51} & c_{52} & c_{53} & c_{54} & c_{55} & c_{56} \\ c_{61} & c_{62} & c_{63} & c_{64} & c_{65} & c_{66} \end{pmatrix} = \begin{pmatrix} c_{11} & c_{12} & c_{13} & c_{14} & c_{15} & c_{16} \\ c_{21} & c_{22} & c_{23} & c_{24} & c_{25} & c_{26} \\ c_{31} & c_{32} & c_{33} & c_{34} & c_{35} & c_{36} \\ -c_{41} & -c_{42} & -c_{43} & -c_{44} & -c_{45} & -c_{46} \\ -c_{51} & -c_{52} & -c_{53} & -c_{54} & -c_{55} & -c_{56} \\ c_{61} & c_{62} & c_{63} & c_{64} & c_{65} & c_{66} \end{pmatrix} \quad (2.1-16)$$

Hence, 8 of the elastic constants vanish. This leaves 13 elastic constants. However, there is freedom to choose the x-y co-ordinates in the reflection plane. This reduces the degrees of freedom by one, so only 12 constants describe a monoclinic crystal medium. Application of this method for the case of media with hexagonal symmetry shows that (Landau and Lifschitz 1959) there are only 5 independent elastic constants.

## Intuitive Arguments

The use of group theory in determining the number of independent elastic constants for a particular crystal is precise, but other means are available to study the elastic tensor for media with different symmetries. As Feynman (1966) states:

" There is a branch of mathematics called 'group theory' that deals with such subjects, but usually you can figure out what you want with common sense."

The simplest elastic material to consider is one that is homogeneous and isotropic. When this material is stretched by a force  $F$ , the amount of extension  $\Delta l$  is related to the force by Young's Modulus

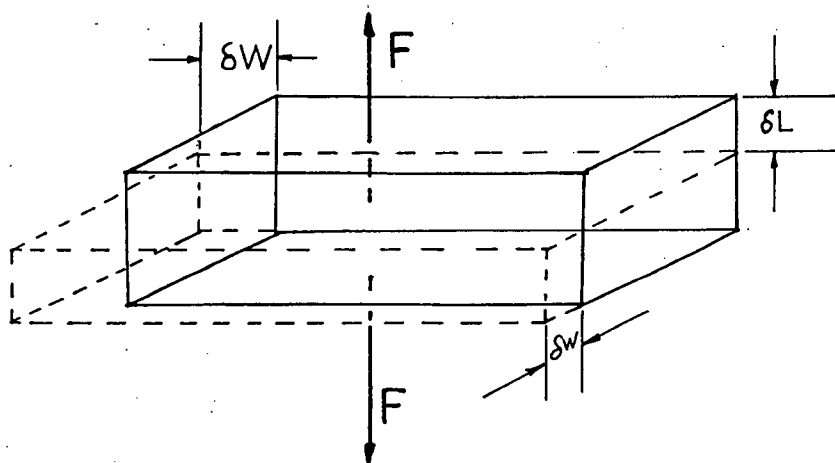
$$F = Y \Delta l \quad (2.1-17)$$

As well the bar contracts perpendicularly to the direction of stretch. The change in width per unit width is related by Poisson's ratio to the change in length per unit length.

$$\frac{\Delta w}{w} = -\sigma \frac{\Delta l}{l} \quad (2.1-18)$$

The above stretching experiment can be done in any orientation, since the medium is isotropic. Hence only two elastic constants are needed to describe a homogeneous, isotropic medium.

The next type of elastic material to be considered is one resembling plywood in geometrical structure. It is composed of infinitesimally thin laminae. Each lamina can be viewed as isotropic and hence is symmetric about the z axis. To determine the minimum number of elastic constants for this medium, two experiments suffice. Apply an extension normal to the laminae



There are lateral contractions  $\delta W$ , equal and parallel to the planes of the laminae. For this case a Young's Modulus and Poisson ratio can be measured. The amount of extension in this case is determined by the weakest lamina, and the lateral contraction  $\delta W$  is the same along the  $x$  and  $y$  axes. Now repeat the experiment with  $F$  parallel to the laminae. The physical situation is different, since it is the strongest lamina which determines the amount of extension. There are two Poisson ratios, because lateral contraction perpendicular to the applied force  $F$  is both parallel to and perpendicular to the symmetry axis of the laminae. These two experiments show that this material (known as transversely isotropic) has five elastic constants. Backus

(1962) showed how one could calculate the elastic constants of a transversely isotropic medium, which is dynamically equivalent to a finely layered isotropic medium by the application of an analogous argument. Also, it is important to note that the transversely isotropic medium is equivalent to a medium with hexagonal symmetry, since its elastic properties can be described in terms of five elastic constants.

A more complicated type of elastic medium can be now examined. It can be viewed as finely-layered, but in three orthogonal directions. In this case an extension along each of the x, y, and z axes would allow measurement of a Young's Modulus and two Poisson ratios. This gives a total of nine elastic constants. Such an elastic medium is called orthotropic. Orthotropic materials are especially important as they are considered to be among the main constituents of the upper mantle. (Green & Liebermann (1976))



## Section 2 - Solutions of the Equations of Motion

As seen in Section 1, the equations of motion with no body forces, are written (in Cartesian co-ordinates) as

$$\rho \frac{\partial^2 u_i}{\partial t^2} = \frac{\partial}{\partial x_j} \left( c_{ijkl} \frac{\partial u_k}{\partial x_l} \right) \quad (2.2-1)$$

In solving such a system of differential equations, the salient features can be obtained by using plane waves as trial solutions. Let

$$u_i = A_i e^{i\omega[\rho_k x_k - t]} \quad (2.2-2)$$

where  $A_i$  is the amplitude,

$\rho_k$  is the slowness

(the summation convention is implied on appropriate repeated indices). Substitution of (2.2-2) into (2.2-1) gives

$$(\rho \delta_{ik} - \rho_j \rho_l C_{ijkl}) A_k = 0 \quad (2.2-3)$$

Equation (2.2-3) has a solution when the determinant of the coefficients of  $A_k$  vanishes. Thus the solution to (2.2-1) reduces to the solution of an eigenvalue problem. That is,

$$\det(\rho \delta_{ij} - \rho_j \rho_l C_{ijkl}) = 0 \quad (2.2-4)$$

Equation (2.2-4) is a sextic in the components of  $p$ . It also can be viewed as a cubic in  $\rho_i \rho_j$ . This cubic has three roots, each root describing a quadratic form in the components of  $p$ . Thus each root of (2.2-4) represents a quadric surface known as the slowness surface. There is a corresponding eigenvector for each root. The eigenvector represents the displacement associated with the particular root. The existence of three roots corresponds to three different polarizations of displacement. These polarizations are still orthogonal but are not pure mode vibrations. (Musgrave (1970)) That is, they do not align either parallel to or perpendicular to the wave propagation,

as do P or S waves propagating in an isotropic medium. For each polarization of the motion, the corresponding quadric surface provides a constraint on the components of  $\mathbf{p}$  i.e. on the plane waves which are allowed to propagate. It is known that the most general solution of equation (2.2-1) is an envelope of all plane waves, which are allowed by the roots of (2.2-4) (Kraut 1963; Duff 1975; Courant & Hilbert 1966). This envelope is known as the wave surface (Kraut 1963; Musgrave 1970).

## Construction of Wave Surface - Analytic Treatment

The analytic construction of the wave surface can be obtained by differentiating the phase function (chosen for convenience at  $t=1$ ) with respect to the parameters (the components of the slowness) subject to the constraint that the slowness vectors trace out a three sheeted slowness surface (Fowler 1929; Lighthill 1960; Duff 1975; Musgrave 1970). Let the equation of the  $j$ th sheet of the slowness surface be  $G_j(p)=0$ . The phase function is  $p_k x_k - 1 = 0$ . To find the envelope of all plane waves the method of Lagrange multipliers is used, and then  $p_k$  is eliminated from the two equations:

$$\frac{\partial}{\partial p_k} (p_k x_k - 1 + \lambda G_j(p)) = 0 \quad (2.2-5)$$

and

$$p_k x_k - 1 = 0 \quad (2.2-6)$$

The co-ordinates of the envelope are

$$x_k = \frac{\frac{\partial G_j}{\partial p_k}}{\rho_k \frac{\partial G_j}{\partial p_k}} \quad (2.2-7)$$

Equation (2.2-7) shows that the co-ordinates  $X_k$  of the wave surface  $W$  are related to the normals of the slowness surface  $S$ . (Note that  $j$  refers to the  $j$ 'th sheet of the slowness surface.)

The above calculation is identical to the traditional stationary phase approach. That is, it is required to find the stationary points of the phase

$$\Theta(k_\ell, x_\ell) = K_\ell x_\ell - \omega(k_\ell) t \quad (2.2-8)$$

where  $k_\ell$  are the components of the wave number. The angular frequency,  $\omega$ , is related to the wave number by the dispersion relation obtained by solving for the  $j$ th eigenvalue, using an eigenvalue equation identical to (2.2-4). Therefore, the stationarity condition is

$$\frac{\partial \theta}{\partial k_x} = 0 \quad \text{or} \quad x_x = \left( \frac{\partial \omega}{\partial k_x} \right) t \quad (2.2-9)$$

But  $\partial \omega / \partial k_x$  are the components of the group velocity. Equation (2.2-9), which is simply the equation of the rays for a homogeneous anisotropic medium, demonstrates that the co-ordinates of the wave surface at one second can be obtained by calculating the group velocity for all angles defined by the allowable wave vectors. In general the vector  $\partial \omega / \partial k_x$  is not parallel to  $k_x$ . This implies that in a homogeneous anisotropic medium, the slowness, and hence the phase velocity, are not in the same direction as the group velocity. All the physical peculiarities of waves travelling in such media are derivable from that simple result.

## Construction of Wave Surface- Geometrical Derivation

The shape of the wave surface may be obtained by a geometrical argument. In the last section, it has been shown that the components of the group velocity generate the wave surface at  $t=1$  second. Since the direction of the group velocity is given by the normal to the slowness surface, the slowness corresponding to the group velocity (the group slowness) may be easily determined. Its reciprocal is the group velocity. For the case of a slowness curve (slowness surface for a two dimensional problem in the X-Z plane), the geometric construction proceeds as follows (Fig 2.1):

- 1) For the slowness vector OB at an angle  $\theta$ , find the corresponding unit normal vector  $\hat{n}$ ; the components of  $\hat{n}$  are the directional cosines for the line RS;
- 2) Find the group slowness, corresponding to the direction of  $\hat{n}$ . Its magnitude is the perpendicular distance from the origin to the line RS and its direction is given by the angle  $\phi$ , which is  $\arctan(\hat{n}_y/\hat{n}_x)$ ;
- 3) Take the reciprocal of the magnitude of the group slowness vector OC. The vector OD at the same angle as OC is the group velocity corresponding to the slowness vector OB.

If steps one, two, and three are repeated for all angles  $\theta$ , the two dimensional wave surface can be traced out. The complete slowness surface and wave surface for a transversely isotropic material are illustrated in

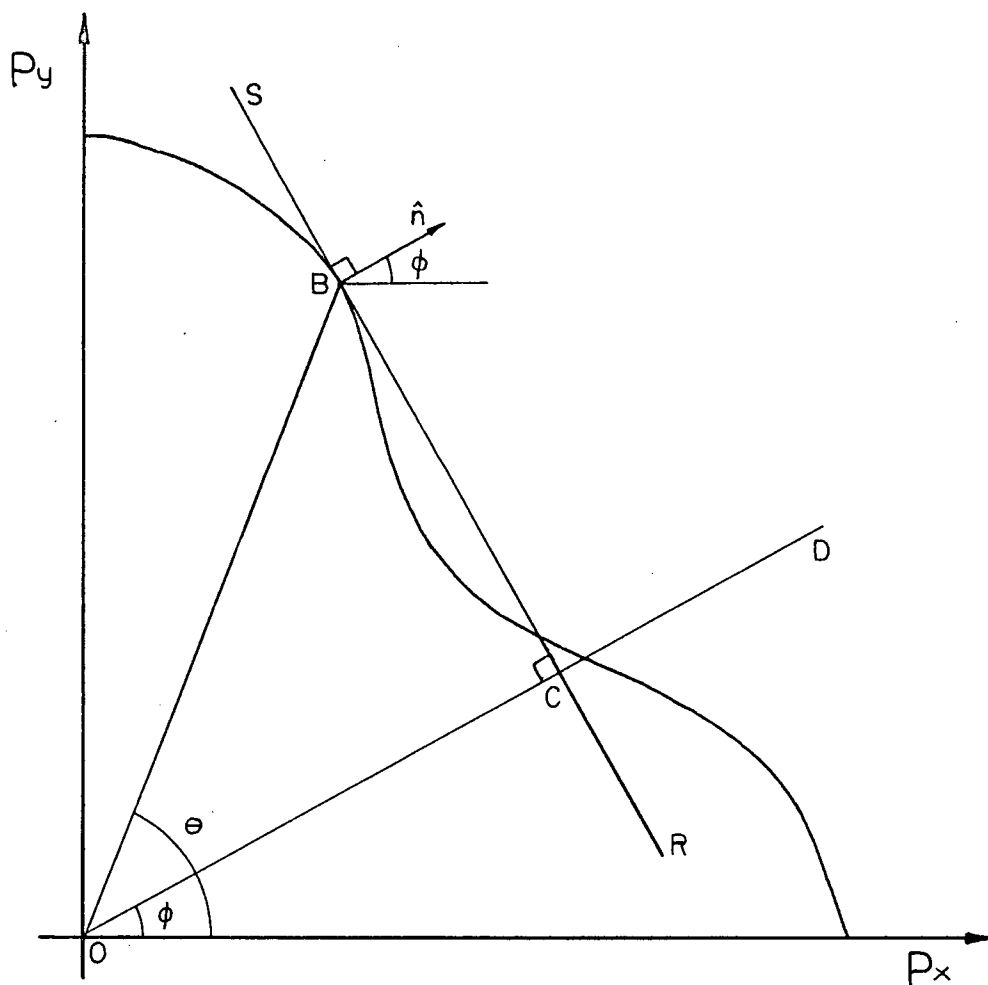


Figure 2.1 Geometric construction of wave surface from slowness surface

Figure 2.2 .

The geometric construction described above has its origin in projective geometry (Klein 1939; Poncelet 1822; Napoleoni 1977, personal communication; Courant & Hilbert 1966; Briot & Bouquet 1896). In the terms of projective



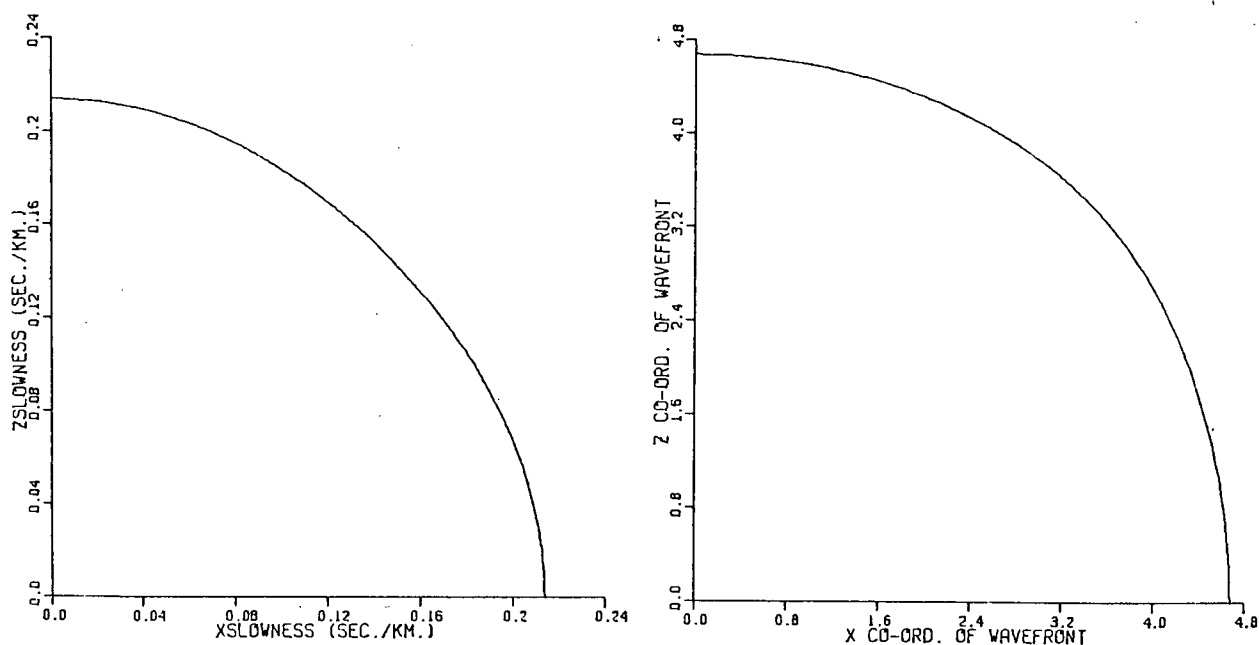


Figure 2.2 Slowness and wave surface for a transversely isotropic medium. Polar reciprocal construction was used to construct the wave surface.

geometry, the slowness surface and wave surface are known as polar reciprocals with respect to the unit sphere (a circle in two dimensions). To see that, the following definitions (for the two dimensional case) are in order:

- 1) "If  $P, Q$  are points on the diameter  $AB$  of a circle such that  $AB:PQ$  is harmonic and if  $QR$  is drawn parallel to the tangent of  $A$  then  $QR$  is called the polar of  $P$  with respect to the circle and  $P$  is called the pole of  $QR$ ." (Fig 2.3 ). If  $O$  is the center of the circle, it follows at once that  $OP \cdot OQ = \text{radius squared}$ ." (Durell 1947).
- 2) A surface  $W$ , consisting of a locus of poles whose polars with respect to the unit circle are the tangents to a surface  $S$ , is said to be the polar reciprocal of  $S$  with respect to the unit circle.

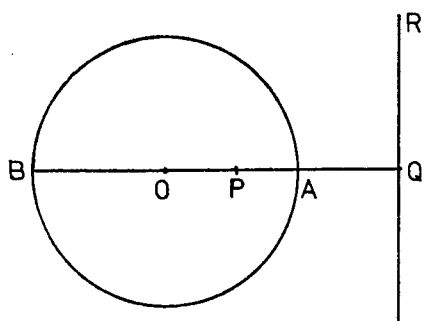
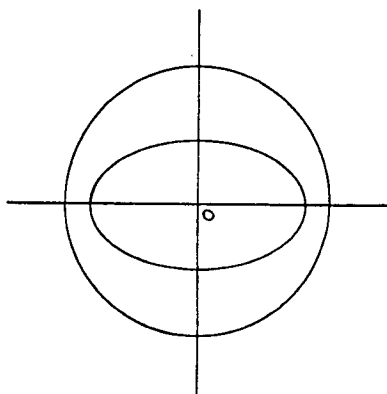


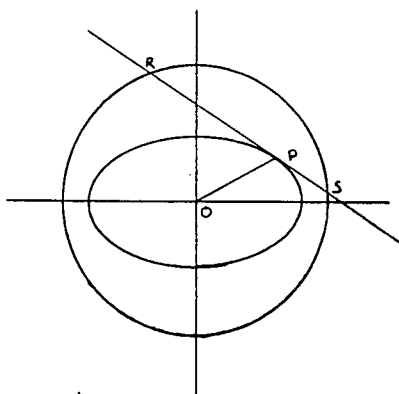
Figure 2.3 Diagram illustrating definition of pole and polar.

To see that definition (2) describes the relation of the wave surface to the slowness surface, it is sufficient to show that the construction implied by (2) is identical to the one described previously.

First imbed a surface  $S$  inside the unit circle as follows. Then



Draw a tangent at P. This tangent cuts the circle at R and S



Construct the pole D of RS. Now by symmetry, the line OD bisects the angle RDS, and intersects line RS at Q in a right angle. Hence, by definition (1) (Napoleoni 1977, personal communication)  $OQ \cdot OD = 1$  or  $OD$  is  $(1/OQ)$ . The above construction, therefore, is identical to that

described using arguments of group velocity. In three

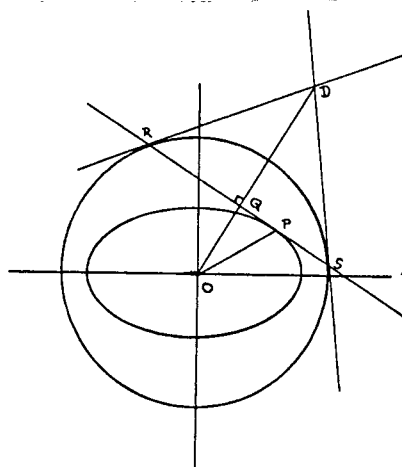


Figure 2.4 Construction of the polar reciprocal surface

dimensions, analogous definitions hold. To obtain these analogies simply substitute the words polar planes, tangent planes, and spheres for polar lines, tangents, and circles.

## Properties of the Wave Surface

Although the derivation of the wave surface from the slowness surface is based on a simple geometrical construction, the surfaces that result sometimes have peculiar features. From a mathematical viewpoint, these peculiarities are the singular points of the wave surface. There are two types of singularities: cusps and double points. It is easier to see how the two types of singularities arise if a plane section of the slowness surface is considered.

The first type of singularity to be investigated will be a double point. (A', B', fig.2.7) In Figure 2.5, points A and B of the slowness surface (one quadrant shown) share the same tangent line RS with normal  $\hat{n}$ . Hence, the corresponding group velocities must be in the same direction. By the construction shown in figure 2.4 the magnitude of the corresponding group velocities is the reciprocal of the length OP. This proves that the points A and B map onto the same point of the wave surface. In the three dimensional case, a cone of slowness vectors would share the same tangent plane and map onto one point of the wave surface. This phenomenon is known as internal conical refraction (Landau and Lifshitz 1960). From Fig 2.5, it is clear that at a neighboring point of A, D, and at a

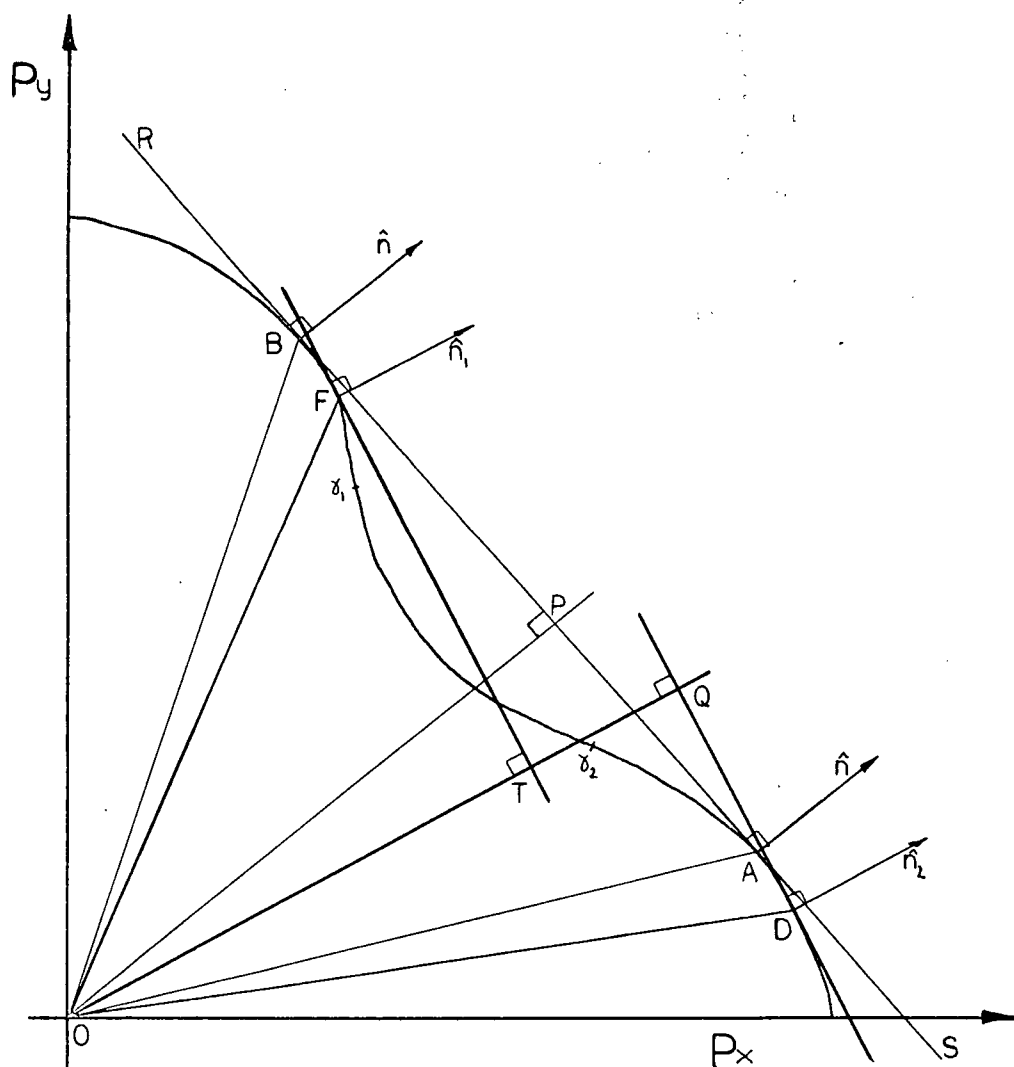


Figure 2.5 Points A and B on slowness surface sharing a common tangent, resulting in a double point on the wave surface.

neighboring point of B, F, the directions of the group velocity are the same, but the magnitudes are different. This is illustrated in Fig. 2.6, where the two tangent lines XZ and UV are parallel but the perpendicular distance

from 0 to the tangent line XZ is less than that to the line UV. Thus point F has a larger group velocity associated

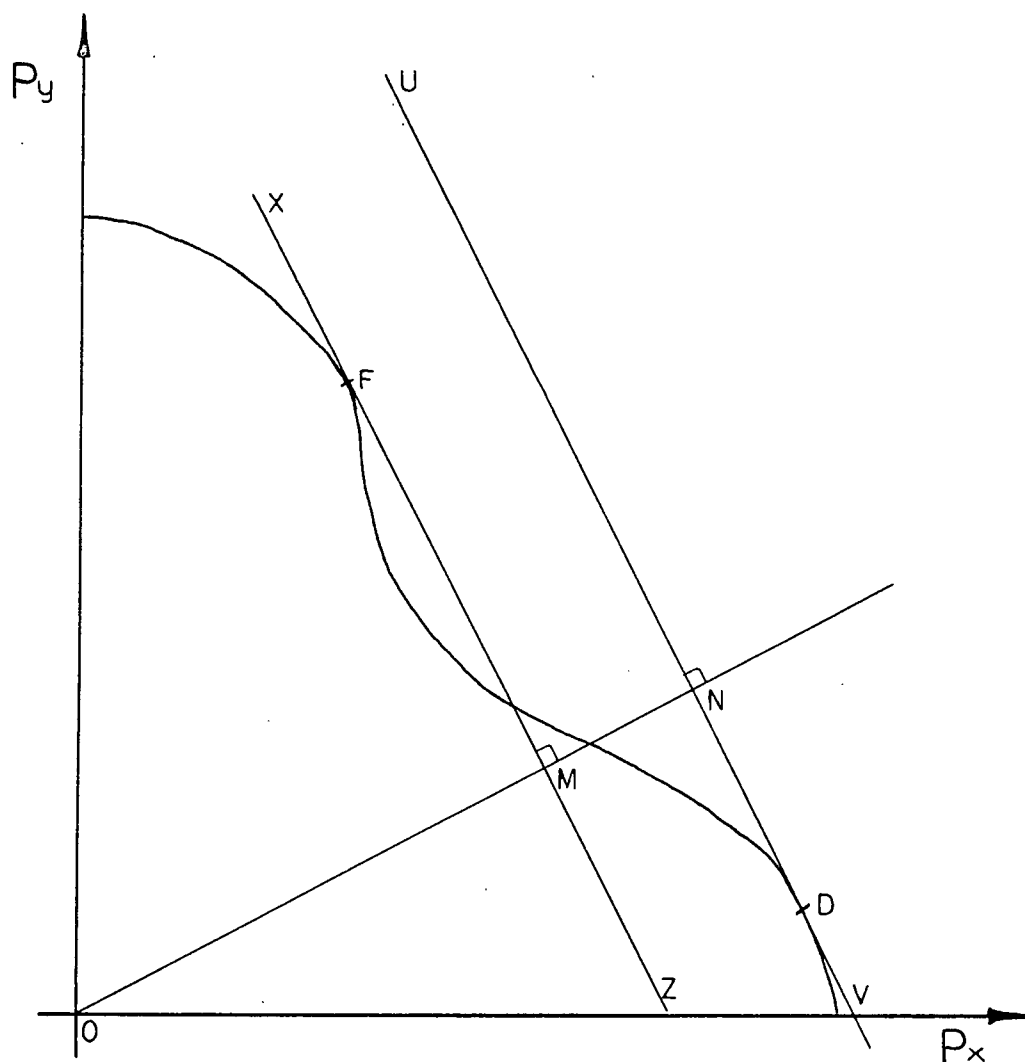


Figure 2.6 Differing group velocity magnitudes in the neighborhood of points A and B which share a common tangent.

with it than point D. The wave surface for Fig. 2.5 is shown in Fig. 2.7 with the group velocities of the corresponding slownesses labelled with dashes. The point A'

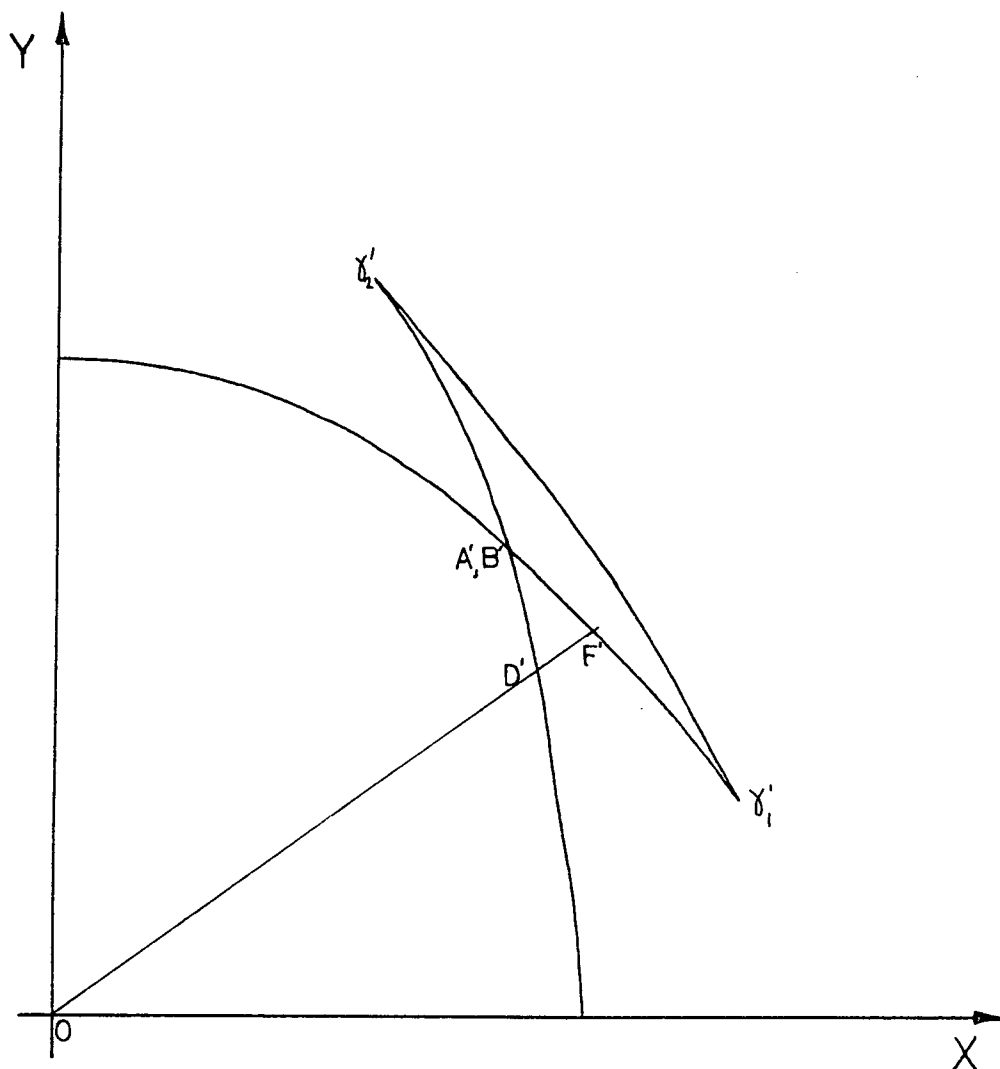


Figure 2.7 Illustration of wave surface with singularities corresponding to slowness surface of figure 2.5

or  $B'$  (which is identical) is the double point and here the wave surface intersects itself. In Fig. 2.7 the other singularity mentioned previously is also present, the cusp.

The cusp arises because of an inflection point on the slowness curve (or surface). At the inflection point,



( $\chi_1, \chi_2$  in fig. 2.5) the tangent becomes stationary. The pole of the corresponding tangent must also become stationary. This pole, which represents the group velocity at the inflection point of the slowness curve, is the tip of cusp ( $\chi_1', \chi_2'$  in Fig. 2.7). If the curve in Fig. 2.7 is given parametrically by  $X(t)$ , and  $Y(t)$ , then the stationarity condition described above is simply

$$\begin{aligned} \dot{X}(t) &= 0 & \dot{Y}(t) &= 0 \\ ' &\equiv d/dt \end{aligned} \quad (2.2-10)$$

From classical differential geometry, (Fowler 1929; Eisenhart 1968) equation (2.2-10), is the known condition for a singular point of a curve. The additional constraint that

$$(\ddot{X}(t))^2 + (\ddot{Y}(t))^2 \neq 0 \quad (2.2-11)$$

is sufficient to prove that the singular point is indeed a cusp.

Let the slowness surface be given parametrically as

$$r = f(t) \quad (2.2-12)$$

Then

$$\begin{aligned} x(t) &= f(t) \cos(t) \\ y(t) &= f(t) \sin(t) \end{aligned} \quad (2.2-13)$$

where  $x(t)$ ,  $y(t)$  are the co-ordinates of a point on the slowness curve for any given  $t$ . At an inflection point of the slowness surface,

$$\frac{d^2 y}{dx^2} = 0 \quad (2.2-14)$$

or parametrically,

$$\ddot{x}\dot{y} - \dot{y}\ddot{x} = 0 \quad (2.2-15)$$

Using equation (2.2-13) for the definition of  $x(t)$  and  $y(t)$ , it is easy to show that equation (2.2-15) becomes

$$f^2 - f\ddot{f} + 2\dot{f}^2 = 0 \quad (2.2-16)$$

Equation (2.2-16) is the condition for an inflection point, when a curve is given in polar co-ordinates (Fowler 1929). For the given slowness curve, the corresponding wave surface (in two dimensions) is

$$\begin{aligned} X(t) &= \frac{\sqrt{f^2 + \dot{f}^2}}{f^2} \cos(\alpha(t) + t) \\ Y(t) &= \frac{\sqrt{f^2 + \dot{f}^2}}{f^2} \sin(\alpha(t) + t) \end{aligned} \quad (2.2-17)$$

where  $X(t)$  and  $Y(t)$  are the co-ordinates of a point on the wave surface and

$$\alpha(t) = \text{TAN}^{-1} \left( \frac{-\dot{f}}{f} \right) \quad (\text{Fig. 2.8})$$

Equation (2.2-17) can be simplified to

$$\begin{aligned} X(t) &= \frac{1}{f^2} (f \cos t + \dot{f} \sin t) \\ Y(t) &= \frac{1}{f^2} (-\dot{f} \cos t + f \sin t) \end{aligned} \quad (2.2-18)$$

Now compute  $\dot{X}(t)$  and  $\dot{Y}(t)$ :

$$\dot{X}(t) = \frac{-2\dot{f}}{f^3} [f \cos t + \dot{f} \sin t] + \frac{1}{f^2} [2\dot{f} \cos t + f \sin t - f \sin t] \quad (2.2-19)$$

and

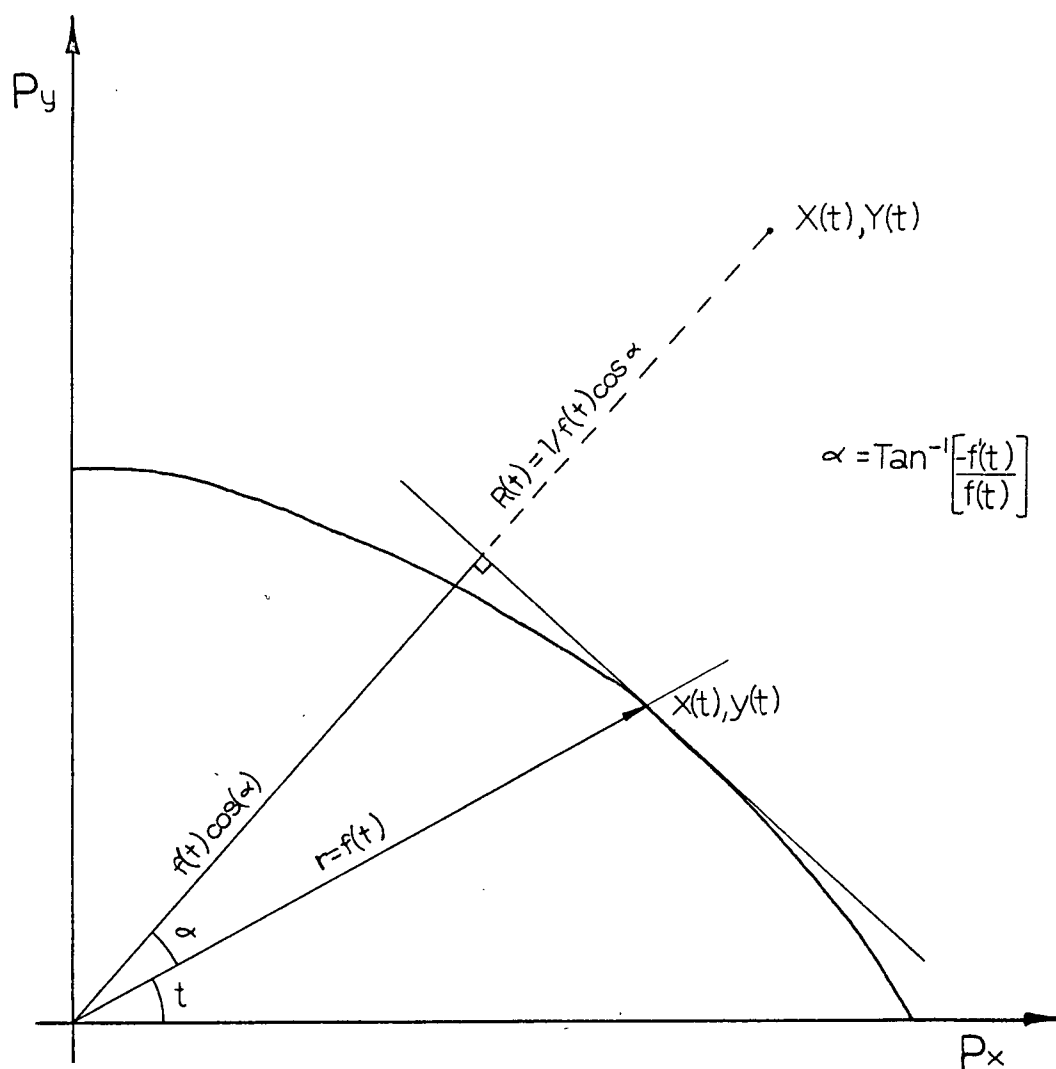


Figure 2.8 parametric representation of the slowness surface used to construct the wave surface

$$\dot{y}(t) = \frac{-2\dot{f}}{f^3} [-f \cos t + f \sin t] + \frac{1}{f^2} [-\ddot{f} \cos t + 2\dot{f} \sin t + f \cos t] \quad (2.2-20)$$

Simplifying:

$$\begin{aligned}\dot{X}(\hat{t}) &= \frac{-\sin t}{f^3} [f^2 - f\ddot{f} + 2\dot{f}^2] \\ \dot{Y}(\hat{t}) &= \frac{\cos t}{f^3} [f^2 - f\ddot{f} + 2\dot{f}^2]\end{aligned}\quad (2.2-21)$$

However, at the inflection point, at  $x(t), y(t)$ ,

$$f^2 + f\ddot{f} + 2\dot{f}^2 = 0$$

(by equation (2.2-16)). This proves that at the point of the wave surface corresponding to  $x(t), y(t)$ ,  $\dot{X}(\hat{t}) = \dot{Y}(\hat{t}) = 0$ .

It remains to show that the second derivative is non-zero at  $t = \hat{t}$ . To do this it is necessary to compute  $\ddot{X}(\hat{t})$  and  $\ddot{Y}(\hat{t})$ . Now  $\ddot{X}(\hat{t}) + \ddot{Y}(\hat{t}) = 0$  only if, at  $t = \hat{t}$ ,

$$\frac{d}{dt} (f^2 - f\ddot{f} + 2\dot{f}^2) = 0 \quad (2.2-22)$$

or

$$2f\dot{f} - f\ddot{f} + 3\dot{f}\ddot{f} = 0$$

To prove that equation (2.2-22) cannot hold, it is necessary to revert to the slowness surface. For the slowness surface

$$\frac{d^3 y}{d x^3} \neq 0. \quad \text{Parametrically,}$$

$$\frac{d^3y}{dx^3} = \frac{\dot{x}\ddot{y} - \dot{y}\ddot{x}}{\dot{x}^3} - \frac{3\ddot{x}(\dot{x}\ddot{y} - \dot{y}\ddot{x})}{\dot{x}^4} \quad (2.2-23)$$

At  $t = \hat{t}$  equation (2.2-23) becomes

$$\left. \frac{d^3y}{dx^3} \right|_{t=\hat{t}} = \left. \frac{\dot{x}\ddot{y} - \dot{y}\ddot{x}}{\dot{x}^3} \right|_{t=\hat{t}} \quad (2.2-24)$$

as  $\ddot{x}\ddot{y} - \ddot{y}\ddot{x}$  vanishes identically at  $t=\hat{t}$ . If the parametric equations of the slowness surface (2.2-13) are used then

$$\left. \frac{d^3y}{dx^3} \right|_{t=\hat{t}} = -\dot{f}\ddot{f} + 3\dot{f}\ddot{f} + 2\dot{f}\ddot{f} \Big|_{t=\hat{t}} \neq 0 \quad (2.2-25)$$

Thus (2.2-22) cannot be satisfied, and indeed the singular point is a cuspidal one.

Another way of proving the condition for the existence of the cusp is based on a construction given here in two dimensions involving the velocity curve (or surface). Suppose that the phase velocity is specified as a function of angle

$$c = g(\theta) \quad (2.2-26)$$

That is, for each angle  $\theta$  a plane wave with unit normal  $\hat{k}$  is propagated and its phase velocity  $c$  is measured. To find the group velocity, rewrite (2.2-26) as

$$\omega = \kappa g(\theta) \quad (2.2-27)$$

Following Backus (1970), the group velocity is obtained from (2.2-27) by differentiation, using the gradient operator in polar co-ordinates. The components of the group velocity in the  $\theta$  and  $\kappa$  directions are given as

$$\begin{aligned} v_{g\theta} &= g'(\theta) \\ v_{g\kappa} &= g(\theta) \end{aligned} \quad (2.2-28)$$

From (2.2-28) a physical picture of the group velocity can be obtained. The group velocity is a vector whose  $\kappa$  component is the phase velocity, and whose  $\theta$  component is  $g'(\theta)$ . Thus the angle the group velocity makes with the phase velocity is  $\tan^{-1}(g'(\theta)/g(\theta))$ . This proves the important result noted by many authors (Landau & Lifschitz 1960; Witham 1974). It is clear from figure 2.8 that the group velocity leads or lags the phase velocity by the angle  $\alpha$ .

Suppose that it leads the phase velocity of the plane wave propagating at an angle  $\Theta$ .<sup>1</sup> Then with respect to  $\Theta=0$ , the angle the group velocity makes is

$$\rho = \Theta + \tan^{-1} \left( \frac{g'(\Theta)}{g(\Theta)} \right) \quad (2.2-29)$$

As long as  $dp/d\theta$  is  $>0$ , the group velocity will lead the phase velocity. But when  $dp/d\theta < 0$ , it will lag. Therefore, the critical point is at

$$dp/d\theta = 0 \quad (2.2-30)$$

From (2.2-29), it follows that

$$g''(\theta) + g(\theta) = 0 \quad (2.2-31)$$

at the critical point. The above condition for a cuspidal point in the wave surface has been obtained by Witham (1974) and Potsma (1955) using a slightly different argument. Musgrave (1957) has also given proofs of the existence of cuspidal points, but his arguments are somewhat different from those used here. He has also derived the conditions

---

<sup>1</sup>Note:  $t$  in figure 2.8 is equivalent to  $\Theta$ , the variable which relates phase velocity to the angle of propagation.



that the elastic constants must obey in order that cuspidal edges exist in the three dimensional problem.

A detailed study of the wave surface, which is the Green's Function for a point source in homogeneous, anisotropic media is important, since the qualitative features of waves propagating in such media can readily be derived. The singular points correspond to the focussing of energy. Thus in computing seismograms in anisotropic media, it is expected that these focussing effects should appear if the cusps in the wave surface are large enough.

### CHAPTER III

#### Introduction

Following the discussion of the basic physics of waves propagating in anisotropic media, it is a straightforward matter to investigate the kinematics of these waves. In particular, attention will be focussed on transversely isotropic media . As indicated in Chapter I and II, the main emphasis of this thesis will be the analytic derivation and numerical calculation of synthetic seismograms in transversely isotropic media.

The study of the kinematics of plane waves is usually approached via asymptotic ray theory (Cerveny 1972), or by the consideration of the jumps in dynamical quantities across the wavefronts (Vlaar 1968). As will be shown in this chapter the two methods are completely equivalent, although details differ. Once the ray theory has been developed, p-delta curves (Wiggins 1973; Bullen 1965; McMechan 1976) will be constructed. These p-delta curves will then be utilized directly in the next chapter for the construction of synthetic seismograms .

A visual presentation of the rays is easily obtainable, once part of the numerical schemes for integration of the ray equations have been derived. A new hybrid scheme of integration will be developed, based on work of Gauss,

Kantorovich (1934), Krylov (1962), and Chapman (1971).

## Ray Theory Part I

The methods of ray theory have been used in optics since Newton's time. Not until Hamilton's derivation of the principle of least action was a connection made between optics and mechanics. It is precisely this connection which is utilized so effectively in seismology.

Following the derivation presented in Methods of Mathematical Physics Vol II (Courant & Hilbert 1966) many Russian seismologists (Alekseyev (1961); Yeliseyevnin (1964); Babich 1961) have successfully applied the ray method in detail and Cervený (1972) has applied the method to general anisotropic media. The specific case of transverse isotropy has been considered by Daley and Hron (1977). A summary of their basic results will be outlined below.

The equations of motion to be considered were derived in Chapter II:

$$\rho \frac{\partial^2 u_k}{\partial t^2} = \frac{\partial}{\partial x_j} \left( C_{ijkl} \frac{\partial u_k}{\partial x_l} \right) \quad (3.1-1)$$

The basic assumption of the ray method is that

$$\frac{C_{ijkl}}{\partial (C_{ijkl})} \ll \lambda$$

(no summation here) where  $\lambda$  is the wavelength under consideration. With this condition, it is possible to express the displacements in terms of an asymptotic expansion :

$$u_k = \sum_{n=0}^{\infty} u_k^n(x_1, x_2, x_3) \frac{e^{i\omega(t-\tau)}}{(i\omega)^n} \quad (3.1-2)$$

where

$u_k^n$  = vector amplitude

$\tau$  = phase of the wavefront

$\omega$  = angular frequency.

Substitution of (3.1-2) into (3.1-1) and consideration of the terms involving  $\omega$  yields the following eigenvalue problem:

$$(\rho_l \rho_j c_{ijkl} - \rho \delta_{ij}) u_k^{(0)} = 0 \quad (3.1-3)$$

$$\rho_l = \frac{\partial \tau}{\partial x_l}$$

The superscript 0 refers to the zeroth order term of the asymptotic series (3.1-2). Equation (3.1-3) is identical to the eigenvalue problem posed in the previous chapter. If the elastic tensor is scaled by the density, equation (3.1-3) becomes:

$$(\rho_l \rho_j \alpha_{ijkl} - \delta_{ij}) u_k^{(0)} = 0 \quad (3.1-4)$$

where  $\alpha_{ijkl} = \frac{c_{ijkl}}{\rho}$

Equation (3.1-4) has three eigenvalues whose numerical values, when set equal to one, define three orthogonal eigenvectors, the polarizations of particle motion. In particular, if the eigenproblem associated with the matrix  $[\rho_j \rho_l \alpha_{ijkl}]$  is rewritten as

$$(p_l p_j \alpha_{ijkl} - G \delta_{ij}) u_k^{(0)} = 0 \quad (3.1-5)$$

then, the condition  $G=1$ , corresponds to the equation (3.1-4) above. It is instructive to determine the eigenvalues  $G_j$  ( $j=1, 2, 3$ ) associated with (3.1-5), and set  $G_j = 1$ . In order that a solution of (3.1-5) exists

$$\det(p_l p_j \alpha_{ijkl} - G \delta_{ij}) = 0 \quad (3.1-6)$$

Since each  $G_j$  is a function of the  $p_i$ , a partial differential equation for the wavefront has been obtained:

$$G_m(p_i, x_i) = 1 \quad (3.1-7)$$

Equation (3.1 - 7) can be solved by the methods of characteristics (Courant & Hilbert 1966). The solution is defined by the equations

$$\frac{dx_i}{ds} = \frac{\partial G_m}{\partial p_i} \quad (3.1-8)$$

$$\frac{\partial p_i}{\partial s} = -\frac{\partial G_m}{\partial x_i}$$

where  $s$  is a parameter along the ray.

If equation (3.1 - 8) is to be recast in terms of  $\mathcal{T}$ , the phase of the wavefront, an additional result must be utilized. This result is obtained by application of Euler's theorem on homogeneous functions to the eigenvalues  $G_m$ . That is,

$$p_i \frac{\partial G_m}{\partial p_i} = 2 G_m \quad (3.1-9)$$

or

$$p_i \frac{\partial G_m}{\partial p_i} = 2$$

or as can be seen from (3.1-2), the phase of the wavefront is defined by:



$$t = \tau(x_i) \quad (3.1-10)$$

Upon differentiation of (3.1-10) with respect to  $t$ , the result obtained is

$$1 = p_i \frac{dx_i}{d\tau} \quad (3.1-11)$$

A combination of (3.1-8), (3.1-9) and (3.1-11) changes the form of the ray equations. Expressed in terms of the phase of the wavefront  $\mathcal{T}$ , equations (3.1-8) become

$$\frac{dx_i}{d\tau} = \frac{1}{2} \frac{\partial G}{\partial p_i} \quad (3.1-12)$$

$$\frac{\partial p_i}{\partial t} = -\frac{1}{2} \frac{\partial G}{\partial x_i}$$

The above theoretical derivation may be elucidated if the example of transverse isotropy is considered. The elastic tensor (Cerveny & Psencik 1972) for a transversely isotropic medium is

$$\begin{bmatrix} a_{11} & a_{12} & a_{13} & 0 & 0 \\ 0 & a_{11} & a_{13} & 0 & 0 \\ 0 & 0 & a_{33} & 0 & 0 \\ 0 & 0 & 0 & a_{55} & 0 \\ 0 & 0 & 0 & 0 & a_{66} \end{bmatrix} \quad (3.1-13)$$

$$\text{with } a_{12} = a_{11} - 2a_{66}$$

The ray will lie entirely in the  $(X_1, X_3)$  plane if the source lies in the  $(X_1, X_3)$  plane and the inhomogeneity depends only on  $X_3$ . With these restrictions, substitution of (3.1-13) into (3.1-16) yields the following determinantal equation (Daley and Hron 1977):

$$\det \begin{bmatrix} p_1^2 A_{11} + p_3^2 A_{55} - G & 0 & p_1 p_3 (A_{13} + A_{66}) \\ 0 & p_1^2 A_{66} + p_3^2 A_{55} & 0 \\ p_1 p_3 (A_{13} + A_{66}) & 0 & p_1^2 A_{55} + p_3^2 A_{33} - G \end{bmatrix} = 0 \quad (3.1-14)$$

The roots are given by solving the cubic

$$(p_1^2 A_{66} + p_3^2 A_{55} - G) \times (p_1^2 A_{11} + p_3^2 A_{55} - G) \cdot (p_1^2 A_{55} + p_3^2 A_{55} - G) - p_1^2 p_3^2 (A_{13} + A_{55})^2 = 0 \quad (3.1-15)$$

One obvious root is  $G_2 = p_1^2 A_{66} + p_3^2 A_{55}$ . The other two roots are determined by the quadratics

(3.1-16)

$$G^2 - KG + L = 0$$

$$\text{where } K = (A_{11} + A_{55}) p_1^2 + (A_{33} + A_{55}) p_3^2$$

$$L = (A_{11} p_1^2 + A_{55} p_3^2)(A_{55} p_1^2 + A_{33} p_3^2) - (A_{13} + A_{55})^2 p_1^2 p_3^2$$

The solutions to these quadratics are

$$G_1 = \frac{1}{2} ( \kappa + \sqrt{\kappa^2 - 4L} ) \quad (3.1-17)$$

$$G_3 = \frac{1}{2} ( \kappa - \sqrt{\kappa^2 - 4L} )$$

If  $G_1$  and  $G_3$  respectively are set equal to one, then each equation in (3.1-17) is an algebraic relation between the horizontal and vertical slownesses for compressional and shear waves respectively. The ray equations describing the ray trajectory may now be derived using (3.1-7) and (3.1-12): for example, the trajectories for vertically polarized quasi-compressional waves are

$$\frac{dx}{dz} = \frac{1}{2} \frac{1}{\sqrt{\kappa^2 - 4L}} \frac{\partial}{\partial p_1} (\kappa - L)$$

$$\frac{dz}{dz} = \frac{1}{2} \frac{1}{\sqrt{\kappa^2 - 4L}} \frac{\partial}{\partial p_3} (\kappa - L) \quad (3.1-18)$$

The two equations in (3.1-18) may be combined into a single ray equation

$$\frac{dx}{dz} = \frac{p_1}{p_3} \left\{ \frac{(A_{11} + A_{33}) - [2A_{11}A_{33}p_1^2 + p_3^2(A_{33}^2 + A_{11}A_{33}(A_{13} + A_{31})^2)]}{(A_{33} + A_{33}) - [2A_{33}A_{33}p_3^2 + p_1^2(A_{33}^2 + A_{33}A_{33}(A_{13} + A_{31})^2)]} \right\} \quad (3.1-19)$$

Equation (3.1-19) is identical to that inferred from Cervený and Psencik (1972).

## Ray Theory Part II

Another approach to the ray trajectory calculations, involving considerations of the discontinuities of the particle velocity across a surface travelling through  $X_i$ -space, has been developed by Vlaar (1968). His approach to ray theory will be derived below for vertically inhomogeneous, transversely isotropic media. Cylindrical coordinates will be utilized, so that the cylindrical symmetry of the medium may be exploited. As well, the final algebraic results will be proven identical to those obtained in Part I.

As Vlaar's notation will be used throughout, the following definitions are in order:

- a) the wavefront will be denoted by  $\Gamma$ ;
- b) A field quantity  $f$ , before the wavefront has passed, will be designated by  $f^-$ . After the wavefront has passed, the field quantity will be signified by  $f^+$ ;
- c) The jump in the field quantity  $f$  is shown as  $(f^*) = (f^+) - (f^-)$ , with both  $f^+$  and  $f^-$  being evaluated at the appropriate time and location
- d) The position of the wavefront at time  $t$  can be written as

$$\psi(r, \theta, z) - t = 0$$

Immediately some results may be derived from the above.

Since

$$f^*(r, \theta, z) = f^+(r, \theta, z, t = \psi(r, \theta, z)) \\ - f^-(r, \theta, z, t = \psi(r, \theta, z))$$

then

$$\frac{df^*}{dt} = (\nabla f)^* \cdot \underline{v} + \left( \frac{\partial f}{\partial t} \right)^* \quad (3.2-1)$$

$$\text{where } \nabla = \left( \frac{\partial}{\partial r}, \frac{1}{r} \frac{\partial}{\partial \theta}, \frac{\partial}{\partial z} \right)$$

$$\underline{v} = \left( \frac{dr}{dt}, r \frac{d\theta}{dt}, \frac{dz}{dt} \right)$$

As well, on the wavefront  $\psi(r, \theta, z) - t = 0$ .

Differentiation of this relation yields

$$\nabla \psi \cdot \underline{v} = 1 \quad (3.2-2)$$

Equation (3.2-2), analogous to (3.1-11) in the last section, has the following physical interpretation. The gradient of  $\psi$  is normal to the wavefront and its components are the components of the slowness vector. Hence, the velocity of the wavefront, normal to itself, has a magnitude of

$1/|\nabla \psi|$ . If the unit normal to the wavefront is denoted by

$n_j$  , then the components of the slowness are given by

$$p_j = n_j |\nabla \psi| = \frac{n_j}{V_n}$$

Equation (3.2-1) can be rewritten as

$$\begin{aligned} \frac{|V|}{V_n} \cos \alpha &= 1 \\ \text{or } V_n &= |V| \cos \alpha \end{aligned} \quad (3.2-3)$$

where  $V_n$  = magnitude of the normal velocity

$|V|$  = magnitude of ray velocity

$\alpha$  = angle between ray velocity vector and unit wavefront normal.

From (3.2,1-3) and (3) algebraic relations between the jumps in stress and in particle velocity may be derived.

Since  $\dot{u}_i^* = 0$ , the jump in the particle velocity is zero, it follows that  $d u_i^* / dt = 0$ . On application of this result to equation (3.2-1) , the ensuing equation is obtained:



$$\frac{\partial u_i^*}{\partial t} = -(\nabla u_i)^* \cdot \underline{v}_r \quad (3.2-4)$$

$$\frac{\partial u_i}{\partial t} = -|(\nabla u_i)^*| |\underline{v}_r| \cos \alpha$$

where  $\cos \alpha$  is the same as in (3.2-3). Substitution of  $\underline{v}_n$  for  $|\underline{v}_r| \cos \alpha$  and noting that  $|(\nabla u_i)^*| = \left(\frac{\partial u_i}{\partial n}\right)^*$  if  $n$  is defined as the unit normal to the wavefront, yields the final result

$$\left(\frac{\partial u_i^*}{\partial n}\right) \underline{v}_n = -\frac{\partial u_i^*}{\partial t} \quad (3.2-5)$$

Further reduction of (3.2-5) is essential in inferring the final algebraic equation relating jumps in particle velocity across the wavefront to the corresponding jumps in stresses. This reduction is achieved by multiplying (3.2-5) by the components of  $\underline{n}$ ,  $n_j$  and using the fact that  $n_j \left(\frac{\partial u_i}{\partial n}\right)^* = (\nabla u_i)^*_j$ . Then, in component form equation (3.2-5) becomes

$$(\nabla u_i)_j^* \cdot \underline{v}_n = -\eta_j \left( \frac{\partial u_i^*}{\partial t} \right) \quad (3.2-6)$$

or

$$(\nabla u_i)_j^* = -\rho_j \left( \frac{\partial u_i^*}{\partial t} \right)$$

Equation (3.2-6) relates the jump in the  $j$ th component of the gradient of particle displacement to the jump in particle velocity across the wavefront. This equation is the desired one required for calculation of ray trajectories since it is known that the characteristics are carriers of jumps in dynamical quantities. However, another relation is needed before the jumps in the stress across the wavefront can be related to the particle's velocity. Details of the derivation are given in Vlaar's paper (1968). The required equation which relates the discontinuity in stress across the wavefront, to the jump in momentum is

$$\sigma_{ij}^* \eta_j + \rho v_n (\dot{s}_i)^* = 0 \quad (3.2-7)$$

Combination of equations (3.2-6) and (3.2-7) will result in an eigenvalue problem similar to those discussed previously. As before, a system of partial differential equations associated with the eigenvalue problem can be elucidated.

The solution of these equations yields the ray trajectories.

The ray trajectories, obtained indirectly from equations (3.2-6) and (3.2-7) are of course identical to those calculated earlier. To demonstrate the equivalence of the two approaches, the example of a vertically inhomogeneous, transversely isotropic medium will again be examined. In this following example, the cylindrical symmetry of the medium is exploited.

Since the medium is cylindrically symmetric, all  $\theta$  derivatives are zero. The strains are given as

$$\begin{aligned} \epsilon_{rr} &= \frac{\partial u_r}{\partial r} & \epsilon_{r\theta} &= \frac{1}{2} \left( \frac{\partial u_\theta}{\partial r} - \frac{u_\theta}{r} \right) \\ \epsilon_{rz} &= \frac{1}{2} \left( \frac{\partial u_r}{\partial z} + \frac{\partial u_z}{\partial r} \right) & \epsilon_{\theta\theta} &= \frac{1}{2} \frac{\partial u_\theta}{\partial z} \\ \epsilon_{zz} &= \frac{\partial u_z}{\partial z} & \epsilon_{\theta r} &= \frac{u_r}{r} \end{aligned} \quad (3.2-8)$$

Since the jumps of the tractions across the wavefront are needed in equation (3.2-7), it is necessary to obtain the jumps in the stresses. Where the discontinuities in derivatives are required, equation (3.2-6) is used. Therefore, the required jumps in strain are

$$\begin{aligned}
\epsilon_{rr}^* &= -p_r(\dot{u}_r)^* & \epsilon_{\theta\theta} &= 0 \\
\epsilon_{r\theta}^* &= -\frac{1}{2} p_r(\dot{u}_r)^* & \epsilon_{rz}^* &= -\frac{1}{2} (p_z(\dot{u}_r)^* + p_r(\dot{u}_z)^*) \\
\epsilon_{zz}^* &= -p_z(\dot{u}_z)^* & \epsilon_{z\theta}^* &= -\frac{1}{2} p_z(\dot{u}_\theta)^*
\end{aligned} \tag{3.2-9}$$

where  $p_r, p_z, p_\theta$  are the components of the slowness.  $(\dot{u}_r)^*, (\dot{u}_z)^*, (\dot{u}_\theta)^*$  are the jumps in particle velocity. The corresponding jumps in the traction are obtained by using the constitutive relations relating strain and stress (equation (3.2-9)). These are:

$$\begin{aligned}
\sigma_{rr}^* &= c_{11}(-p_r(\dot{u}_r)^*) + c_{13}(-p_z(\dot{u}_z)^*) \\
\sigma_{\theta\theta}^* &= c_{11}(-p_r(\dot{u}_r)^*) + 2c_{66}p_r(\dot{u}_r)^* + c_{13}(-p_z(\dot{u}_z)^*) \\
\sigma_{zz}^* &= c_{13}(-p_r(\dot{u}_r)^*) + c_{33}(-p_z(\dot{u}_z)^*) \\
\sigma_{\theta z}^* &= c_{55}(-p_z(\dot{u}_\theta)^*) \\
\sigma_{zr}^* &= c_{55}(-p_z(\dot{u}_r)^* - p_r(\dot{u}_z)^*) \\
\sigma_{r\theta}^* &= c_{66}(-p_r(\dot{u}_\theta)^*)
\end{aligned} \tag{3.2-10}$$

where  $C_{ij} = A_{ij} \rho$  with  $A_{ij}$  defined previously. (see 3.1-4.) Substitution of (3.2-10) into (3.2-7) and use of the facts that  $p_j = \frac{n_j}{V_n}$  and  $p_\theta = 0$  (since  $\frac{\partial}{\partial \theta} = 0$ ) yields

$$\begin{bmatrix} -\rho_r^2 c_{11} - \rho_z^2 c_{55} + \rho & 0 & -\rho_r \rho_z (c_{13} + c_{31}) \\ 0 & -\rho_r^2 c_{66} - \rho_z^2 c_{55} + \rho & 0 \\ -\rho_z \rho_r (c_{55} + c_{13}) & 0 & -c_{33} \rho_z^2 - c_{55} \rho_r^2 + \rho \end{bmatrix} \begin{pmatrix} (\dot{u}_r)^* \\ (\dot{u}_z)^* \\ (\dot{u}_\theta)^* \end{pmatrix} = 0$$

(3.2-11)

Equation (3.2-11) has a solution if the determinant of the coefficient matrix vanishes. The resultant cubic in

$\rho_r^2, \rho_z^2$ , is identical to that derived in Part I, equation (3.1-15). To prove this equivalence introduce again the scaled elastic constants  $A_{ij} = c_{ij}/\rho$ . Upon computing the determinant and setting it to zero, the following cubic is obtained.

$$(-\rho_r^2 A_{66} - \rho_z^2 A_{55} + 1) \{ (-\rho_r^2 A_{11} - \rho_z^2 A_{55} + 1)(-\rho_z^2 A_{33} - \rho_r^2 A_{55} + 1) - \rho_r^2 \rho_z^2 (A_{13} + A_{31})^2 \} = 0$$

(3.2-12)

Equation (3.2-12) becomes equation (3.2-15) of Part I if  $\rho_r$  and  $\rho_z$  are identified with  $\rho_1$  and  $\rho_3$ . Since equation

(3.2-12) is a cubic relation between  $p_r^2$  and  $p_z^2$ , three solutions of  $p_z$  as a function of  $p_r$  can be obtained, each of which corresponds to a particular polarization of particle motion. One obvious solution of (3.2-12) is

$$p_z = \sqrt{\frac{1}{A_{ss}}(1 - p_r^2 A_{ss})}$$

This solution can be identified with horizontally polarized shear waves. The other two solutions are:

$$p_z = \pm \sqrt{\frac{b \pm \sqrt{b^2 - 4ac}}{2a}}$$

$$\begin{aligned} \text{where } b &= (A_{13} + A_{ss})^2 p_r^2 - A_{33}(p_r^2 A_{11} - 1) \\ &\quad - A_{ss}(A_{ss} p_r^2 - 1) \\ a &= A_{13} A_{33} \\ c &= (A_{11} p_r^2 - 1)(A_{ss} p_r^2 - 1) \end{aligned} \quad (3.2-13)$$

In equation (3.2-13) the outer '+' and '-' signs corresponds to up or downgoing waves, while the inner '+' sign can be identified with quasi-shear waves, and the inner '-' sign can be identified with quasi-compressional waves. If equation 3.2-13 is written as  $p_z^2 = f_i(p_r, z) = F_i(p_r, p_z) = 0$ , then the corresponding ray equations are (Vlaar 1968):

$$\begin{aligned}
 \frac{dr}{ds} &= \frac{\partial F}{\partial p_r} & \frac{dz}{ds} &= \frac{\partial F}{\partial p_z} \\
 \frac{dp_r}{ds} &= -\frac{\partial F}{\partial r} & \frac{dp_z}{ds} &= -\frac{\partial F}{\partial z}
 \end{aligned}
 \tag{3.2-14}$$

The equation necessary to compute the ray trajectory is

$$\frac{dr}{dz} = \frac{-1}{2p_z} \frac{\partial f_i}{\partial p_r} = -\frac{1}{2\sqrt{f_i}} \frac{\partial f_i}{\partial p_r}
 \tag{3.2-15}$$

where the subscript  $i$  refers to the two possible polarizations of motion. Equation (3.2-15) is identical to the ray equations obtained earlier for a planar, vertically inhomogeneous, transversely isotropic medium. Since the medium is cylindrically symmetric, simply replace  $r$  by  $x$ .

Calculation of t-delta and p-delta curves.

### Theory

The results of the previous section allow the calculation of t-delta curves and p-delta curves which have found such broad application in the calculation of synthetic seismograms. Integration of the equation

$$\frac{dr}{dz} = -\frac{1}{2\sqrt{f_i}} \frac{\partial f_i}{\partial p_r} \quad (3.3-1)$$

given in the previous section, will determine the distance to the turning point for a given ray parameter (horizontal slowness) in a particular vertically inhomogeneous, transversely isotropic medium. The travel time can be obtained from the relation

$$\frac{dt}{dz} = \frac{1}{2\lambda p_z} \quad (3.3-2)$$

where

$$\lambda = \left( p_r \frac{\partial F}{\partial p_r} + p_z \frac{\partial F}{\partial p_z} \right)$$



$$\text{or} \quad \frac{dt}{dz} = \frac{2p_z^2 - p_r \partial f_i / \partial p}{2\sqrt{f_i}} = p_z + p_r \frac{dr}{dz} \quad (3.3-3)$$

Note that (3.3-3) can be immediately integrated to give the one way travel time as

$$t = \int_0^z \sqrt{f_i} d\zeta + p_r r \quad (3.3-4)$$

The equations which will be used to calculate both p-delta and t-delta curves are obtained by multiplying the right hand side of (3.3-1) and (3.3-3) by (3.3-2), since the material is laterally homogeneous.

In order that the calculations of p-delta and t-delta curves proceed accurately and efficiently, a hybrid computational scheme based on the work of Chapman (1971) and Kantorovich (1934) is utilized. Kantorovich's method is used to subtract out the singularity which can be integrated analytically. The remainder of the integral is integrated using a fancy Gaussian integration scheme described in Approximate Calculation of Integrals. Chapman's usage of the fancy Gaussian method is extended, in that the technique

is applied also to the integrals with square root singularities.

The hybrid technique described above is necessary due to the singular behaviour of the ray integrals near the turning point. For example, in the case of an isotropic, vertically inhomogeneous medium, the ray integrals are

$$X(p) = 2p \int_0^{z_t} \frac{d\xi}{\sqrt{1/v^2(\xi) - p^2}} \quad (3.3-4a)$$

and

$$\tau(p) = 2 \int_0^{z_t} \sqrt{\frac{1}{v^2(\xi)} - p^2} d\xi \quad (3.3-4b)$$

where  $t(p)$  is the two-way vertical delay time.

The integrand in (3.3-4b) has an integrable singularity since  $p = 1/v(z_t)$ . That the singularity is integrable can be seen by a change of variable  $u = \frac{1}{v^2(\xi)} - p^2$ . Then, for example,

$$X(p) = -2p \int_0^{1/v^2(\xi) - p^2} \frac{1}{\sqrt{u}} \frac{d\xi}{du} du \quad (3.3-5)$$

If  $v(\xi)$  is monotonic and smooth  $d\xi/du$  will be smooth, and the behavior of the integral will be dominated by the

singularity at  $u = 0$ , (corresponding to the turning point).

If the function is more complicated, an artifice due to Kantorovich (1934) may be used. Suppose the integral in question is of the form

$$I = \int_a^b \phi(\psi(x)) dx \quad (3.3-6)$$

where  $\phi(\psi(x))$  is some composite function. Also suppose that at  $x = a$ ,  $\psi(x) = 0$  and as a result  $\phi(0)$  diverges, i.e.  $\phi(u)$  could be  $\frac{1}{\sqrt{u}}$ . The procedure is to expand  $\psi(x)$  about  $x = a$ , to as many terms as desired. For example,

$$\psi(x) = \underbrace{\psi(a)}_0 + \psi'(a)(x-a) \quad (3.3-7)$$

In (3.3-6), then, add and subtract  $\phi(\psi'(a)(x-a))$  to obtain

$$I = \int_a^b \phi(\psi'(a)(x-a)) dx + \int_a^b \phi(\psi(x)) - \phi(\psi'(a)(x-a)) dx \quad (3.3-8)$$

Since  $\phi$  usually is a simple function like  $\sqrt{x}$ , the first term in (3.3-8) can be integrated analytically. The second term is regular about the singular point, at least to first order in  $x$ . Hence, a numerical method, such as Gaussian integration may be employed.

The above technique may now be applied to the particular ray integral necessary for the calculation of  $p$ -delta curves in transversely isotropic, vertically inhomogeneous media. Recall that

$$X(p) = \int_0^{z_t} \frac{-\partial f_i / \partial p_r}{\sqrt{f_i}} dy \quad (3.3-9)$$

where  $z_t$  = the depth at the turning point and

$$f_i = \frac{b \pm \sqrt{b^2 - 4ac}}{2a} \quad \begin{array}{l} i=1 \text{ choose } + \\ i=2 \text{ choose } - \end{array} \quad (3.3-9.1)$$

$$b = (A_{13} + A_{55})^2 p_r^2 - A_{33}(A_{11} p_r^2 - 1) - A_{55}(A_{55} p_r^2 - 1)$$

$$a = (A_{11} + A_{33})$$

$$c = (A_{11} p_r^2 - 1)(A_{55} p_r^2 - 1)$$

$p_r$  = ray parameter

$A_{13}, A_{33}, A_{55}, A_{11}$  are the reduced elastic constants ( $c_{13}/\rho$  etc.).

At the turning point  $z_t$ ,  $f_i = 0$ . If the wave being considered is quasi-compressional, then  $f_2 = 0$  at  $z_t$  with the corresponding ray parameter chosen to be  $p_r = \frac{1}{\sqrt{A_{11}}}$ .

Conversely, if the wave is a quasi-shear wave, the corresponding ray parameter is  $p_r = \frac{1}{\sqrt{A_{55}}}$ . In equation (3.3-9), the integrand may be rewritten as

$$\sqrt{\frac{1}{\frac{f_i}{(\partial f_i)^2} \frac{\partial f_i}{\partial p_r}}} \quad (3.3-10)$$

The function in (3.3-10) is now a composite function of the form mentioned previously with

$$\phi(z) = \frac{1}{\sqrt{z}} \quad \psi(z) = \frac{f_i}{\left(\frac{\partial f_i}{\partial p_r}\right)^2}$$

Adherence to the prescription outlined previously necessitates calculation of  $\left. \frac{d\psi}{dz} \right|_{z_t}$ . After lengthy algebra, it may be shown that at the turning point

$$\frac{d\psi}{dz} = \frac{C_z/b}{C_{pr}^2/b^2} = \frac{C_z b}{C_{pr}} \quad (3.3-11)$$

where

$$C_z = \frac{d}{dz} \left\{ (A_{11} p_r^2 - 1)(A_{ss} p_r^2 - 1) \right\}$$

$$C_{pr} = \frac{\partial}{\partial p_r} \left\{ (A_{11} p_r^2 - 1)(A_{ss} p_r^2 - 1) \right\}$$

Expansion of  $\psi$  about the turning point yields

$$\psi(z) = \psi(z_t) + \left( \frac{d\psi}{dz_t} \right) (z - z_t)$$

$$\psi(z) = \frac{c_z b}{c_{pr}^2} (z - z_t) = u(z - z_t) \quad (3.3-12)$$

$$\text{where } u = \frac{c_z b}{c_{pr}^2}$$

Substitution of (3.3-12) into (3.3-9), and use of (3.3-8) yields

$$X(p_r) = \int_0^{z_t} \frac{1}{\sqrt{-u(z-z_t)}} d\zeta + \int_0^{z_t} \frac{1}{\sqrt{\frac{f_i}{\left( \frac{\partial f_i}{\partial p_r} \right)^2}}} - \frac{1}{\sqrt{-u(z-z_t)}} d\zeta$$

The first term in (3.3-13) may be integrated analytically.

As mentioned previously, the second term, which is not singular, can be integrated numerically using a Gaussian method. However, since the integrand in the second term in (3.3-13) still behaves like  $1/\sqrt{\mathcal{P}}$ , it is

convenient to recast the integrand in the form  $h(s)/\sqrt{\mathcal{P}}$ .

This is first accomplished by a simple change of variables

$v = z_t - \bar{z}$ . Then, let  $\frac{f_t(s)}{(\frac{\partial f_t}{\partial p})^2} = g(v)$ . The integrand in the second term in (3.3-13) is written as

$$\frac{1}{\sqrt{g(v)}} - \frac{1}{\sqrt{-uv}} \quad (3.3-14)$$

Equation (3.3-14) is identical to

$$\frac{1}{\sqrt{-uv}} \left( \sqrt{\frac{-uv}{g(v)}} - 1 \right) = \frac{h(v)}{\sqrt{v}} \quad (3.3-15)$$

where

$$h(v) = \sqrt{\frac{v}{g(v)}} - \frac{1}{\sqrt{u}} \quad (3.3-16)$$

To integrate an integral of the form

$$I = \int_0^1 \frac{h(v)}{\sqrt{v}} dv \quad (3.3-17)$$

a Gaussian method is used. The method is slightly more elaborate than usual, and the polynomials which are orthogonal on  $(0,1)$  with respect to the weight function  $\frac{1}{\sqrt{v}}$  are closely related to the Legendre polynomials, which are orthogonal on the interval  $[-1,1]$  with respect to a unit weight function. The polynomials are (Krylov 1962):



$$Q_N(x) = P_{2N}(\sqrt{x})$$

where  $P_{2n}(x)$  are the Legendre polynomials of even order. Given the above formula, the integral (3.3-17) can be calculated numerically as

$$\int_0^1 \frac{h(v)}{\sqrt{v}} dv = \sum_{k=1}^n A_k h(x_k) \quad (3.3-18)$$

where  $X_k$  are the squares of positive roots of the Legendre polynomials

and  $A_k$  are weights obtainable directly from the weights used in ordinary Gaussian integration.

Usually  $X_k$ , and  $A_k$  are obtained directly from tables.

The numerical algorithm elucidated above, a hybrid of techniques of Kantorovich and Krylov, can also be used in the calculation of integrals of the form

$$I = \int_0^1 \sqrt{g(x)} dx \quad (3.3-19)$$

Such integrals arise in the calculation of  $\tau(p)$ , the vertical delay time. P-delta curves calculated using the

above method are presented in Chapter V along with the calculation of synthetic seismograms.

## CHAPTER IV

### Solutions Of The Equations Of Motion

The results in Chapter III were derived so that the kinematics of the wave propagation could be explained in terms of rays,  $p$ -delta and  $t$ -delta curves. These results will be utilized in Chapter V, which is concerned with the seismogram calculation. It is first necessary to solve the relevant equations of motion and include the source terms.

The solutions of the equations of motion, in the elastodynamic case have been known for some time. (Love 1945). Most often the solution is obtained in terms of plane waves. (Musgrave 1970). In the case of vertically inhomogeneous media, the horizontal co-ordinates are Fourier transformed, and the resultant equations are a set of coupled ordinary differential equations, to be solved as a function of  $z$ . (Chapman 1977b, gives an excellent review of the method.) These coupled equations are solved using either a numerical scheme, (Gilbert & Backus 1966) or an asymptotic method, which incorporates the wave kinematics described in Chapter III.

In the solution of these coupled equations, the horizontal slowness,  $p$ , and the angular frequency  $\omega$ , appear

as parameters. The solution is then inverse transformed to obtain displacements and stresses as a function of  $(r, z, t)$ . It is the evaluation of the inverse transform to which much attention has been paid viz. Chapman (1974a), Wiggins (1976), Helmberger (1968), Fuchs and Muller (1971), Helmberger and Wiggins (1974). Very recently, it has been discovered that an adequate approximation to the first motion represented on the seismogram can be obtained using the equal phase method (Chapman 1976a) or equivalently disk ray theory (Wiggins 1976). Chapter V will be concerned with the application of the above approximation to vertically inhomogeneous, transversely isotropic, elastic media.

## Section 1. Development of the Equations of Motion

When the earth may be regarded as vertically inhomogeneous, transversely isotropic, and elastic in its dynamic response to an applied force, the equations of motion and stress-strain relations can be readily derived. In order to incorporate the source description into the formulation, it is expedient to use the formalism developed by Takeuchi and Saito (1972). In the case of a flat earth and the vertical symmetry axis possessed by a transversely isotropic medium, vector cylindrical harmonics are employed. Then the displacement and stresses can be expanded as follows:

$$\underline{u} = e^{-i\omega t} \sum_m \frac{1}{2\pi} \int_0^\infty k dk \left\{ \bar{u}_z R_k^m(r, \theta) + \bar{u}_r S_k^m(r, \theta) + \bar{u}_\theta T_k^m(r, \theta) \right\}$$

$$\underline{\sigma} = e^{-i\omega t} \sum_m \frac{1}{2\pi} \int_0^\infty k dk \left\{ \bar{\sigma}_{zz} R_k^m(r, \theta) + \bar{\sigma}_{zr} S_k^m(r, \theta) + \bar{\sigma}_{z\theta} T_k^m(r, \theta) \right\}$$

(4.1-1)

where  $\underline{\sigma}$  = stress vector in the z direction

$\underline{u}$  = displacement vector and

$$R_{\kappa}^m(r, \theta) = J(\kappa r) e^{im\theta} \quad \hat{e}_z = Y_{\kappa}^m \hat{e}_z$$

$$S_{\kappa}^m(r, \theta) = \frac{1}{\kappa} \frac{\partial Y_{\kappa}^m}{\partial r} \hat{e}_r + \frac{1}{\kappa r} \frac{\partial Y_{\kappa}^m}{\partial \theta} \hat{e}_{\theta} \quad (4.1-2)$$

$$T_{\kappa}^m(r, \theta) = \frac{1}{\kappa r} \frac{\partial Y_{\kappa}^m}{\partial \theta} \hat{e}_r - \frac{1}{\kappa} \frac{\partial Y_{\kappa}^m}{\partial r} \hat{e}_{\theta}$$

with  $\hat{e}_r, \hat{e}_{\theta}, \hat{e}_z$  the unit vectors in the  $r, \theta, z$  directions.

The cylindrical harmonics  $R_{\kappa}^m, S_{\kappa}^m, T_{\kappa}^m$  are simplified when there is a vertical symmetry axis since  $\frac{\partial}{\partial \theta} \equiv 0$  ( $m=0$ ). They become:

$$\begin{aligned}
\underline{R}_\kappa^o &= J_o(\kappa r) \hat{e}_z \\
\underline{S}_\kappa^o &= \frac{1}{\kappa} \frac{\partial}{\partial r} [J_o(\kappa r)] \hat{e}_r \\
\underline{T}_\kappa^o &= -\frac{1}{\kappa} \frac{\partial}{\partial r} [J_o(\kappa r)] \hat{e}_\theta
\end{aligned} \tag{4.1-3}$$

The cylindrical harmonic expansion (4.1-1) can be applied to the equations of motion and the constitutive relations as outlined in the paragraphs below.

Continuing with the formalism of Takeuchi and Saito (1972) , the strain-displacement relations are given as

$$\begin{aligned}
\epsilon_{rr} &= \frac{\partial u_r}{\partial r} & \epsilon_{zz} &= \frac{\partial u_z}{\partial z} & \epsilon_{\theta\theta} &= \frac{u_r}{r} \\
\epsilon_{r\theta} &= \frac{1}{2} \left\{ \frac{\partial u_\theta}{\partial r} - \frac{u_\theta}{r} \right\} & \epsilon_{rz} &= \frac{1}{2} \left\{ \frac{\partial u_r}{\partial z} + \frac{\partial u_z}{\partial r} \right\} & & \\
\epsilon_{\theta z} &= \frac{1}{2} \frac{\partial u_\theta}{\partial z}
\end{aligned} \tag{4.1-4}$$

where  $e_{ij}$  =  $ij$ th component of strain

$u_j$  =  $j$ th component of displacement.

The above strain-displacement relations are substituted into

the constitutive relations as outlined below:

$$\begin{aligned}
 \sigma_{rr} &= A \frac{1}{r} \frac{\partial}{\partial r} (r u_r) - 2N \frac{u_r}{r} + F \frac{\partial u_z}{\partial z} \\
 \sigma_{\theta\theta} &= A \frac{1}{r} \frac{\partial}{\partial r} (r u_r) - 2N \frac{\partial u_r}{\partial r} + F \frac{\partial u_z}{\partial z} \\
 \sigma_{zz} &= F \left( \frac{1}{r} \frac{\partial}{\partial r} (r u_r) \right) + C \frac{\partial u_z}{\partial z} \\
 \sigma_{\theta z} &= L \frac{\partial u_\theta}{\partial z} \quad \sigma_{r\theta} = N \left\{ \frac{\partial u_\theta}{\partial r} - \frac{u_\theta}{r} \right\} \\
 \sigma_{rz} &= L \left\{ \frac{\partial u_z}{\partial r} + \frac{\partial u_r}{\partial z} \right\}
 \end{aligned} \tag{4.1-5}$$

where  $\sigma_{ij}$  =  $ij$ th component of stress ( $i = r, \theta, z$ ;  $j = r, \theta, z$ ), and  $A, C, F, N, L$  are the 5 elastic parameters describing a transversely isotropic medium. Then equations (4.1-5) are substituted into the equations of motion below (4.1-6) to obtain equations (4.1-7).

The equations of motion are



$$\frac{\partial \sigma_{rr}}{\partial r} + \frac{\partial \sigma_{\theta z}}{\partial z} + \frac{\sigma_{rr} - \sigma_{\theta\theta}}{r} + \rho f_r = \rho \ddot{u}_r$$

$$\frac{\partial \sigma_{r\theta}}{\partial r} + \frac{\partial \sigma_{\theta z}}{\partial z} + \frac{2\sigma_{r\theta}}{r} + \rho f_\theta = \rho \ddot{u}_\theta \quad (4.1-6)$$

$$\frac{\partial \sigma_{rz}}{\partial r} + \frac{\partial \sigma_{zz}}{\partial z} + \frac{\sigma_{rz}}{r} + \rho f_z = \rho \ddot{u}_z$$

where  $\rho$  = density

$$\ddot{\phantom{x}} = \frac{\partial^2}{\partial t^2}$$

$f_r, f_\theta, f_z$  = components of the body forces and,

$\sigma_{ij}$  =  $ij$ th components of stress. Substitution of (4.1-5)

into (4.1-6) results in the following set of equations:

$$\begin{aligned}
A \frac{\partial}{\partial r} \left\{ \frac{1}{r} \frac{\partial}{\partial r} (r u_r) \right\} + F \frac{\partial}{\partial r} \left( \frac{\partial u_z}{\partial z} \right) + \frac{\partial \sigma_{rz}}{\partial z} + \rho f_r &= \rho \ddot{u}_r \\
N \frac{\partial}{\partial r} \left\{ \frac{1}{r} \frac{\partial}{\partial r} (r u_\theta) \right\} + \frac{\partial \sigma_{\theta z}}{\partial z} + \rho f_\theta &= \rho \ddot{u}_\theta \\
\frac{1}{r} \frac{\partial}{\partial r} \left\{ r \sigma_{rz} \right\} + \frac{\partial \sigma_{zz}}{\partial z} + \rho f_z &= \rho \ddot{u}_z
\end{aligned} \tag{4.1-7}$$

Equation set (4.1-7) and the constitutive relations

$$\begin{aligned}
\sigma_{rr} &= A \frac{1}{r} \frac{\partial}{\partial r} (r u_r) - 2N \frac{u_r}{r} + F \frac{\partial u_z}{\partial z} \\
\sigma_{\theta\theta} &= A \frac{1}{r} \frac{\partial}{\partial r} (r u_r) - 2N \frac{\partial u_r}{\partial r} + F \frac{\partial u_z}{\partial z} \\
\sigma_{zz} &= F \left( \frac{1}{r} \frac{\partial}{\partial r} (r u_r) \right) + C \frac{\partial u_z}{\partial z} \\
\sigma_{\theta z} &= L \frac{\partial u_\theta}{\partial z} \quad \sigma_{r\theta} = N \left\{ \frac{\partial u_\theta}{\partial r} - \frac{u_\theta}{r} \right\} \\
\sigma_{rz} &= L \left\{ \frac{\partial u_z}{\partial r} + \frac{\partial u_r}{\partial z} \right\}
\end{aligned} \tag{4.1-8}$$

completely define the differential system to be solved. Before applying the cylindrical harmonic expansion it is useful to rewrite the two sets of equations (4.1-7), and (4.1-8) such that all  $z$  derivatives appear on the left hand

side and the right hand side has only  $\frac{\partial}{\partial r}$  operators and body force components. Written in this manner, the complete system is

$$\frac{\partial u_r}{\partial z} = \frac{\sigma_{rz}}{L} - \frac{\partial u_z}{\partial r} \quad (4.1-9-1)$$

$$\frac{\partial u_\theta}{\partial z} = \frac{1}{L} \sigma_{\theta z} \quad (4.1-9-2)$$

$$\frac{\partial u_z}{\partial z} = -\frac{F}{C} \left\{ \frac{1}{r} \frac{\partial}{\partial r} (r u_r) \right\} + \frac{1}{C} \sigma_{zz} \quad (4.1-9-3)$$

$$\frac{\partial \sigma_{zz}}{\partial z} = \rho \ddot{u}_z - \frac{1}{r} \frac{\partial}{\partial r} (r \sigma_{rz}) - \rho f_z \quad (4.1-9-4)$$

$$\frac{\partial \sigma_{rz}}{\partial z} = \rho \ddot{u}_r - A \frac{\partial}{\partial r} \left\{ \frac{1}{r} \frac{\partial}{\partial r} (r u_r) \right\} - F \frac{\partial}{\partial r} \left\{ \frac{\partial u_z}{\partial z} \right\} - \rho f_r$$

(4.1-9-5)

$$\frac{\partial \sigma_{\theta z}}{\partial z} = \rho \ddot{u}_\theta - N \frac{\partial}{\partial r} \left\{ \frac{1}{r} \frac{\partial}{\partial r} (r u_\theta) \right\} - \rho f_\theta$$

(4.1-9-6)

The six equations above separate into two systems, a fourth order system, and a second order system. These are

$$\frac{\partial u_r}{\partial z} = \frac{\sigma_{rz}}{L} - \frac{\partial u_z}{\partial r}$$

$$\frac{\partial u_z}{\partial z} = -\frac{F}{C} \frac{1}{r} \frac{\partial}{\partial r} (r u_r)$$

(4.1-10)

$$\frac{\partial \sigma_{rz}}{\partial z} = \rho \ddot{u}_r - A \frac{\partial}{\partial r} \left\{ \frac{1}{r} \frac{\partial}{\partial r} (r u_r) \right\} - F \frac{\partial}{\partial r} \left\{ \frac{\partial u_z}{\partial z} \right\} - \rho f_r$$

$$\frac{\partial \sigma_{rz}}{\partial z} = \rho \ddot{u}_r - \frac{1}{r} \frac{\partial}{\partial r} (r \sigma_{rz}) - \rho f_z$$

and

$$\frac{\partial u_\theta}{\partial z} = \frac{1}{c} \phi_{\theta z} \quad \frac{\partial \phi_{\theta z}}{\partial z} = \rho \ddot{u}_\theta - N \frac{\partial}{\partial r} \left\{ \frac{1}{r} \frac{\partial}{\partial r} (r u_\theta) \right\} - \rho f_\theta$$

(4.1-11)

Equation set (4.1-10) corresponds to the differential system describing P-SV waves in an isotropic medium, while the second order system (4.1-11) is analogous to that describing SH propagation. In the ensuing discussion only the "P-SV" system, equation set (4.1-10), will be considered.

Now, the formalism developed earlier may be applied to equation set (4.1-10). Only one trick is used and that is the fact that the operator  $\left\{ \frac{1}{r} \left[ \frac{\partial}{\partial r} r \frac{\partial}{\partial r} \right] \right\}$  has the eigenvalue  $-\omega^2 \rho^2$ , when it is applied to  $J_0(\omega \rho r)$  (recall  $k = \omega \rho$ ). The transformed set of equations is then derived by substitution of (4.1-1) (with  $m=0$ ) into equation set (4.1-10). Thus the following system is obtained

$$\frac{\partial \bar{u}_r}{\partial z} = \frac{\bar{\sigma}_{rz}}{L} - \omega \rho \frac{\partial \bar{u}_z}{\partial r}$$

$$\frac{\partial \bar{u}_z}{\partial z} = \frac{F}{C} \omega \rho \bar{u}_r + \frac{1}{C} \bar{\sigma}_{zz}$$

(4.1-12)

$$\frac{\partial \bar{\sigma}_{rz}}{\partial r} = -\rho \omega^2 \bar{u}_r - \left(A - \frac{F^2}{C}\right) (-\omega^2 \rho^2) \bar{u}_r - \frac{F}{C} \omega \rho \bar{\sigma}_{zz} - \rho \bar{f}_r$$

$$\frac{\partial \bar{\sigma}_{zz}}{\partial z} = -\rho \omega^2 \bar{u}_z + \omega \rho \bar{\sigma}_{rz} - \rho \bar{f}_z$$

where  $\bar{u}_z, \bar{u}_r$  are the coefficients of  $\underline{R}_k^\circ$  and  $\underline{S}_k^\circ$  in (4.1-1a)  
 $\bar{\sigma}_{zz}, \bar{\sigma}_{rz}$  are the coefficients of  $\underline{R}_k^\circ$  and  $\underline{S}_k^\circ$  in (4.1-1b) and  
 $w$  = angular frequency

$\rho$  = horizontal slowness

$k = wp$  = wavenumber.

Alternatively  $\bar{u}_r, \bar{u}_z, \bar{\sigma}_{rz}, \bar{\sigma}_{zz}$  can be viewed as the Bessel transforms of  $u_r, u_z, \sigma_{rz}, \sigma_{zz}$ . This is not strictly correct, as can be seen by examination of  $\underline{S}_k^\circ$  which is accompanied by the  $\frac{\partial}{\partial r}$  differential operator. The details of the source terms will be described below, but first it is instructive to cast (4.1-12) as the matrix differential equation

$$\frac{d\bar{V}}{dz} = [A] \bar{V} + \rho \bar{f}$$

$$\bar{V} = \begin{pmatrix} \bar{u}_r \\ \bar{u}_z \\ \bar{\sigma}_{rz} \\ \bar{\sigma}_{zz} \end{pmatrix} \quad \bar{f} = \begin{pmatrix} 0 \\ 0 \\ -\bar{f}_r \\ -\bar{f}_z \end{pmatrix} \quad (4.1-13)$$

$$[A] = \begin{pmatrix} 0 & -\omega \rho & \frac{1}{L} & 0 \\ \frac{F\omega}{c} & 0 & 0 & \frac{1}{c} \\ -\omega^2 & (A - \frac{F}{c})\omega^2 \rho^2 & 0 & -\frac{f\omega \rho}{c} \\ 0 & 0 & -\rho\omega^2 & 0 \end{pmatrix}$$

Equation (4.1-13) can be altered so that  $\omega$  does not appear at all in  $[A]$ . That equation is

$$\frac{d\bar{V}'}{dz} = -i\omega [A'] \bar{V}' + \rho \bar{F}$$

(4.1-14)

$$\bar{V}' = \begin{pmatrix} -i\omega \bar{V}_1 \\ -i\omega \bar{V}_2 \\ v_3 \\ -i v_4 \end{pmatrix} = \begin{pmatrix} \bar{V}_1 \\ \bar{V}_2 \\ \bar{V}_3 \\ \bar{V}_4 \end{pmatrix}$$

$$[A'] = \begin{pmatrix} 0 & \rho & 1/L & 0 \\ \frac{F_p}{c} & 0 & 0 & 1/c \\ \rho - (A - F/c)\rho & 0 & 0 & F_p/c \\ 0 & \rho & \rho & 0 \end{pmatrix}$$

$$\bar{F} = \begin{pmatrix} 0 \\ 0 \\ -\bar{f}_r \\ i\bar{f}_r \end{pmatrix}$$



## Section 2. Details of the Source

The power of the vector cylindrical harmonic expansion was perhaps not too evident in the last section. One could ask "Why not use Bessel transforms directly?" The answer is given in this section. A vector cylindrical harmonic decomposition is the best one for describing the most general types of sources. An expansion identical to that of (4.1-1) can be written for a point force of magnitude  $G$  acting at  $(r_0, \theta_0, z_0)$  and pointing in the "m" direction, i.e., if

$$\rho f(r, \theta, z, \omega) = e^{-i\omega t} \frac{\delta(r-r_0) \delta(\theta-\theta_0) \delta(z-z_0)}{r_0} \underline{\tilde{m}} \quad (4.2-1)$$

where

$$\underline{\tilde{m}} = m_r \underline{\tilde{e}}_r + m_\theta \underline{\tilde{e}}_\theta + m_z \underline{\tilde{e}}_z$$

then

$$\rho \underline{\tilde{f}} = e^{-i\omega t} \frac{1}{2\pi} \int_0^\infty k dk \int_0^{2\pi} d\phi \underline{\tilde{m}} (\underline{\tilde{F}}_z \underline{\tilde{R}}_k + \underline{\tilde{F}}_r \underline{\tilde{S}}_k + \underline{\tilde{F}}_\theta \underline{\tilde{T}}_k) \quad (4.2-2)$$

where

$$\begin{aligned}\bar{F}_z &= \delta(z-z_0) \int_0^\infty r dr \int_0^{2\pi} d\phi \cdot \underline{R}_k^{m*} \cdot \underline{m} \frac{\delta(\phi-\phi_0) \delta(r-r_0)}{r_0} \\ &= \delta(z-z_0) m_z Y_k^m \Big|_{\substack{r=r_0 \\ \theta=\theta_0}}\end{aligned}$$

and similarly

$$\begin{aligned}\bar{F}_r &= \delta(z-z_0) \left[ \frac{m_r}{k} \frac{\partial Y_k^{m*}}{\partial r} + \frac{m_\theta}{kr} \frac{\partial Y_k^{m*}}{\partial \theta} \right]_{\substack{r=r_0 \\ \theta=\theta_0}} \\ \bar{F}_\theta &= \delta(z-z_0) \left[ \frac{m_r}{kr} \frac{\partial Y_k^{m*}}{\partial \phi} - \frac{m_\theta}{kr} \frac{\partial Y_k^{m*}}{\partial \theta} \right]_{\substack{r=r_0 \\ \theta=\theta_0}}\end{aligned}$$

In order to obtain more general sources, only the superposition of point sources acting in different directions need be considered. Suppose there exists a point force of magnitude  $G$  acting in the direction " $\hat{m}$ " separated by  $|\delta r_0|$  from a force acting in the direction " $-\hat{m}$ ", then

$$\rho \bar{f}_j = e^{-i\omega t} \left\{ j(\underline{r}_0 + \delta \underline{r}_0) - j(\underline{r}_0) \right\} \quad (4.2-3)$$

where  $G$  = magnitude of the force

$$\underline{r}_0 = (r_0, \theta_0, z_0)$$

$j$  =  $j$ th expansion coefficient of the force i.e. coefficient of  $R_K^m$ ,  $S_K^m$  or  $T_K^m$  in the expansion (4.1-1). In (4.2-3), which represents a couple force, now multiply and divide the right hand side by  $|\delta r_0|$  and let  $\delta r_0 \rightarrow 0$ . Then, letting  $G|\delta r_0|$  be the moment of the couple force it follows that

$$\rho \bar{f}_j = e^{-i\omega t} G |\delta r_0| \nabla \bar{F}_j \cdot \underline{n} \quad (4.2-4)$$

where

$$\underline{n} = \frac{\delta \underline{r}_0}{|\delta r_0|}$$

$r_0, \theta_0, z_0$  are the source co-ordinates and

$$\nabla = \left( \frac{\partial}{\partial r_0}, \frac{1}{r_0} \frac{\partial}{\partial \theta_0}, \frac{\partial}{\partial z_0} \right)$$

$\bar{F}_j$  = jth component in the cylindrical harmonic expansion of the force as given in equation (4.2-2) The term on the right hand side of equation (4.2-4) may be written as a directional derivative, yielding

$$\rho \bar{f}_j = e^{-i\omega t} \left\{ G |\delta r| \frac{\partial \bar{F}_j}{\partial n_1} + n_z \frac{\partial \bar{F}_j}{\partial z_0} \right\} \quad (4.2-5)$$

or if unit moment is considered,

$$\rho \bar{f}_j = e^{-i\omega t} \left\{ \frac{\partial \bar{F}_j}{\partial n_1} + n_z \frac{\partial \bar{F}_j}{\partial z_0} \right\} \quad (4.2-6)$$

where

$$\frac{\partial}{\partial n_1} = n_r \frac{\partial}{\partial r_0} + \frac{n_\theta}{r_0} \frac{\partial}{\partial \theta_0}$$

Application of the above results to equations (4.1-14) of the last section is straightforward since all that is needed is substitution of  $\bar{F}_r$ ,  $\bar{F}_z$  into (4.2-6) dropping the explicit time dependence  $e^{-i\omega t}$  and then substituting into (4.1-14). For simplicity expressions will be evaluated for  $r=r_0=0$ . Since only the zeroth order term in the cylindrical harmonic expansion is being considered  $\bar{F}_r$  and  $\bar{F}_z$  simplify considerably. Thus from (4.2-2)

$$\bar{F}_r = \delta(z-z_0) \left\{ \frac{m_r}{k} \frac{\partial}{\partial r} (J_0(kr)) \right\}_{\substack{r=r_0 \\ \theta=\theta_0}} \quad (4.2-7)$$

and

$$\bar{F}_z = \delta(z-z_0) \left\{ m_z J_0(kr) \right\}_{\substack{r=r_0 \\ \theta=\theta_0}}$$

Then substitution of (4.2-7) into (4.2-6) results in

$$\rho \bar{f}_r = e^{i\omega t} \left\{ \frac{\partial}{\partial \eta_1} \left[ \delta(z-z_0) \frac{m_r}{\kappa} \frac{\partial}{\partial r} (J_0(\kappa r)) \right] \right\}_{\substack{r=r_0 \\ \theta=\theta_0}} + n_z \frac{\partial}{\partial z_0} \left[ \delta(z-z_0) \frac{m_r}{\kappa} \frac{\partial}{\partial r} (J_0(\kappa r)) \right]_{\substack{r=r_0 \\ \theta=\theta_0}} \quad (4.2-8)$$

and

$$\rho \bar{f}_z = e^{i\omega t} \left\{ \frac{\partial}{\partial \eta_1} \left[ m_z J_0(\kappa r) \delta(z-z_0) \right] \right\}_{\substack{r=r_0 \\ \theta=\theta_0}} + n_z \frac{\partial}{\partial z_0} \left[ m_z J_0(\kappa r) \delta(z-z_0) \right]_{\substack{r=r_0 \\ \theta=\theta_0}} \}$$

The following facts are then used to simplify the expressions in (4.2-8):

$$\begin{aligned}
(1) \quad J_0(kr) \Big|_{\substack{r=r_0=0 \\ \theta=\theta_0}} &= 1 \\
(2) \quad J_0'(kr) \Big|_{\substack{r=r_0=0 \\ \theta=\theta_0}} &= 0 \\
(3) \quad \frac{\partial \bar{F}_r}{\partial r_0} &= -\frac{1}{2} K m_r \delta(z-z_0) \quad \text{and} \quad \frac{1}{r} \frac{\partial \bar{F}_r}{\partial \theta_0} = -\frac{1}{2} K m_\theta \delta(z-z_0)
\end{aligned}
\tag{4.2-9}$$

This results in

$$\begin{aligned}
\rho \bar{f}_r &= -\frac{1}{2} K (n_r m_r + n_\theta m_\theta) \delta(z-z_0) \\
\rho \bar{f}_z &= -m_z n_z \delta'(z-z_0)
\end{aligned}
\tag{4.2-10}$$

where: 1) the explicit harmonic time dependence has been removed;

2) " / " indicates differentiation with respect to the argument

of the delta function;

3)  $n_r$  ,  $n_\theta$  ,  $n_z$  define direction of the couple;

4)  $m_r$  ,  $m_\theta$  ,  $m_z$  define direction of the force;

Insertion of (4.2-10) into the source term in equation (4.1-14) yields

$$\rho \underline{F} = \begin{pmatrix} 0 \\ 0 \\ \frac{1}{2} \kappa (n_r m_r + n_\theta m_\theta) \delta(z-z_0) \\ -i m_z n_z \delta'(z-z_0) \end{pmatrix} \quad (4.2-11)$$

Addition of three orthogonal couples together produces an explosion source given by

$$\rho \underline{F} = \begin{pmatrix} 0 \\ 0 \\ k p \delta(z-z_0) \\ -i \delta'(z-z_0) \end{pmatrix} \quad (4.2-12)$$

where  $k=wp$ . It is equation (4.2-12) which will be used as a source in all seismogram calculations in Chapter V.



### Section 3. Solution of the Homogeneous System Using Airy Functions

Consider the homogeneous differential system obtained by dropping the force term in (4.1-14)

$$\frac{d\bar{V}'}{dz} = -i\omega [A'] \bar{V}' \quad (4.3-1)$$

A fundamental matrix satisfies (4.3-1) (Gilbert & Backus 1966), i.e.

$$\frac{d[H]}{dz} = -i\omega [A'] [H] \quad (4.3-2)$$

In order to solve for the fundamental matrix  $[H]$  it is instructive and useful to use the asymptotic formalism developed by Wasow (1965), Chapman (1974b), and Woodhouse (1977)

First recall that

$$[A'] = \begin{pmatrix} 0 & p & 1/L & 0 \\ \frac{F_p}{C} & 0 & 0 & 1/C \\ p - (A - F/C)p & 0 & 0 & F_p/C \\ 0 & p & p & 0 \end{pmatrix} \quad (4.3-3)$$

So that algebraic calculations may be later simplified let

$$z = p \text{ (no relation to depth variable } z)$$

(4.3-4)

$$w = 1/L$$

$$Y = pF/C$$

$$t = 1/C$$

$$x = p - (A - F^2/C)p$$

It is easiest to describe the complicated set of calculations which follow in a manner analogous to a cooking recipe.

Step 1: Find a Block Diagonal Transformation for (4.3-2).

It is desired to find a transformation which puts the matrix  $[A]$  in (4.3-2) in block diagonal form. The

eigenvalues of each block will be the square of the eigenvalues in the original matrix  $[A]$  (Woodhouse 1977, personal communication). The original eigenvalues of  $[A]$  are the up and downgoing vertical wave numbers. Thus for some matrix  $[R] = (r_1, r_2, r_3, r_4)$  let

$$[A][R] = [R] \left( \begin{array}{cc|cc} 0 & 1 & & 0 \\ n_x^2 & 0 & & \\ \hline & 0 & 0 & 1 \\ & & n_\beta^2 & 0 \end{array} \right)$$

(4.3-5)

or

$$\begin{aligned} [A]r_1 &= n_x^2 r_2 & [A]r_3 &= n_\beta^2 r_4 \\ [A]r_2 &= r_1 & [A]r_4 &= r_3 \end{aligned}$$

From (4.3 - 5), it is seen that  $[R]^{-1}[A][R] = \text{Required Block Diagonal Matrix}$

To find  $[R]$  it is requisite that the eigenvectors of the matrix  $[A]^2$  be found. The matrix  $[A]^2$  is

$$[A]^2 = \begin{pmatrix} wx+yz & 0 & 0 & tz+wy \\ 0 & yz+pt & tz+wy & 0 \\ 0 & py+zx & xw+yz & 0 \\ py+zx & 0 & 0 & pt+yz \end{pmatrix} \quad (4.3-6)$$

The eigenvalues of (4.3-6) are  $n_\alpha^2$  and  $n_\beta^2$  (represented from here as  $\alpha^2$  and  $\beta^2$ ), the vertical wave numbers squared for quasi-compressional and quasi-shear waves. The eigenvector matrix  $[R]$  is

$$[R] = \begin{pmatrix} \hat{e}_\alpha(ptw - tz^2 - wLA_2) & 0 & 0 & -\hat{e}_\beta(tz + wy) \\ 0 & -\hat{e}_\alpha(tz + wy) & \hat{e}_\beta(twx - tLB_2 - wy^2) & 0 \\ 0 & \hat{e}_\alpha(pt + yz - LA_2) & \hat{e}_\beta(-txz + yz^2 - yLB_2) & 0 \\ \hat{e}_\alpha(-pwy + yz^2 - zLA_2) & 0 & 0 & \hat{e}_\beta(wx + yz - LB_2) \end{pmatrix} \quad (4.3-7)$$

and its inverse is

$$[R]^{-1} = \begin{pmatrix} \hat{E}_x(\rho t + yz - LAz) & 0 & 0 & -\hat{E}_x(tz + wy) \\ 0 & \hat{E}_x(-\rho wy + yz^2 - LAz) & \hat{E}_x(\rho tw - tz^2 - wLAz) & 0 \\ 0 & \hat{E}_p(wx + yz - LBz) & -\hat{E}_p(tz + wy) & 0 \\ \hat{E}_p(-txz + yz - yLBz) & 0 & 0 & -\hat{E}_p(twx - tLBz - wy^2) \end{pmatrix}$$

(4.3-8)

The normalization factors have been chosen to satisfy energy flux conditions, which will be described later.

So, step 1 is completed, since the required transformation has been found. Application of the transformation  $[H] = [R][H']$  results in (4.3-2) becoming

$$\frac{d[R][H']}{dz} = -i\omega[A'][R][H'] \quad (4.3-9)$$

or

$$\frac{d[H']}{dz} = -i\omega \left\{ [R]^{-1} [A'] [R] - [R]^{-1} \frac{d[R]}{dz} [H'] \right\} \quad (4.3-10)$$

The reason for the second term is that the parameters of density and stiffness do depend on the depth. Therefore  $\frac{d[R]}{dz} \neq 0$ . Note, however, that if high frequencies are considered, the first term on the right hand side of (4.3-10) is dominant. Hence, (4.3-10) is an asymptotic expansion and can be written as

$$\frac{d[H']}{dz} = s \sum_{j=0}^1 \frac{[M'_j]}{s^j} [H'] \quad (4.3-11)$$

where  $s = -i\omega$

$$\text{and } [M'_0] = [R]^{-1} [A] [R] = \left( \begin{array}{cc|cc} 0 & 1 & 0 & 0 \\ LA2 & 0 & 0 & 0 \\ \hline 0 & 0 & 0 & 1 \\ 0 & 0 & LB2 & 0 \end{array} \right)$$

and

$$[M'_1] = [R]^{-1} \frac{d[R]}{dz}$$

Step 2: Find a Block Diagonal Transformation for all orders in (4.3-11)

In order to implement this step, it is important to realize that  $[R]^{-1} \frac{d[R]}{dz}$  has the same form as  $[R]$ . This transformation allows separation of the block diagonal components from the non block diagonal components of  $[R]^{-1} \frac{d[R]}{dz}$ . Following Chapman (1974b) a transformation is constructed such that

$$[H'] = [B][H^2] \quad (4.3-12)$$

with the conditions that

$$(1) \quad \frac{d[H^2]}{dz} = s \sum_{k=0}^{\infty} \frac{[M_k^2]}{s^k} [H^2]$$

$$(2) \quad [B] = \sum_{l=0}^{\infty} s^{-l} [B]_l$$

Now to first order in  $s$ , substitution of (4.3-12) into (4.3-11) gives

$$\frac{d[B]}{dz} [H^2] + [B] \frac{d[H^2]}{dz} = s \sum_{j=0}^1 \frac{[M_j^2]}{s} ([B][H^2]) \quad (4.3-13)$$

Substitution of conditions (1) and (2) into (4.3-13), taking only powers up to  $s^{-1}$  yields



$$\begin{aligned}
& \left( \frac{d[B_0]}{dz} + \frac{1}{S} \frac{d[B_1]}{dz} \right) [H^2] + \left( [B_0] + \frac{[B_1]}{S} \right) (s[M_0^2] + [M_1^2]) [H^2] \\
& = (s[M_0^2] + [M_1^2]) \left( [B_0] + \frac{[B_1]}{S} \right) [H^2]
\end{aligned}
\tag{4.3-14}$$

Consideration of coefficients of  $s$  and  $1$  in (4.3-14)

requires that:

$$a) \quad [B_0][M_0^2] = [M_0^2][B_0]$$

and

(4.3-15)

$$b) \quad \frac{d[B_0]}{dz} + [B_0][M_1^2] + [B_1][M_0^2] = [M_0^2][B_1] + [M_1^2][B_0]$$

From a) it is evident that

$$[B_0] = I \quad \text{and} \quad [M_0^2] = [M_0^1]$$

and from b)

$$[M_1^2] = [M_1^1] + [M_0^2][B_1] - [B_1][M_0^2]$$

Now the structures of the above matrices are known, and

equations such as

$$[M_i'] = [M_i] + [M_0'] [B_i] - [B_i] [M_0']$$

(4.3-16)

can be solved recursively (Wasow 1965). In particular

$$[M_0'] = \left( \begin{array}{cc|cc} 0 & 1 & & \\ LA2 & 0 & & \\ \hline & & 0 & 1 \\ & & LB2 & 0 \end{array} \right)$$

$$[M_i'] = [R]^{-1} \frac{d[R]}{dz} = \left( \begin{array}{cc|cc} g_{11} & 0 & 0 & g_{14} \\ 0 & g_{22} & g_{23} & 0 \\ \hline 0 & g_{32} & g_{33} & 0 \\ g_{41} & 0 & 0 & g_{44} \end{array} \right)$$

where  $g_{ij}$  is the  $ij$ th element of the matrix

As Wasow (1965) and Chapman (1974b) point out, the matrices have an "anti" block-diagonal structure so that recurrence formulae may be used to calculate the elements. The salient features of the above calculation are that

$$[M_i^2] = \left( \begin{array}{cc|cc} g_{11} & 0 & 0 & 0 \\ 0 & g_{22} & 0 & 0 \\ \hline 0 & 0 & g_{33} & 0 \\ 0 & 0 & 0 & g_{44} \end{array} \right) \quad (4.3-17)$$

and that the trace of the blocks is zero, i.e.,

$g_{11} + g_{22} = 0$  and  $g_{33} + g_{44} = 0$ . The first terms in the transformation have now been found, and the system (4.3-11) may be written as

$$\frac{d[H^2]}{dz} = S \sum_{k=0}^{\infty} \frac{[M_k^2]}{S^k} [H^2] \quad (4.3-18)$$

where the main concern is with the first two terms in (4.3-18). Since the  $[M_k^2]$  are all block diagonal, the fourth order system in (4.3-18) decouples into two first order systems. Symbolically this decoupling is written as

$$[M^2] = [M^{\omega}] \oplus [M^{2\beta}]$$

where  $\oplus$  denotes the direct sum. In the system under consideration

$$[M_o^{\alpha}] = \begin{pmatrix} 0 & 1 \\ LA2 & 0 \end{pmatrix} \quad [M_o^{\beta}] = \begin{pmatrix} 0 & 1 \\ LB2 & 0 \end{pmatrix} \quad (4.3-19)$$

Step 3: Convert each of the decoupled 2 by 2 systems into the Airy Equation and solve using Hankel Functions

The calculations outlined below will be done for only one of the two by two systems, the quasi-compressional one. Consideration of the first two terms in the asymptotic series on the right hand side of (4.3-18) yields the desired 2 by 2 system of differential equations:

$$\frac{d[H^{\alpha}]}{dz} = s \sum_{k=0}^1 \frac{[M^{\alpha}]_k}{s^k} [H^{\alpha}] \quad (4.3-20)$$

where the superscript  $\alpha$  indicates that the  $2 \times 2$  system corresponding to quasi-compressional waves is considered and

$$[M_0^{2\alpha}] = \begin{pmatrix} 0 & 1 \\ LA2 & 0 \end{pmatrix} \quad [M_1^{2\alpha}] = \begin{pmatrix} g_{11} & 0 \\ 0 & g_{22} \end{pmatrix} \quad (4.3-21)$$

To convert (4.3-20) into an Airy equation let

$$[H^{2\alpha}] = [C][H^{2\alpha}] \quad (4.3-22)$$

$$\text{and let } h = \left[ \frac{3}{2} \int_{z_\alpha}^z \omega n_\alpha(\xi, p) d\xi \right]^{2/3}$$

where

$w$  = angular frequency

$n_\alpha = \sqrt{LA2} = \text{vertical wave number}$

$z_\alpha = \text{turning point } (n_\alpha(z_\alpha, p) = 0)$

$z = \text{level at which solution is considered}$

Substitution of the above transformation into (4.3-20)

results in

$$\begin{aligned} \frac{d[H^{3\alpha}]}{dh} &= \left(\frac{dh}{dz}\right)^{-1} s \left[ [C]^{-1} [M_o^{3\alpha}] [C] \right] [H^{3\alpha}] \\ &\quad - [C]^{-1} \frac{d[C]}{dh} [H^{3\alpha}] + \left(\frac{dh}{dz}\right)^{-1} \left[ [C]^{-1} [M_i^{3\alpha}] [C] \right] [H^{3\alpha}] \end{aligned} \quad (4.3-23)$$

or

$$\frac{d[H^{3\alpha}]}{dh} = s [M_o^{3\alpha}] [H^{3\alpha}] + [M_i^{3\alpha}] [H^{3\alpha}] \quad (4.3-24)$$

with

$$[M_o^{3\alpha}] = \left(\frac{dh}{dz}\right)^{-1} [C]^{-1} [M_o^{3\alpha}] [C]$$

and

$$[M_i^{3\alpha}] = \left(\frac{dh}{dz}\right)^{-1} [C]^{-1} [M_i^{3\alpha}] [C] - [C]^{-1} \frac{d[C]}{dh}$$

In order to evaluate the right hand side of (4.3-24), the expressions for  $[C]$  and  $\left(\frac{dh}{dz}\right)^{-1}$  must be determined.  $[C]$  is chosen so that the first term on the right hand side of (4.3-24) is  $\begin{pmatrix} 0 & 1 \\ h & 0 \end{pmatrix} [H^{3\alpha}]$ , and  $\left(\frac{dh}{dz}\right)^{-1}$  can be evaluated from the expression for  $h$  (see 4.3-22). Then,

$$\frac{dh}{dz} = \omega^{-1} n_{\alpha}^{-1} h'^{1/2} \quad (4.3-25a)$$

and

$$[c] = \begin{pmatrix} 1 & 0 \\ 0 & n_{\alpha} h'^{1/2} \end{pmatrix} = \begin{pmatrix} 1 & 0 \\ 0 & h'/\omega \end{pmatrix} \quad (4.3-25b)$$

where

$$h' = \frac{dh}{dz}$$

$n_{\alpha}$  = vertical wave number

$\omega$  = angular frequency

Insertion of the above two expressions into (4.3-24) results in

$$\frac{d[H^*]}{dz} = -i \begin{pmatrix} 0 & 1 \\ h & 0 \end{pmatrix} [H^*] + \begin{pmatrix} (h')^{-1}g & 0 \\ 0 & (h')^{-1}g - \left(\frac{h'}{w}\right)^{-1} \frac{d}{dh} \left(\frac{h'}{w}\right) \end{pmatrix} \quad (4.3-26)$$

From (4.3-26) it is clear that the first matrix is the coefficient of  $w^0$  in an asymptotic expansion and the second matrix on the right hand side has powers of  $w$  in it from the  $(h')^{-1}$  terms. Therefore a further transformation may be used (Wasow 1965; Chapman 1974b) to solve (4.3-26). It is given as

$$[H^*] = \sum_{K=0}^{\infty} \frac{[D_K^*] h}{s^{-K}} [H^*] \quad (4.3-27)$$

and  $[H^{4\alpha}]$  satisfies the equation

$$\frac{d[H^{4\alpha}]}{dz} = -i \begin{pmatrix} 0 & 1 \\ h & 0 \end{pmatrix} [H^{4\alpha}] \quad (4.3-28)$$

with the  $[D_K^\alpha]$  obtained by substitution of (4.3-27) into (4.3-26). Again a set of recurrence relations is the outcome. These are:



$$[M_0^{\alpha}][D_k^{\alpha}] - [D_k^{\alpha}][M_0^{\alpha}] = [E_k^{\alpha}] \quad (4.3-29)$$

with

$$\begin{aligned} [E_k^{\alpha}] &= 0 \quad \text{when } k=0 \\ &= [D_{k-1}^{\alpha}]' - \sum_{j=1}^k [M_j^{\alpha}][D_{k-j}^{\alpha}] \end{aligned}$$

Wasow shows that a system such as (4.3-29) has a solution if and only if

$$\text{tr}[E_k^{\alpha}] = 0 \quad \text{and} \quad \text{tr}([E_k^{\alpha}][M_0^{\alpha}]) = 0 \quad (4.3-30)$$

Such being the case, relations (4.3-30) can be used to find the required  $[D_k^{\alpha}]$ . The principal concern here is to obtain  $[D_0^{\alpha}]$ , the first term in the transformation (4.3-27). As can be seen from (4.3-29), since  $[E_0^{\alpha}] = 0$ , the most general solution of  $[D_0^{\alpha}]$  is

$$[D_0^{\alpha}] = g_1(h)I + g_2(h)[M_0^{\alpha}] \quad (4.3-31)$$

To determine  $g_1$  and  $g_2$ , the trace relations (4.3-30) are used for  $[E_1^{\alpha}]$ . First, it is necessary to calculate  $[E_1^{\alpha}]$ , which is done from the equation

$$[E_i] = [D_o^\alpha]' - [M_i^\alpha][D_o^\alpha] \quad (4.3-32)$$

Substitution of  $[M_i^{\beta\alpha}]$ ,  $[D_o^\alpha]$ , and  $[D_o^\alpha]'$  into (4.3-32) and use of (4.3-26) results in

$$[E_i^\alpha] = \begin{pmatrix} g_1' & g_2' \\ hg_2' + g_2 & g_1' \end{pmatrix} - \begin{pmatrix} (h')^{-1} g_{11} g_1 & (h')^{-1} g_{11} g_2 \\ hg_2 \left\{ g_{22} (h')^{-1} - \left( \frac{h'}{\omega} \right)^{-1} \frac{d}{dh} \left( \frac{h'}{\omega} \right) \right\} & g_1 \left\{ (h')^{-1} g_{22} - \left( \frac{h'}{\omega} \right)^{-1} \frac{d}{dh} \left( \frac{h'}{\omega} \right) \right\} \end{pmatrix}$$

(4.3-33)

Taking the trace of  $[E_i^\alpha]$  and setting it equal to zero yields

$$g_1' - (h')^{-1} g_{11} g_1 + g_1' - (h')^{-1} g_{11} g_1 + g_1 \left( \frac{h'}{\omega} \right)^{-1} \frac{d}{dh} \left( \frac{h'}{\omega} \right) = 0$$

or

$$\frac{2g_1'}{g_1} = -\left(\frac{h'}{w}\right) \alpha \left(\frac{h'}{w}\right) \quad (4.3-34)$$

which has the solution (assuming  $(h(z)) = 1$ )

$$g_1 = \frac{\sqrt{(h'/w)_{z=z_\alpha}}}{\sqrt{(h'/w)}} \quad (4.3-35)$$

or

$$g = \frac{\sqrt{n_\alpha(\rho, z_\alpha) h^{-1/2}(z_\alpha)}}{\sqrt{n_\alpha(\rho, z) h^{-1/2}(z)}} = e_1 n_\alpha^{1/2} h^{1/4}(z)$$

where

$$e_1 = \sqrt{n_\alpha(z_\alpha) h^{-1/2}(z_\alpha)}$$

An identical analysis shows that  $g_2$  in (4.3-31) must be zero in order that  $[D_0^\alpha]$  be regular at  $z=z_\alpha$ , the turning point.

Therefore

$$[D_0^\alpha] = e_1 n_\alpha^{-1/2} h^{1/4}(z) \begin{pmatrix} 1 & 0 \\ 0 & 1 \end{pmatrix} \quad (4.3-36)$$

What is left now is the solution of (4.3-28).

Step 4: The solution of Equation (4.3-28).

In order to solve equation (4.3-28) consider first a column of  $[H^{4\alpha}]$ . Call it  $\underline{y}$ . Then (4.3-28) becomes

$$\frac{d\underline{y}}{dh} = -i \begin{pmatrix} 0 & 1 \\ h & 0 \end{pmatrix} \underline{y} \quad \text{where } \underline{y} = \begin{pmatrix} y_1 \\ y_2 \end{pmatrix} \quad (4.3-37)$$

From (4.3-37) it is observed that

$$\frac{d^2 y_1}{dh^2} = -i \frac{dy_2}{dh} = -h y_1(h) \quad (4.3-38)$$

Equation (4.3-38) has the solution

$$y_1 = h^{1/2} \left( c_1 f_1 \left( \frac{2}{3} h^{3/2} \right) + c_2 f_2 \left( \frac{2}{3} h^{3/2} \right) \right)$$

where  $f_1$  and  $f_2$  are Hankel functions of the  $1/3$  order and first and second kind respectively. The constants  $C_1$  and  $C_2$  may be arbitrarily chosen and, hence  $C_1$  and  $C_2$  will be picked to be a phase factor times other constants which will be absorbed as the calculation proceeds. Therefore

$$y_1 = h^{1/2} (c_1 H_{1/3}'(\frac{2}{3} h^{3/2}) + c_2 H_{1/3}^2(\frac{2}{3} h^{3/2})) \quad (4.3-39)$$

To find the other independent solutions, the differential equation and the properties of the Hankel functions are used. Thus

$$\begin{aligned} y_1'(h) = & \frac{1}{2} h^{-1/2} c_1 H_{1/3}' + c_1 h H_{1/3}' \\ & + \frac{1}{2} h^{-1/2} c_2 H_{1/3}^2 + c_2 h H_{1/3}^2' \end{aligned} \quad (4.3-40)$$

Application of formulas in (4.1-27) in Abramowitz and Stegun (1965) for derivatives of the Hankel functions e.g.

$$H_m'(u) = H_{m-1}'(u) - \frac{m}{u} H_m'(u)$$

And of the identity

$$H_{-1/3}' = e^{2\pi i/3} H_{2/3}'$$

to (4.3-40) results in

$$y_1'(h) = (c_1 h H_{2/3}^1 e^{2\pi i/3} + c_2 h H_{2/3}^2 e^{-2\pi i/3})$$

Choice of  $c_1 = e^{5\pi i/12}$  and  $c_2 = e^{-5\pi i/12}$  together with the relation  $y_2 = i y_1'$  yields

$$y_2 = h(-e^{7\pi i/12} H_{2/3}^1 + e^{-7\pi i/12} H_{2/3}^2)$$

Therefore the columns of  $[H^{4\alpha}]$  are

$$[H^{4\alpha}] = h^{1/2} \begin{pmatrix} e^{5\pi i/12} H_{1/3}^1 & e^{-5\pi i/12} H_{1/3}^2 \\ -e^{7\pi i/12} H_{2/3}^1 h^{1/2} & e^{-7\pi i/12} H_{2/3}^2 h^{1/2} \end{pmatrix} \quad (4.3-41)$$

Step 5: Complete solution of the decoupled 2x2 and 4x4 systems

The complete solution of the 2x2 system for quasi-compressional waves is obtained by multiplying all the

transformations and the solution (4.3-41) together. Therefore  $[H^{2\alpha}] = [C][D_0^\alpha][H^{4\alpha}]$ , or combining results of equations (4.3-25) (b), (4.3-36) and (4.3-41), the fundamental matrix solution of the 2x2 system is

$$\begin{aligned}
 [H^{2\alpha}] &= \begin{pmatrix} 1 & 0 \\ 0 & n_\alpha h^{-1/2} \end{pmatrix} \cdot e_1 n_\alpha h^{1/4} \begin{pmatrix} 1 & 0 \\ 0 & 1 \end{pmatrix} [H^{4\alpha}] \\
 &= e_1 n_\alpha h^{3/4} \begin{pmatrix} e^{5\pi i/12} H_{1/3}^1 & e^{-5\pi i/12} H_{1/3}^2 \\ -n_\alpha e^{7\pi i/12} H_{2/3}^1 & n_\alpha e^{-7\pi i/12} H_{2/3}^2 \end{pmatrix} \quad (4.3-42)
 \end{aligned}$$

The constant  $e_1$  can be absorbed into the definition of  $C_1$  and  $C_2$  described previously. Also,  $h^{3/4}$  can be written as

$$h^{3/4} = \left[ \frac{3}{2} \int_{z_\alpha}^z \omega n_\alpha d\xi \right]^{2/3 \cdot 3/4} = (\omega Q_\alpha)^{1/2} \left( \frac{3}{2} \right)^{1/2} \quad (4.3-43)$$

where:

$$Q_\alpha = \int_{z_\alpha}^z n_\alpha(\rho, \xi) d\xi$$

where

$\omega$  = angular frequency

Recall also that the argument of the Hankel functions is  $\frac{2}{3} h^{3/2}$  or  $(\omega Q_\alpha)$ . Therefore, the fundamental solution (4.3-42) becomes

$$[H^{2\alpha}] = \frac{1}{\sqrt{2n_\alpha}} \left( \frac{\pi}{2} \omega Q_\alpha \right)^{1/2} \begin{pmatrix} e^{5\pi i/12} H_{1/3}'(\omega Q_\alpha) & e^{-5\pi i/12} H_{1/3}^2(\omega Q_\alpha) \\ -e^{7\pi i/12} n_\alpha H_{2/3}'(\omega Q_\alpha) & e^{-7\pi i/12} H_{2/3}^2(\omega Q_\alpha) n_\alpha \end{pmatrix} \quad (4.3-44)$$

A completely analogous solution exists for the 2x2 system related to quasi-shear waves. That is

$$[H^{2\beta}] = \frac{1}{\sqrt{2n_\beta}} \left( \frac{\pi}{2} \omega Q_\beta \right) \begin{pmatrix} e^{5\pi i/12} H(\omega Q_\beta) & e^{-5\pi i/12} H_{1/3}^2(\omega Q_\beta) \\ -e^{7\pi i/12} n_\beta H_{2/3}'(\omega Q_\beta) & e^{-7\pi i/12} n_\beta H_{2/3}^2(\omega Q_\beta) \end{pmatrix}$$

Thus, the complete solution for the fundamental matrix, using only the first term in the  $[\beta]$  transformation ( $[\beta_0] = I$ , in equation (4.3-12)), is

$$[H] = \underline{R} \cdot \underline{I} \cdot [ [H^{2\alpha}] \oplus [H^{2\beta}] ] \quad (4.3-45)$$

The columns of  $[H]$  are given below  
column 1



$$\frac{\hat{\varepsilon}_\alpha}{\sqrt{2n_\alpha}} \left[ \frac{\pi \omega Q_\alpha}{2} \right]^{1/2} \begin{bmatrix} (\rho t w - t z^2 - \omega L A z) e^{5\pi i/12} H_{1/3}'(\omega Q_\alpha) \\ LA(tz + wy) e^{7\pi i/12} H_{2/3}'(\omega Q_\alpha) \\ -LA(\rho t + yz - LAz) e^{\pi i/12} H_{1/3}'(\omega Q_\alpha) \\ (-\rho wy + yz - zLAz) e^{\pi i/12} H_{4/3}'(\omega Q_\alpha) \end{bmatrix}$$

column 2

$$\frac{\hat{\varepsilon}_\alpha}{\sqrt{2n_\alpha}} \left[ \frac{\pi \omega Q_\alpha}{2} \right]^{1/2} \begin{bmatrix} (\rho t w - t z^2 - \omega L A z) e^{-5\pi i/12} H_{1/3}^2(\omega Q_\alpha) \\ -LA(tz + wy) e^{-7\pi i/12} H_{2/3}^2(\omega Q_\alpha) \\ LA(\rho t + yz - LAz) e^{-\pi i/12} H_{2/3}^2(\omega Q_\alpha) \\ (-\rho wy + yz - zLAz) e^{-5\pi i/12} H_{2/3}^2(\omega Q_\alpha) \end{bmatrix}$$

column 3

$$\frac{\hat{\epsilon}_p}{\sqrt{2n_p}} \left[ \frac{\pi \omega Q_p}{2} \right]^{1/2} \begin{bmatrix} LB(tz+wy) e^{7\pi i/12} H'_{1/3}(\omega Q_p) \\ (twx - tLBz - wy^2) e^{5\pi i/12} H'_{1/3}(\omega Q_p) \\ (-txz + yz - yLBz) e^{5\pi i/12} H'_{1/3}(\omega Q_p) \\ -LB(wx + yz - LBz) e^{7\pi i/12} H'_{1/3}(\omega Q_p) \end{bmatrix}$$

column 4

$$\frac{\hat{\epsilon}_p}{\sqrt{2n_p}} \left[ \frac{\pi \omega Q_p}{2} \right] \begin{bmatrix} -LB(tz+wy) e^{-\pi i/12} H''_{1/3}(\omega Q_p) \\ (twx - tLBz - wy^2) e^{-5\pi i/12} H''_{1/3}(\omega Q_p) \\ (-txz + yz - yLBz) e^{-5\pi i/12} H''_{1/3}(\omega Q_p) \\ (wx + yz - LBz) e^{-7\pi i/12} H''_{1/3}(\omega Q_p) \\ \ast(LB) \end{bmatrix}$$

Asymptotic expansion of the Hankel functions using the relations (4.2-3) and (4.2-4) (Abramowitz & Stegun 1965) allows the fundamental matrix  $[H]$  to be written in a more common form.

$$[H] = [N][\Lambda] \quad (4.3-46)$$

where

$$[\Lambda] = \begin{bmatrix} e^{i\omega Q_d} & & 0 \\ e^{-i\omega Q_d} & & 0 \\ 0 & e^{i\omega Q_p} & \\ 0 & e^{-i\omega Q_p} & \end{bmatrix}$$

and

$$\underline{N} = [\underline{n}_1, \underline{n}_2, \underline{n}_3, \underline{n}_4]$$

with

$$\underline{n}_1 = \epsilon_s \begin{bmatrix} \rho t w - t z^2 - w L A^2 \\ L A (t z + w y) \\ -L A (\rho t + y z - L A^2) \\ -\rho w y + y z^2 - z L A^2 \end{bmatrix}$$

$$\eta_2 = \epsilon_\alpha \begin{bmatrix} \rho t w - t z^2 - w L A^2 \\ -L A (t z + w y) \\ L A (\rho t + y z - L A^2) \\ -\rho w y + y z^2 - z L A^2 \end{bmatrix}$$

$$\eta_3 = \epsilon_\rho \begin{bmatrix} L B (t z + w y) \\ t w x - t L B^2 - w y^2 \\ -t x z + y^2 z - y L B^2 \\ -L B (w x + y z - L B^2) \end{bmatrix}$$

$$\eta_4 = \epsilon_\rho \begin{bmatrix} -L B (t z + w y) \\ t w x - t L B^2 - w y^2 \\ -t x z + y^2 z - y L B^2 \\ L B (w x + y z - L B^2) \end{bmatrix}$$

where  $\epsilon_s = \frac{\hat{\epsilon}_s}{\sqrt{2n_s}}$  and  $\epsilon_p = \frac{\hat{\epsilon}_p}{\sqrt{2n_p}}$

The  $\epsilon$ 's have been chosen as normalizations with respect to unit energy flux (see Chapman 1973 & Biot 1957).

Both forms of the fundamental matrix  $[H]$  and the source vector obtained in Section 2, will be used in the next chapter, in the construction of synthetic seismograms.

## CHAPTER V

### Calculation Of Synthetic Seismograms

#### Introduction

In this final chapter, the basic results of the last three chapters will be incorporated. These results have been obtained with a view to constructing synthetic seismograms in transversely isotropic media. Since the apparatus of ray kinematics has been developed previously, the seismograms will be calculated on that basis.

Chopra (1958) has established the connection between ray theory and saddlepoint methods in elastodynamics. He states that Bromwich was the first to derive a ray series, and since then the correspondence to geometrical optics-reflection and refraction has been well-qualified. But, with the advent of faster computers, more elegant techniques such as Haskell-Thomson propagator matrices, or generalized ray theory have been employed to solve the linear elastodynamic wave equations occurring in seismology. It is interesting to note that developments in synthetic seismology have come full-circle, since the saddlepoint method has again come into vogue, 60 years after Bromwich's work.

The new saddlepoint technique has been called disk ray theory (Wiggins 1976) or the equal phase method (Chapman 1976a). These two approaches were presented simultaneously, and provide a first motion approximation to the motion. Both methods of developing this approximation will be described in the following sections. As well, some seismograms for simple models will be calculated with a view to comparing the results for isotropic and transversely isotropic media.

## Section 1 -Intuitive Development of Disk Ray Theory

Wiggins (1976) has described a method for computing seismograms, based on earlier results (Wiggins and Madrid 1974). The physical basis for computing the seismograms is that the amplitude is proportional to the change in the ray parameter  $p$ . Therefore, given a  $p$ -delta curve for a continuous velocity depth model, the steps to compute the seismogram are:

- 1) Establish the position and time of the geometrical arrival at the receiver position;
- 2) Find the phase arrival times for all rays leaving the source and arriving at the receiver position;  
Rays other than the geometrical ray arrival will be delayed in time with respect to it, a manifestation of Fermat's principle;
- 3) At some time delay relative to the main geometric arrival begin computation of  $dp$  such that one digitization unit of delay time is used up;
- 4) Multiply the  $|dp|$  by a directivity factor, generally dependent on  $p$ ;
- 5) After completing 3 and 4 for the  $p$ -delta curve, convolve the seismogram with an inverse operator which removes the  $1/\sqrt{t}$  behaviour of the seismogram.

The above methodology will now be applied in detail to the transversely isotropic medium.

Consider a suite of rays, leaving the source, as in Fig.5.1. As can be seen, each ray has an associated plane wave front, which is not orthogonal to the ray trajectory.



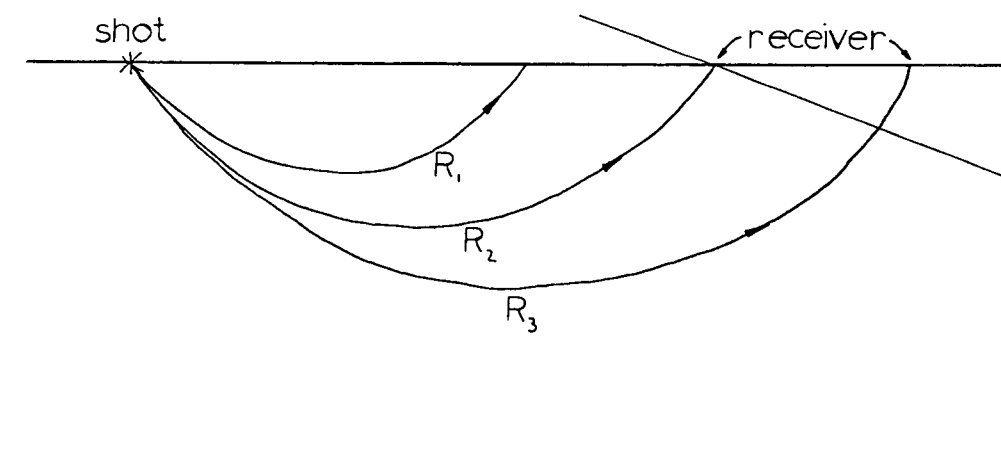


Figure 5.1 - Suite of rays leaving shot

Each of the plane waves (disks) will arrive at the receiver but delayed with respect to the main arrival which is ray 2 in the figure. There may be, however, an objection to using such a ray representation, as both Lighthill (1960) and Crampin (1977) point out. The thesis of their argument,

which is correct, is that in anisotropic media a plane wave front cannot propagate, since energy must be supplied parallel to the wavefront. But, since the source under consideration is a point source, energy is supplied in all directions, as shown in chapter IV. Further evidence for the validity of plane wave models has been provided by the work of Staudt and Cook (1967) (see Fig.5.2). An emitting transducer placed beside a quartz crystal has been used to generate plane wave fronts, which are the vertical lines in the picture. The direction of energy flow, the ray direction, is indicated by the white band in the figure, which is at 45 degrees to the plane wave fronts. The white band is indicative of the direction of energy flow, since this flow affects the optical parameter  $\epsilon$ , which affects the light scattered by the crystal. From the figure, it is clear that energy has been supplied parallel to the wavefront. This energy parallel to the wavefront arises from the fact that there are edge effects from the emitting transducer, i.e. a plane wave is a purely mathematical generalization, albeit a useful one.

Having established the validity of the disk superposition model, it is necessary to find the phase delay time for all disks arriving at the receiver. A simple geometrical argument is illustrated below. From Chapter 3, the arrival time of the disk associated with ray R is

$p_3 X_{R_3} + \tau(p_3)$ . This disk intersects the point  $X_{R_2}$ , the

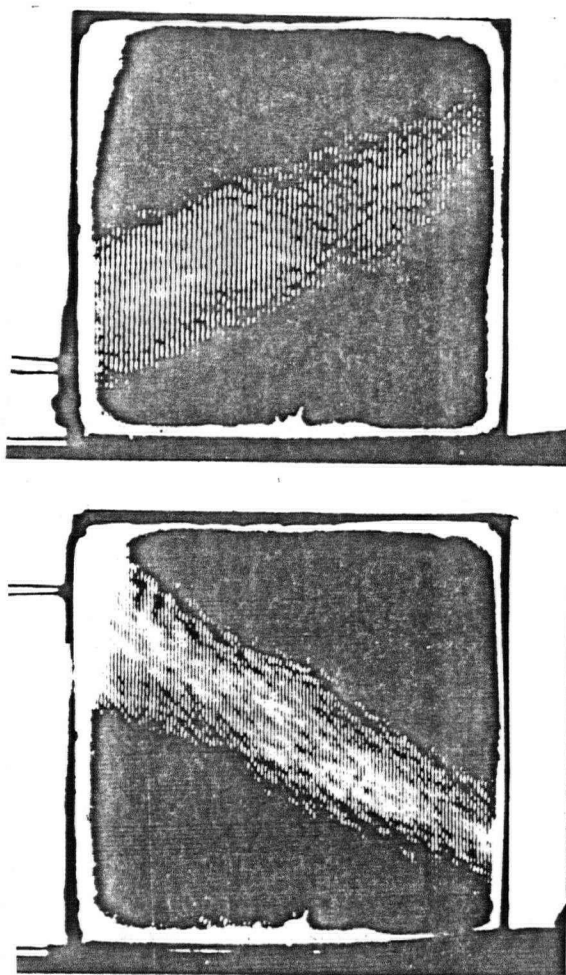


Figure 5.2 - Acoustic plane waves in a quartz crystal (After Staudt and Cook 1967)

geometrical ray arrival distance at some time earlier than

$p_3 x_{R_3} + \tau(p_3)$ . Therefore, time must be subtracted from

$p_3 x_{R_3} + \tau(p_3)$ . This time is given by

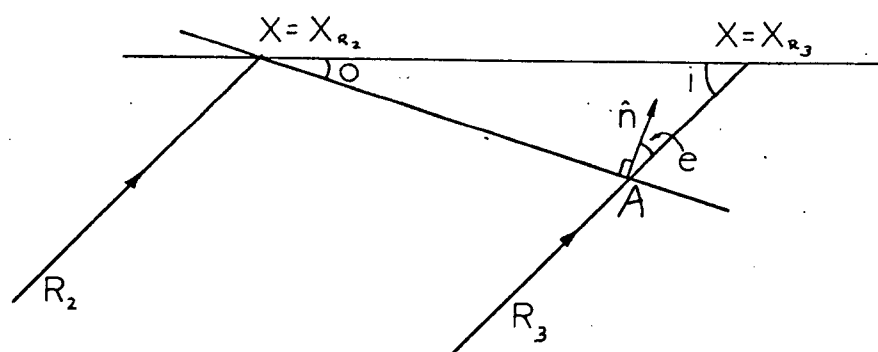


Figure 5.3 - Disk intercepting surface in anisotropic medium

$$\Delta t = \frac{\overline{Ax_{R_3}}}{V_r} \quad (5.1-1)$$

where  $V_r$  = ray velocity

$\overline{AX}_{R_3}$  = distance from the node A to the position

By the law of sines

$$\frac{(X_{R_3} - X_{R_2})}{\sin(\pi/2 + e)} = \frac{\overline{AX}_{R_3}}{\sin(\pi - (\pi/2 + i + e))} \quad (5.1-2)$$

$$\text{or } \overline{AX}_{R_3} = \frac{\sin(\pi/2 - (i + e))(X_3 - X_{R_2})}{\cos e}$$

The time to be subtracted is calculated as

$$\Delta t = \frac{\overline{AX}_{R_3}}{V_r} = \frac{\sin(\pi/2 - (i + e))(X_3 - X_{R_2})}{V_r \cos e} \quad (5.1-3)$$

But  $V_r \cos e = V_p$ , the phase velocity, and

$\sin(\pi/2 - (i + e)) = \cos(i + e)$ . Therefore

$$\Delta t = \frac{\cos(i + e)}{V_p} \cdot (X_{R_3} - X_{R_2}) \quad (5.1-4)$$

From the wave surface-slowness surface construction of Chapter 2,  $\frac{\cos(i + e)}{V_p} = \rho_3$ , the ray parameter of ray  $R_3$ . Thus, the arrival time of the disk associated with ray  $R_3$  at  $X = X_{R_2}$  is

or

$$p_3 X_{R_3} + \tau(p_3) - p_3 (X_{R_3} - X_{R_2})$$

$$t = p_3 X_{R_2} + \tau(p_3)$$

(5.1-5)

Equation (5.1-5), identical to that obtained in the isotropic situation, is used to calculate the  $|dp|$  associated with the phase delay (Fig 5.4).

Application of equation (5.1-5) to the simple p-delta curve in Fig.5.4 demonstrates that the required phase delay of ray  $R_3$ , with respect to the geometrical ray  $R_2$ , is

$$pd = p_3 X_{R_2} + \tau(p_3) - p_2 X_{R_2} - \tau(p_2) \quad (5.1-6)$$

where p.d. is the phase delay.

In Fig. 5.4 p.d. is the area of the triangle OUS. If the slope of the p-delta curve is  $s$ , then

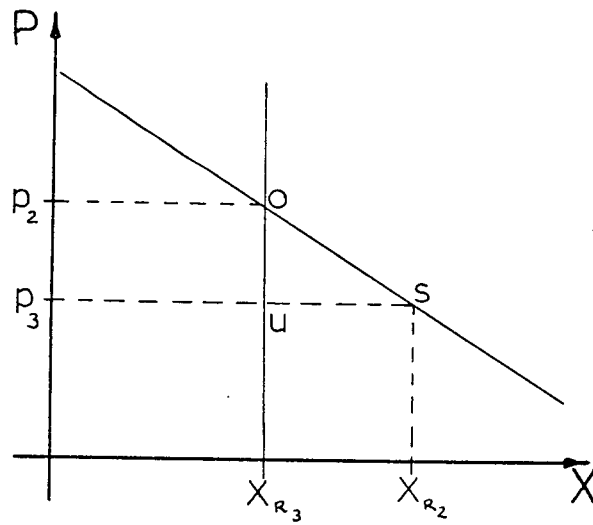


Figure 5.4 - Simple  $p$ -delta curve

(5.1-7)

$$pd = \frac{.5 * (p_3 - p_2)^2}{S}$$

$$\delta p = (2S \delta t)^{1/2}$$

where  $dp = 1-p$

$dt = p.d.$

$S$  = slope of P-Xcurve curve.

As Wiggins points out, the amplitude is given by

$$F(p_2) |\delta p| \quad (5.1-8)$$

where  $F(p_2)$  = directivity at the point  $p=p_2$ .

To construct the seismogram then, it is necessary to compute the amount of  $\delta p$  for the phase delays of  $n \delta t$  where  $n$  is an integer and  $\delta t$  is the digitization interval. For the  $n$ th position in the seismogram, application of equation (5.1-7) gives

$$\delta p_n \propto (S \delta t)^{1/2} (\sqrt{n} - \sqrt{n-1}) \quad (5.1-9)$$

where  $n$  is the integer timing index relative to the main arrival. There are two important points to note about (5.1-9). First, the amplitude is given as



$$A_n = F(\rho_n) |\delta \rho_n| \quad (5.1-10)$$

Second, the seismogram will have a shape like  $t^{-1/2}$  since  $\sqrt{n} - \sqrt{n-1}$  is a finite-difference representation of the derivative of  $t^{-1/2}$ . Therefore after the calculation of all  $A_n$ 's has been completed, the seismogram must be convolved with an inverse operator which removes the  $t^{-1/2}$  dependence. The necessity of such an operator will be proved in Section 3. It is important to note that for computational purposes, Wiggins (1976), has given a 3-point recursion formula for the operator.

## Section 2 The equal phase method JWKB Reflection Coefficient

In the preceding section, an intuitive approach to the first motion approximation in transversely isotropic media was presented. Here, an alternative representation is developed, using the fundamental matrix solutions obtained in chapter IV.

To begin with a solution of the homogeneous system of equations, Equation (4.1-14) must be made valid at the turning point. In order to do this, the method of Chapman (1977a) will be used. In the case of "compressional" waves propagating, the coefficients representing the up and downgoing components must be chosen in a special way. That is, the solution to the homogeneous system,

$$\underline{V} = [H] \begin{pmatrix} ce^{i\alpha} \\ ce^{-i\alpha} \\ 0 \\ 0 \end{pmatrix} \quad (5.2-1)$$

where  $\underline{V}$  = solution vector

$[H]$  = fundamental matrix (H) (4.3-45)

$C$  = amplitude of up and downgoing p-waves

must obey the radiation condition that

$$\lim_{z \rightarrow -\infty} \underline{V}(z) \rightarrow 0$$

The choice of  $z \rightarrow -\infty$  instead of the usual  $+\infty$  is achieved by changing co-ordinates, so that the reference point is the

turning point of the ray. So the object of the exercise is to find the value of  $c$  in (5.2-1). Prior to this, however, some preliminary analysis needs to be done on the representation of the Hankel functions appearing in  $[H]$ .

From Abramowitz and Stegun (1965)

$$H_{1/3}^{(2)}(\xi) = e^{-i\pi/6} \sqrt{\frac{3}{u}} \left( A_i(-u) + i B_i(-u) \right) \quad (5.2-2)$$

where

$$\begin{aligned} \xi &= \omega Q_\alpha \\ u &= \left( \frac{2}{3} \omega Q_\alpha \right)^{2/3} \\ Q_\alpha &= \int_{z_\alpha}^z n_\alpha(p, \xi) d\xi \end{aligned}$$

Below the turning point  $u$  is negative. Therefore,  $-u$  is positive, and since  $B_i(-u) \sim e^{(-u)^{3/2}}$ , for large values of  $(-u)$ , it is required that the quantities in (5.2-1) be chosen so that the  $B_i$ 's do not appear in the final solution for  $\underline{V}$ . This is further illustrated below.

Consideration of the first component of  $\underline{V}$  will be sufficient to calculate  $\alpha$ . Substitution of the fundamental matrix values into (5.2-1) results in the first component of  $\underline{V}$  being calculated as

$$v_1 = bc \left[ e^{5\pi i/2} e^{i\alpha} H_{1/3}^1(\omega Q_\alpha) + e^{-5\pi i/2} e^{-i\alpha} H_{1/3}^2(\omega Q_\alpha) \right] \quad (5.2-3)$$

where

$$b = \frac{\hat{E}_\alpha}{\sqrt{2n_\alpha}} \left[ \frac{\pi \omega Q_\alpha}{2} \right]^{1/2} (\rho T \omega - T z^2 - \omega L A 2)$$

Insertion of asymptotic forms of the Hankel functions, into (5.2-3), neglecting the  $Ai(-u)$  which are bounded results in

$$v_1 \sim bc \left[ e^{-(\pi/6 - \alpha - 5\pi/12)i} Bi(-u) + i e^{(\pi/6 - \alpha - 5\pi/12)i} Bi(-u) \right] \quad (5.2-4)$$

In order that the term in the brackets vanish, it is required that

$$\begin{aligned} -\left(\frac{\pi}{6} - \alpha - \frac{5\pi}{12}\right)i &= \left(\frac{\pi}{6} - \alpha - \frac{5\pi}{12}\right)i \\ \text{or } 2\alpha &= \frac{\pi}{3} - \frac{5\pi}{6} \quad \text{or } \alpha = -\frac{\pi}{4} \end{aligned}$$

The value of  $\alpha$  has been determined so that the solution

(5.2-1) is valid at the turning point, where both up and downgoing waves exist. In order to calculate a reflection coefficient (incident quasi-compressional wave), equation (5.2-1) is premultiplied by  $[N]^{-1}$  the inverse matrix of eigenvectors (see Chapman 1977b). This resolves the physical variables, which are the components of  $\underline{y}$ , into up and downgoing wave components. The first component of  $[N]^{-1} \underline{y}$  will be the reflection coefficient and the second component will represent the incident wave (recall that the origin has been shifted to the turning point). Furthermore, since the solution is to be examined far away from the turning point,  $[H]$  may be written as

$$[H] = \underline{N} [\underline{\Lambda}] \quad (4.3-46)$$

Thus, calculation of the vector, representing all up and downgoing waves above the turning point yields the following:

$$\begin{pmatrix} R \\ R \\ R \\ R \end{pmatrix} = [N]^{-1} [N] [\Lambda] \begin{pmatrix} c e^{-i\pi/4} \\ c e^{i\pi/4} \\ 0 \\ 0 \end{pmatrix} \quad (5.2-5)$$

where  $R_{pp}$  is the reflection coefficient for incident "p" wave;

$R_{ip}$  = incident p-wave amplitude;

$R_{ps}$  = reflected "s" wave converted from p; and

$R_{is}$  = incident "s" wave.

The important result to note about (5.2-5) is that there is no converted quasi-compressional wave due to the "reflection" at the turning point. To actually obtain the value of  $R_{pp}$ , the substitution of

$$[\Lambda] = \begin{pmatrix} e^{i\omega Q_k} & 0 \\ e^{-i\omega Q_k} & 0 \\ 0 & e^{i\omega Q_p} \\ 0 & e^{-i\omega Q_p} \end{pmatrix}$$

into (5.2-5) yields

$$\begin{aligned} R_{PP} &= c e^{-i\pi/4} e^{i\omega Q_\alpha} \\ R_{IP} &= c e^{i\pi/4} e^{-i\omega Q_\alpha} \end{aligned} \quad (5.2-6)$$

In (5.2-6), if a unit incident amplitude is considered,

$$\begin{aligned} c &= e^{-i\pi/4} e^{i\omega Q_\alpha} \\ R_{PP} &= -i e^{2i\omega Q_\alpha} \end{aligned} \quad (5.2-7)$$

Equation (5.2-7) is the famous JWKB reflection coefficient mentioned by Chapman (1976b) and Richards (1973). It can be used to construct seismograms as Chapman has demonstrated. However, as Chapman (1977, personal communication) has pointed out, the result (5.2-7) is not completely general. It does not obey the relation

$$R_{PP}(-\omega) = R_{PP}^*(\omega)$$

which must be true, if the function desired, after an inverse Fourier transform is performed, is to be real. The correct reflection coefficient is

$$R_{pp} = -i \operatorname{sgn}(\omega) e^{2i\omega Q_\alpha} \quad (5.2-8)$$

An analogous coefficient exists for quasi-shear waves:

$$R_{ss} = -i \operatorname{sgn}(\omega) e^{2i\omega Q_\beta} \quad (5.2-9)$$

With the above reflection coefficients, the first motion approximation may be obtained in a straightforward manner.



### Section 3 - The Equal Phase Method - Implementation

With the calculation of the reflection coefficient, the construction of the seismogram proceeds as indicated below.

First, the inhomogeneous matrix equation (4.1-14) must be solved, and then, the solution is substituted into the cylindrical harmonic expansion equation (4.1-1). The solution of the inhomogeneous matrix equation is given as (Chapman 1976b)

$$Y'(z) = [H(z)] \left( [H(z)]^{-1} Y(z_0) + \int_{z_0}^z [H(\xi)]^{-1} W(\xi) d\xi \right) \quad (5.3-1)$$

where  $[H(z)]$  is the fundamental matrix and  $W(\xi)$  is the source term (4.2-12). As  $z_0$  is arbitrary, the first term can be neglected. The second term inside the parentheses in (5.3-1) represents the decomposition of the source vector into its up and downgoing wave components. Substitution of the asymptotic form of the fundamental matrix  $[H]$  (4.3-46) into (5.3-1), and integration across the point of discontinuity,  $z_0$ , yields

$$\underline{S} = \omega \begin{pmatrix} -(z N_{11} + L A N_{21}) \cdot U(z - z_0) \\ -(z N_{11} + L A N_{21}) \cdot U(z_0 - z) \\ -(z N_{13} + L B N_{23}) \cdot U(z - z_0) \\ + (z N_{13} + L B N_{23}) \cdot U(z_0 - z) \end{pmatrix} \quad (5.3-2)$$

where  $\omega$  = angular frequency

$U(z)$  = heaviside step function

$N_{ij}$  =  $ij$ th component of  $[N]$  in (4.3-46)

( Note:  $z$  in  $z N_{11}$  is not the depth but the ray parameter -  
(see (4.3-4))

The first element of  $\underline{S}$ ,  $S_{11}$ , is the amplitude carried by a downgoing quasi-compressional wave, and the third element is the amplitude carried by a downgoing quasi-shear wave. In an isotropic medium  $S_{31}$  and  $S_{41}$  are identically zero, since the explosion source term (4.2-12) generates no shear waves. Thus, in (5.3-2), the first obvious difference between isotropic and transversely isotropic media becomes self-evident.

With an explicit expression for the source, the solution to (4.1-14) for the vertical and horizontal displacements becomes

$\underline{g}$  = source term \* reflection coefficient \* appropriate

eigenvector components (5.3-3)

where

$\underline{g}$  = vector of horizontal and vertical displacements

This will be illustrated below for the case of downgoing quasi-compressional waves.

From (5.3-2), the source term generating downgoing quasi-compressional waves is

$$S_{11} = -\omega (z N_{11} + L A N_{21}) \quad (5.3-4)$$

The reflection coefficient is given as

$$R_{pp} = -i \operatorname{sgn}(\omega) e^{2i\omega Q_\alpha}$$

The relevant eigenvector components are

$$N_{11} = \epsilon_\alpha (\rho t w - t z^2 - \omega L A 2)$$

$$N_{21} = \epsilon_\alpha (t z + \omega y) L A$$

Thus, the solution of equation (4.1-14) for the components representing vertical and horizontal displacements is

$$\begin{pmatrix} \bar{V}_1' \\ \bar{V}_2' \end{pmatrix} = -i \operatorname{sgn}(\omega) e^{i\omega \tau(p)} (-\omega (z N_{11} + L A N_{21})) \begin{pmatrix} N_{11} \\ N_{21} \end{pmatrix}$$

(5.3-5)

where  $\bar{V}_1' = -i\omega \bar{V}_1$  ;  $\bar{V}_2' = -\omega \bar{V}_2$

$\bar{V}_1$  = transformed horizontal displacement

$\bar{V}_2$  = transformed vertical displacement (see (4.1-13), (4.1-14))

$\tau(p) = 2 Q_\alpha$  = the vertical delay time

Expression of  $\bar{V}'$  in terms of the elements of  $\bar{V}$  results in (5.3 - 5 becoming

$$\begin{pmatrix} \bar{V}_1 \\ \bar{V}_2 \end{pmatrix} = \begin{pmatrix} -\operatorname{sgn}(\omega) e^{i\omega \tau(p)} N_{11} \tilde{S}_{11} \\ -i \operatorname{sgn}(\omega) e^{i\omega \tau(p)} N_{21} \tilde{S}_{11} \end{pmatrix} \quad (5.3-6)$$

where  $\tilde{S}_{11} = \frac{-S_{11}}{\omega} = z N_{11} + L A N_{21}$

The problem is almost solved! What is necessary now is to insert  $\bar{V}_1$  and  $\bar{V}_2$  into the cylindrical harmonic expansion, and do the integrations required. Before proceeding with those calculations, it is instructive to note some properties of Bessel functions and their relations to Hankel functions.

The appearance of Bessel functions in the harmonic expansion, or alternatively, the Bessel transform occurs in this elastodynamic problem due to cylindrical symmetry. For example, from (4.1-1) (neglecting constants and the time dependence)

$$u = \int_0^{\infty} \bar{u} \left( \frac{1}{k} \frac{\partial J_0(kr)}{\partial r} \right) k dk \quad (5.3-7)$$

$$w = \int_0^{\infty} \bar{w} J_0(kr) k dk$$

As Chapman (1977a) has noted, it is expedient to convert integrals appearing above to ones where  $\omega$  the angular frequency is real and  $k = \omega p$ . Substitution of  $k = \omega p$  into the integral for  $w$  results in

$$w = \int_0^{\infty} \omega^2 p \bar{w}(p) J_0(\omega p r) dp \quad (5.3-8)$$

Substitution of the relations

$$J_0(\omega pr) = \frac{H'_0(\omega pr) + H''_0(\omega pr)}{2}$$

$$H''_0(-\omega pr) = -H'_0(\omega pr)$$

into (5.3-8) results in

$$w = \frac{1}{2} \omega^2 \int_{-\infty}^{\infty} p \bar{w}(p) H'_0(\omega pr) dp \quad (5.3-9)$$

only if  $\omega > 0$  and  $\bar{w}(p)$  is even in  $p$ . For all real  $\omega$ ,

$$w = \frac{1}{2} |\omega| \omega \int_{-\infty}^{\infty} p \bar{w}(p) H'_0(\omega pr) dp \quad (5.3-10)$$

The contour is chosen to satisfy the radiation condition (Chapman 1977a).

A similar analysis can be applied to the integral for  $u$  through use of the relation

$$\frac{1}{\omega p} \frac{dJ_0(\omega p r)}{dr} = -J_1(\omega p r)$$

Then the expression for  $u$  becomes

$$u = \frac{-1}{2} \omega \int_{-\infty}^{\infty} p \bar{u}(p) H_1'(\omega p r) dp \quad (5.3-11)$$

only if  $\bar{u}(p)$  is odd in  $p$ . Equations (5.3-10) and (5.3-11) will now be used below in the calculation of the inverse transform (or evaluation of the cylindrical harmonic expansion).

In doing the final inverse transform, it must be recalled that the results have been derived for a plane wave of angular frequency  $\omega$ . Therefore, equations (5.3-6) must be multiplied by the source time function transform,  $T(\omega)$ . Then the complete solution for  $u$  (the horizontal displacement) is given as

$$u = v_1 = \frac{1}{8\pi^2} \int_{-\infty}^{\infty} e^{-i\omega t} \omega |\omega| T(\omega) d\omega \cdot \int_{-\infty}^{\infty} -H_1(\omega pr) (-\operatorname{sgn} \omega) e^{i\omega z(p)} N_{11} \tilde{S}_{11} p dp$$

(5.3-12)

and

$$w = v_2 = \frac{1}{8\pi^2} \int_{-\infty}^{\infty} e^{-i\omega t} \omega |\omega| T(\omega) d\omega \cdot \int_{-\infty}^{\infty} H_0(\omega pr) (-i \operatorname{sgn}(\omega)) e^{i\omega z(p)} N_{21} \tilde{S}_{11} p dp$$

(5.3-13)

where (5.3-6), (5.3-10) and (5.3-11) have been used and the inverse time transform has been performed as well.

In order to render (5.3-12) and (5.3-13) in a form suitable for calculation, the asymptotic forms of the Hankel functions are used:



$$H_0' = \sqrt{\frac{2}{\omega p r \pi}} e^{i\omega p r - i\pi/4}$$

$$H_1' = \sqrt{\frac{2}{\omega p r \pi}} e^{i\omega p r - 3\pi i/4}$$

These expansions are substituted into expressions (5.3-12) and (5.3-13), and this fact implies that the curvature of the wavefront is neglected. Thus, the expressions for  $V_1$  and  $V_2$  become

$$V_1 = \frac{1}{8\pi^2} \int_{-\infty}^{\infty} e^{-i\omega t} \omega |\omega| T(\omega) d\omega \cdot \int_{-\infty}^{\infty} \sqrt{\frac{2}{\omega p r \pi}} e^{-3\pi i/4} e^{i\omega(p r + \frac{1}{2} p^2)} (-\text{sgn}(\omega)) N_{11} \tilde{S}_{11} p dp$$

(5.3-14)

and

$$V_2 = \frac{1}{8\pi^2} \int_{-\infty}^{\infty} e^{-i\omega t} \omega |\omega| T(\omega) d\omega \cdot \int_{-\infty}^{\infty} \sqrt{\frac{2}{\omega p r \pi}} e^{-3\pi i/4} e^{i\omega(p r + \frac{1}{2} p^2)} (\text{sgn}(\omega)) N_{21} \tilde{S}_{11} p dp$$

(5.3-15)

To further simplify the above expressions the following

"tricks" are used: 1)  $|\omega| = \omega \text{sgn}(\omega)$

2)  $e^{-3\pi i/4}$  is written as  $(-1) e^{\pi i/4}$

3) the resulting  $(-1)$  is absorbed into the  $\omega$  integral;

4) the convolution theorem is used as well as the following inverse transforms:

$$- \omega^2 \leftrightarrow \frac{d^2}{dt^2}$$

$$e^{\pi i/4} / \sqrt{\omega} \leftrightarrow \frac{H(t)}{\sqrt{\pi t}}$$

These "tricks" result in

$$u = v_1 = \frac{1}{8\pi^3} \frac{d^2}{dt^2} (T(t)) * \frac{H(t)}{\sqrt{\pi}} * \sqrt{\frac{2}{r}} \int_{-\infty}^{\infty} \int_{-\infty}^{\infty} e^{i\omega(\theta(p)-t)} N_{11} \tilde{S}_{11} p^{1/2} dp d\omega$$

(5.3-16)

and

$$w = v_2 = \frac{1}{8\pi^3} \frac{d^2}{dt^2} (T(t)) * \frac{H(t)}{\sqrt{\pi}} * \sqrt{\frac{2}{r}} \int_{-\infty}^{\infty} \int_{-\infty}^{\infty} e^{i\omega(\theta(p)-t)} N_{21} \tilde{S}_{21} p^{1/2} dp d\omega$$

(5.3-17)

where  $\theta(p) = pr + \pi(p)$ , the phase time of all plane waves at the position  $r$ .

$H(t)$  = Heaviside step function.

With the calculation at the present state, it is time to invoke the equal phase method. This is a mathematical statement of the physics developed in Section 1, in which the disk algorithm was explained. The phase  $\theta$  is expanded about the equal phase points  $p_j$  (Chapman 1976b). These  $p_j$  are the ray parameters of rays which, at the receiver position  $r$ , have equal phase delays relative to the main arrival. The contributions from each set of equal phase ray parameters are summed and occur in the seismogram at the

appropriate time. This corresponds exactly to the method explained in Section 1. Note also that, in Section 1, an operator was described, which had to be convolved with the seismogram. If one of the  $\frac{d}{dt}$  operators is considered with the  $\frac{H(t)}{\sqrt{t}}$  term in (5.3-16) or (5.3-17), then this time function  $\frac{d}{dt} \left( \frac{H(t)}{\sqrt{t}} \right)$  is exactly the one described in Section 1.

For the contribution to the seismogram at the  $j$ th equal phase point,  $\Theta(\rho)$  is expanded about  $\rho = \rho_j$

$$\Theta(\rho) = \Theta(\rho_j) + \Theta'(\rho_j)(\rho - \rho_j) \quad (5.3-18)$$

$$\Theta(\rho) - \Theta(\rho_j) = \Theta'(\rho_j)(\rho - \rho_j)$$

Use of (5.3-18) into (5.3-16) and (5.3-17) results in

$$\left( \frac{u}{w} \right)_{\rho=\rho_j} = \frac{1}{8\pi^3} \frac{d}{dt} \left( \frac{H(t)}{\sqrt{t}} \right) * \frac{d}{dt} \left( \frac{H(t)}{\sqrt{t}} \right) * \frac{\sqrt{2}}{\sqrt{r}} \iint_{-\infty}^{\infty} e^{i\omega \theta(\rho_j, r, t)} \begin{pmatrix} N_{11} \\ N_{21} \end{pmatrix} \tilde{S}_{11} \rho'^t d\rho d\omega \quad (5.3-19)$$

To evaluate the double integral in (5.3-19) two steps are taken:

- 1) The limits on the  $\omega$  integral are replaced  $(-\infty, \infty)$  to  $(0, \infty)$  and this gives twice the real part, i.e.,

$$\int_{-\infty}^{\infty} g(\rho) e^{i\omega h(\rho)} d\rho = 2 \operatorname{Re} \int_0^{\infty} g(\rho) e^{i\omega h(\rho)} d\rho$$

2) The  $\omega$  integral is evaluated and the  $p$ -integral is evaluated. Use of the artifices in explicitly doing step (2) is that:

$$\operatorname{Re} \frac{1}{\pi} \int_0^{\infty} \int_{-\infty}^{\infty} h(p) e^{i\omega \theta'(p_j)(p-p_j)} dp d\omega = \int_{-\infty}^{\infty} h(p) \delta(\theta'(p_j)(p-p_j)) dp$$

and

$$\int_{-\infty}^{\infty} h(p) \delta(\theta'(p_j)(p-p_j)) dp = \frac{h(p)}{|\theta'(p)|}$$

$h(p)$  = smooth function of  $p$

Implementation of (1), (2), (3), and (4) yields the final result

$$\left( \frac{u}{w} \right)_{p_j} = \frac{1}{2\sqrt{2} \pi^2} \frac{d}{dt} \left( T(t) \right) * \frac{d}{dt} \left( \frac{H(t)}{\sqrt{t}} \right) * \frac{\tilde{S}_{11}}{\sqrt{r}} p^{1/2} \begin{pmatrix} N_{11} \\ N_{21} \end{pmatrix} \frac{1}{|\theta'(p_j)|}$$

(5.3-20)

Equation (5.3-20) is identical in all respects to that obtained by Chapman (1976b), the only difference being the source factor  $\tilde{S}_{11}$  and the eigenvector components  $N_{11}$  and  $N_{21}$ .

A completely analogous expression exists for quasi-shear waves, the differences being that the phase time is

that appropriate to the wave-type and that the new source term and eigenvector components are:

$$\begin{aligned}\tilde{S}_{11} &= (zN_{13} + LB N_{23}) \\ N_{13} &= \epsilon_p LB (tz + wy) \\ N_{23} &= \epsilon_p (twx - tLBz - wy^2)\end{aligned}\tag{5.3-21}$$

Equations (5.3-20) and (5.3-21) will be used to generate seismograms for very simple transversely isotropic media, as detailed in Section 4.

#### Section 4 -Simple Seismic Calculations

Given the complicated theoretical derivation of the preceding sections, can any simple predictions be made for seismic waves in the case where ray theory is valid? The answer is a definite yes.

For all the calculations of synthetic seismograms in this section, the velocity model chosen was one characteristic of the upper mantle, that is,  $v = 8.1 + .0027 * z$ . Three sets of calculations were done-no anisotropy, 10% anisotropy, and 30% anisotropy. The anisotropy in the model was achieved by increasing the stiffness  $C$  by the appropriate amounts. Increasing  $C$  would effectively increase the vertical velocity. For simplicity, in the following discussion, the model without anisotropy will be referred to as Model 1, those with 10 and 30% anisotropy as Models 2 and 3 respectively.

In figures 5.5, 5.6, 5.7 p-delta curves for compressional waves are plotted for Models 1, 2, and 3. The rays arrive at earlier times and smaller epicentral distances with increasing anisotropy. For example, in figure 5.5, the epicentral distance for  $p = .1$  sec./km. is 4400 km., while in figure 5.7, for the same  $p$ , the distance is 3800 km. Also it is clear from the figures, that apart from kinematic effects, the anisotropy has not affected the

basic shape of the p-delta curve.

Before commenting on the synthetic seismograms calculated from the p-delta curves, it is helpful to consider the directivity functions used in the d. r. t. calculations. The directivity function is taken to mean the product of the source function, the appropriate eigenvector component, and the  $p^{1/2}$  which arises from the expansion of Bessel function. The directivity function assigns an initial "amplitude" to each ray. (Figures 5.8, 5.9, and 5.10 show the horizontal directivity functions for quasi-compressional waves.) It is immediately clear that the anisotropy has had little effect in changing the shape or magnitude of the directivity function for a given ray parameter p. In figures 5.11, 5.12, and 5.13 the directivities for the vertical displacement are illustrated. Again, the increasing anisotropy has not significantly changed the shape of the directivity as a function of p, although the magnitude, in the case of Model 3, has been reduced by about 10%. The most important point to note is that the anisotropy has not introduced any extra bumps on the directivity curve.

Given the above results, it is expected that the main effect of the anisotropy would simply be the advance in time of the main arrival, as the amount of anisotropy is increased. The seismogram for Models 1, 2, and 3 (horizontal displacement) are shown in figures 5.14, 5.15,

and 5.16, while those for vertical displacement are shown in figures 5.17, 5.18, and 5.19. It is clear that the observation of the kinematic effect mentioned above can be seen by comparison of figures 5.14 and 5.16. For example, in figure 5.14, at an epicentral distance of 3100 km., the main pulse arrives at 57 sec. while in figure 5.16 it arrives at 56 sec. The directivity used to construct the seismogram does not affect the pulse for either horizontal or vertical displacement, since it is a smooth function and is not rapidly changing for values of  $p$  in the neighbourhood of .105 sec./km., which corresponds to a delta of 3200 km.

It has been demonstrated that for quasi-compressional ("p") waves, the effect of anisotropy is mainly a kinematic one. What happens in the case of quasi-shear waves? Comparison of p-delta curves shows that for greater anisotropy the epicentral distances are reduced (compare figure 5.21 with 5.20). Hence, the same kinematic effects, mentioned earlier also affect quasi-shear waves for the particular models chosen. However, examination of the directivity curves for horizontal and vertical displacements (figures 5.22 and 5.23 for Model 2 and figures 5.24 and 5.25 for Model 3), shows that the value of the directivity function is much less for quasi-shear waves than for quasi-compressional waves. This is to be expected since in an isotropic medium, the directivity function for an explosion source is zero for shear waves. The directivity values are



somewhat greater for Model 3 than Model 2, since larger amounts of anisotropy generate a greater quasi-shear component.

The relevant seismograms for quasi-shear waves are shown in figures 5.26 - 5.29. Although the seismograms for Model 2 are calculated at different epicentral distances than those in Model 3, it is still clear that the arrivals for Model 3 are earlier than those for Model 2 due to the differing  $p$ -delta curves (see figures 5.20 and 5.21). It is evident from the seismograms that the vertical components are phase shifted 180 degrees relative to the horizontal components. Again due to the smooth, slowly varying directivities, the pulse shapes are not affected by the anisotropy.

Given all the evidence presented thus far, it is possible to answer the question posed at the beginning of this section. It has been demonstrated that for the simple models used in the calculations, the effect of the anisotropy is a kinematic one-the main arrivals are simply advanced in time. The shape of the main arrival is not affected by a smooth, slowly varying directivity function. This situation could be altered if a different range of epicentral distances is considered, or the directivity effects due to free surface are included. To keep the results as simple as possible, no surface conversion coefficient was introduced in the calculation. This may, of

course, be obtained from the eigenvectors calculated in Chapter IV, but the algebra is extremely complicated.

Since the effects of a small amount of anisotropy can be detected using the disk ray method (equal phase method), it is a valuable adjunct to other synthetic seismogram calculation techniques which have been applied to anisotropic media (Keith & Crampin 1977; Daley & Hron 1977).

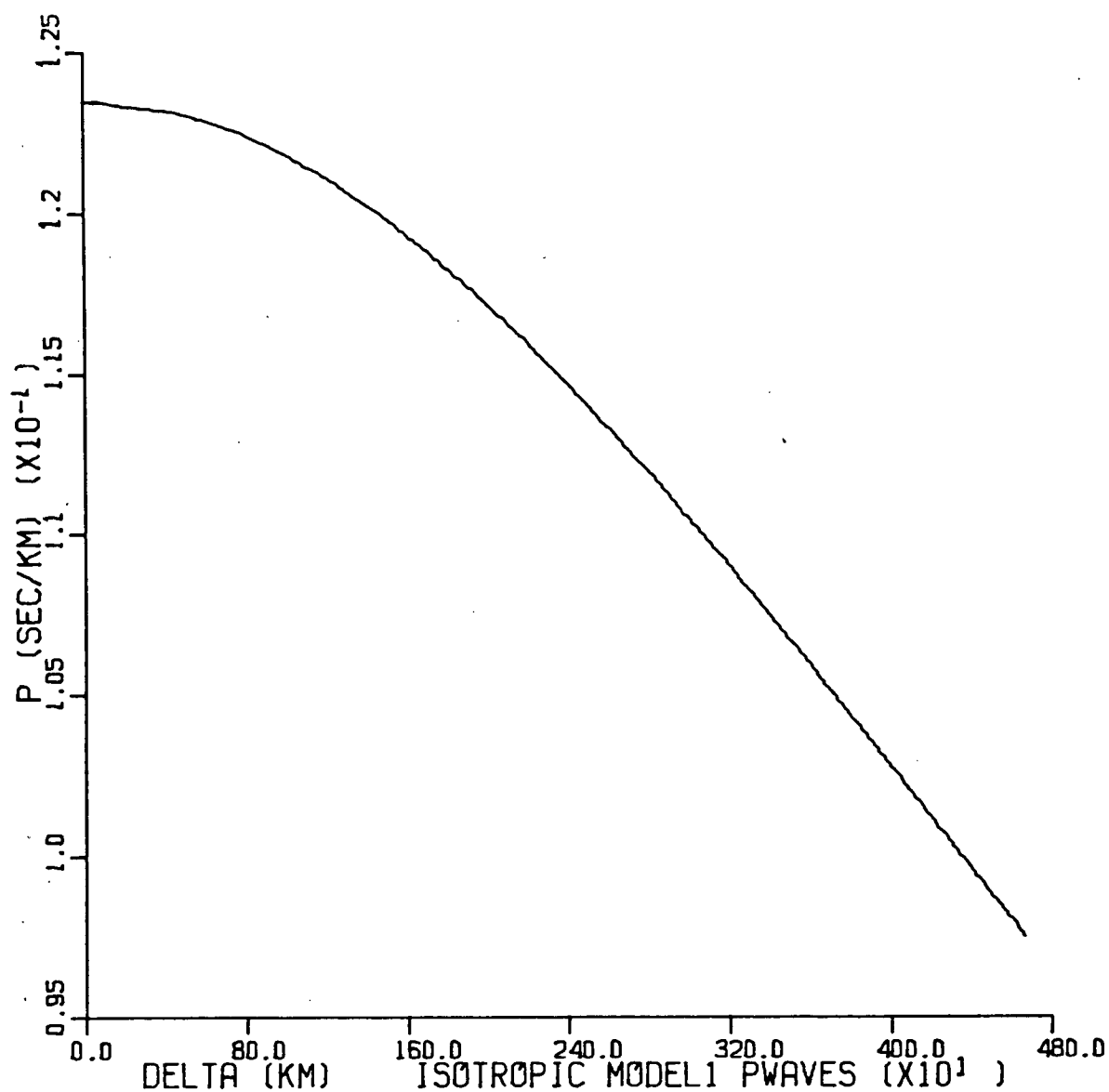


Figure 5.5 P-delta curve for isotropic Model 1 for compressional waves. Mantle model was used ( $v = (8.1 + .0027 * z)$  km./sec.)

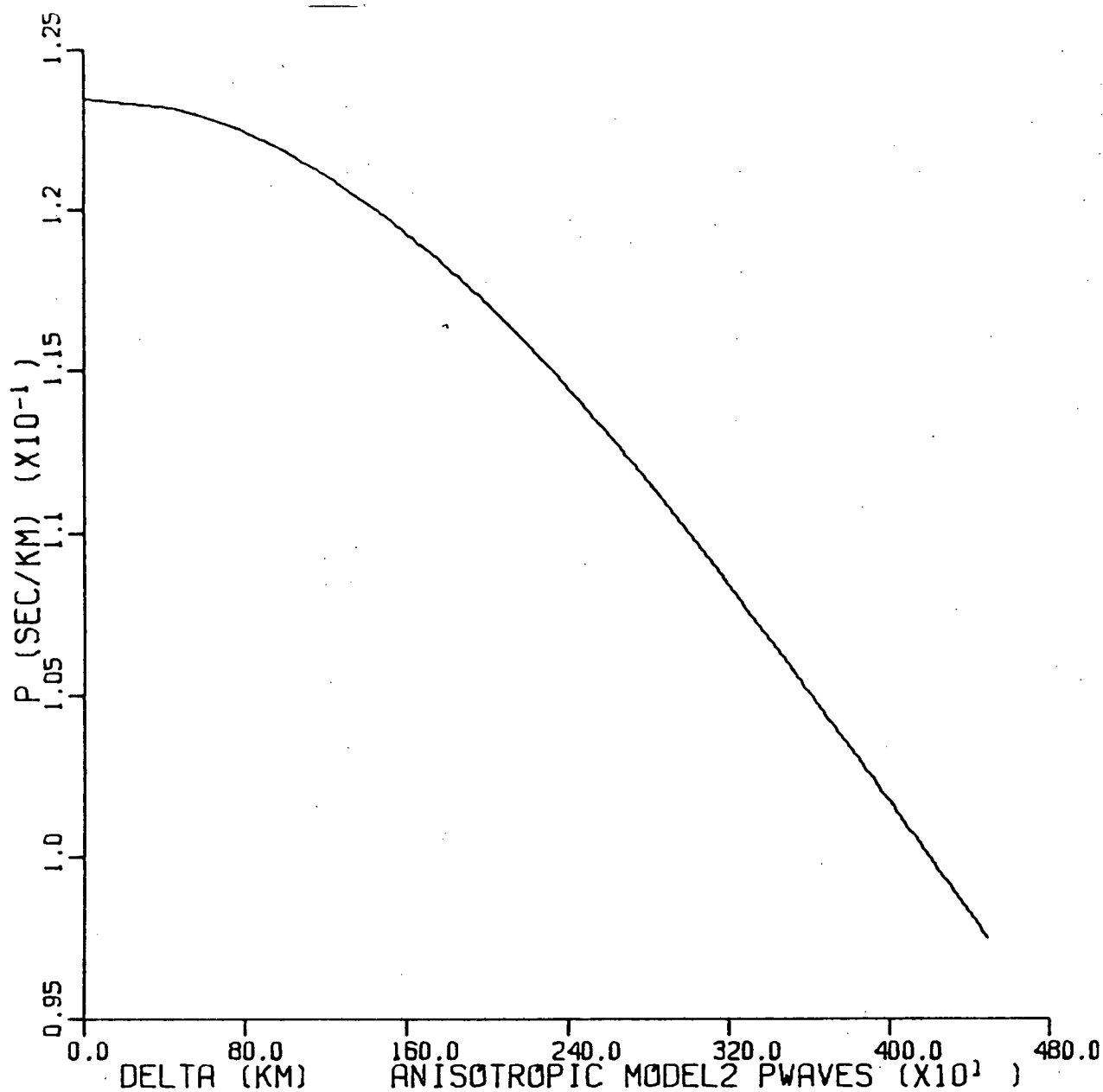


Figure 5.6 P-delta curve for anisotropic Model 2 for quasi-compressional waves. Anisotropy factor is 10%.

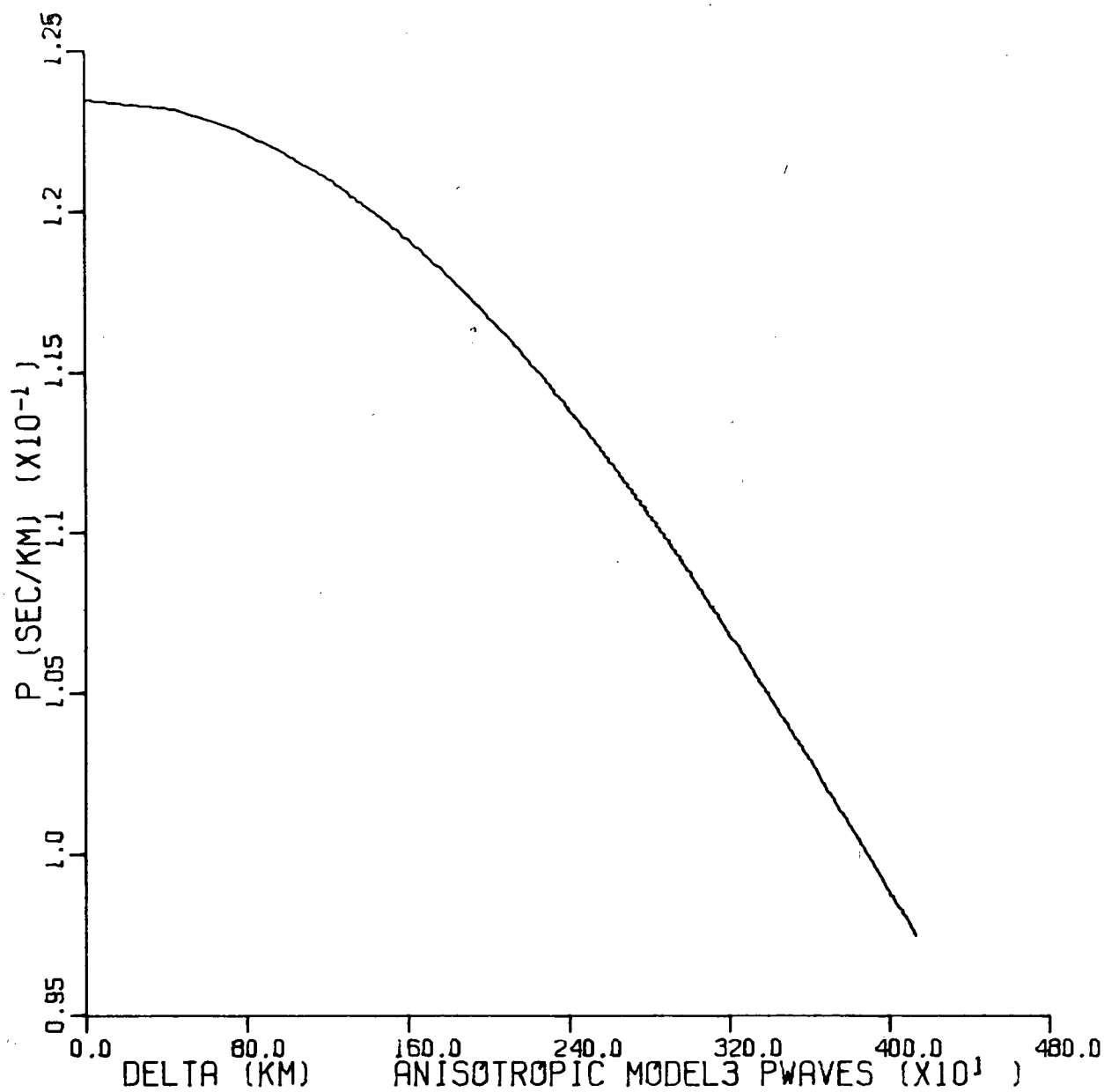


Figure 5.7 P-delta curve for anisotropic Model 3 for quasi-compressional waves. Anisotropy factor is 30%.

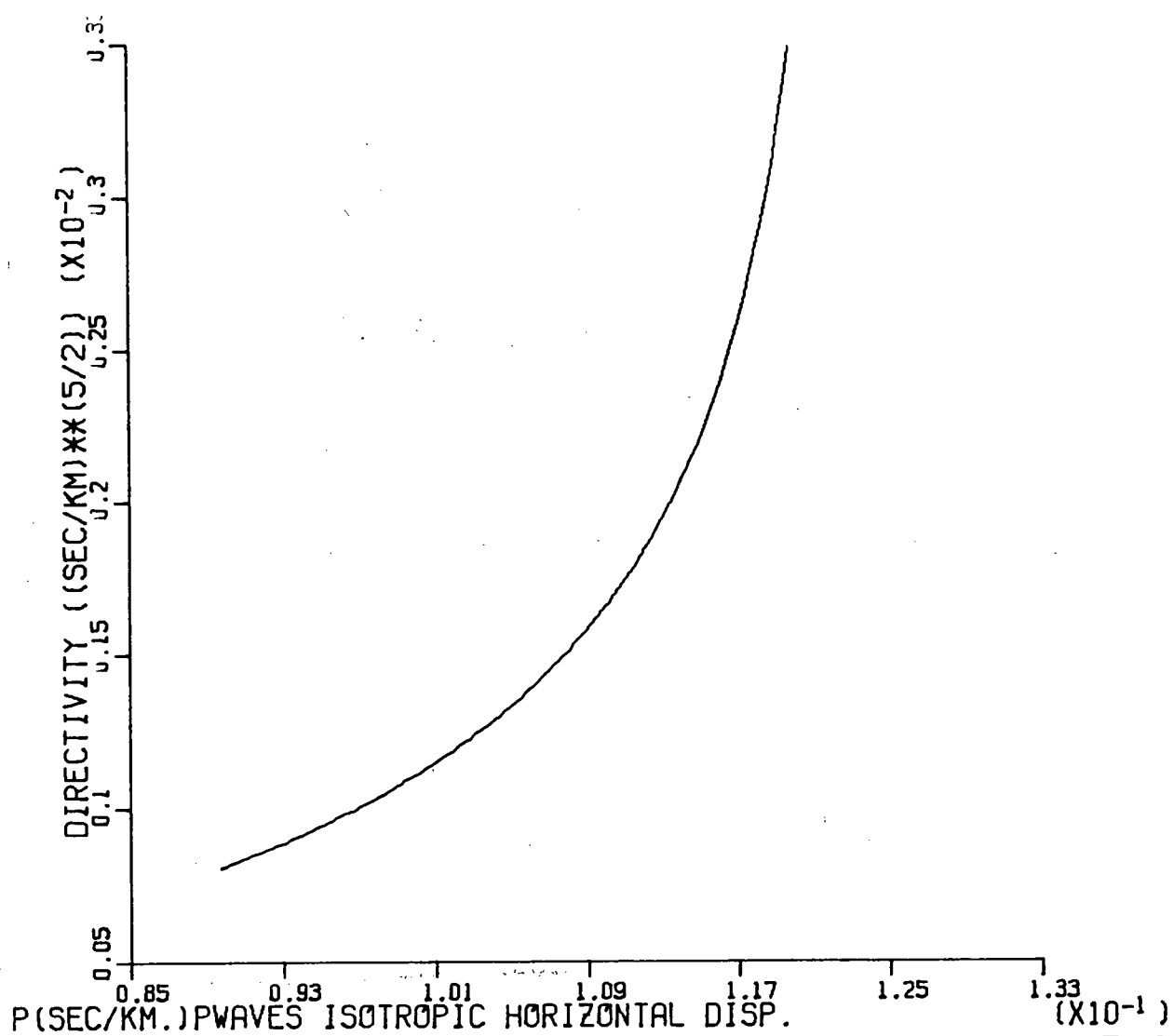


Figure 5.8 Directivity function (compressional waves) for horizontal displacement for isotropic Model 1.

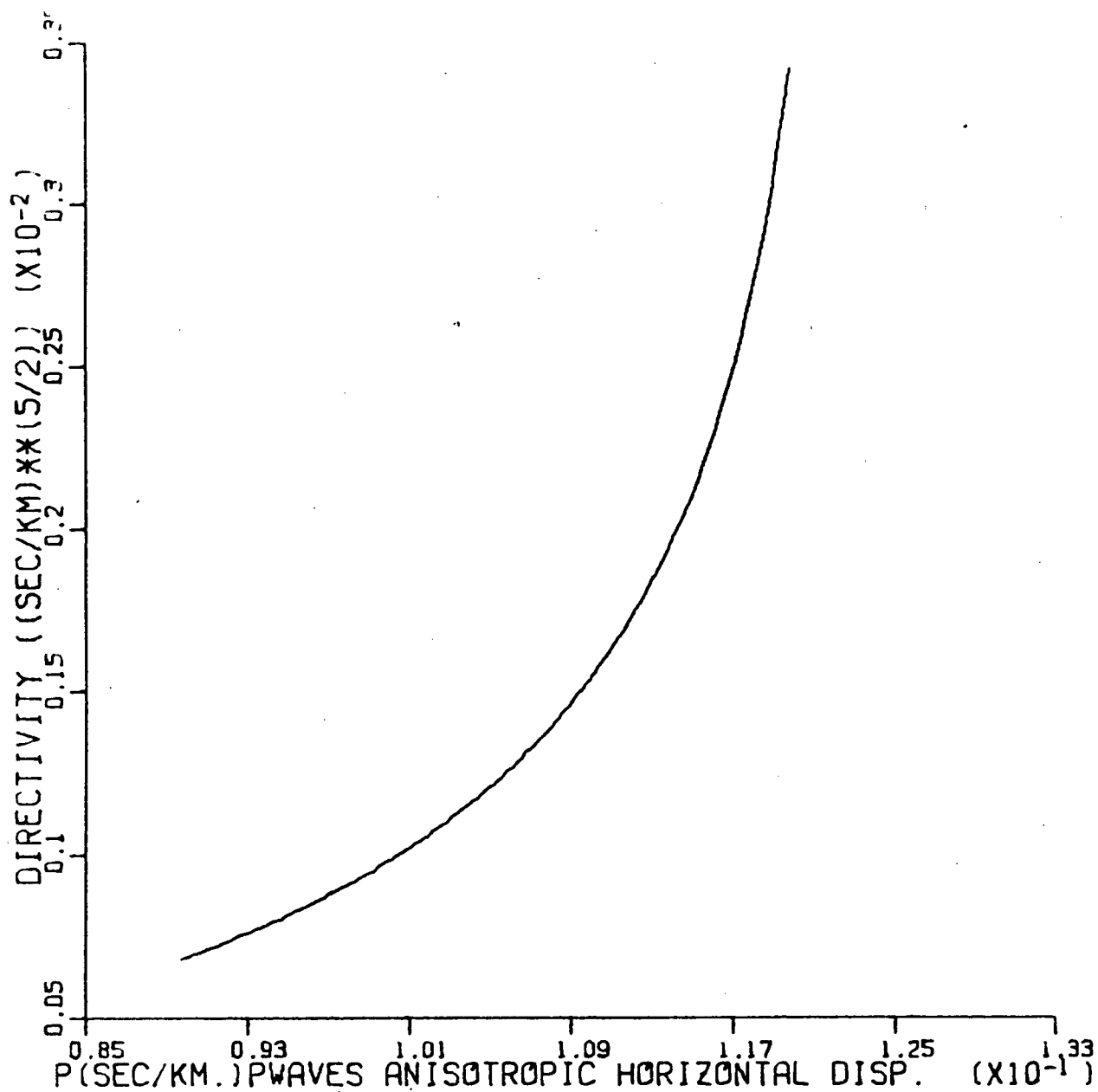


Figure 5.9 Directivity function (quasi-compressional waves)  
for horizontal displacement for anisotropic Model 2. 10%  
anisotropy

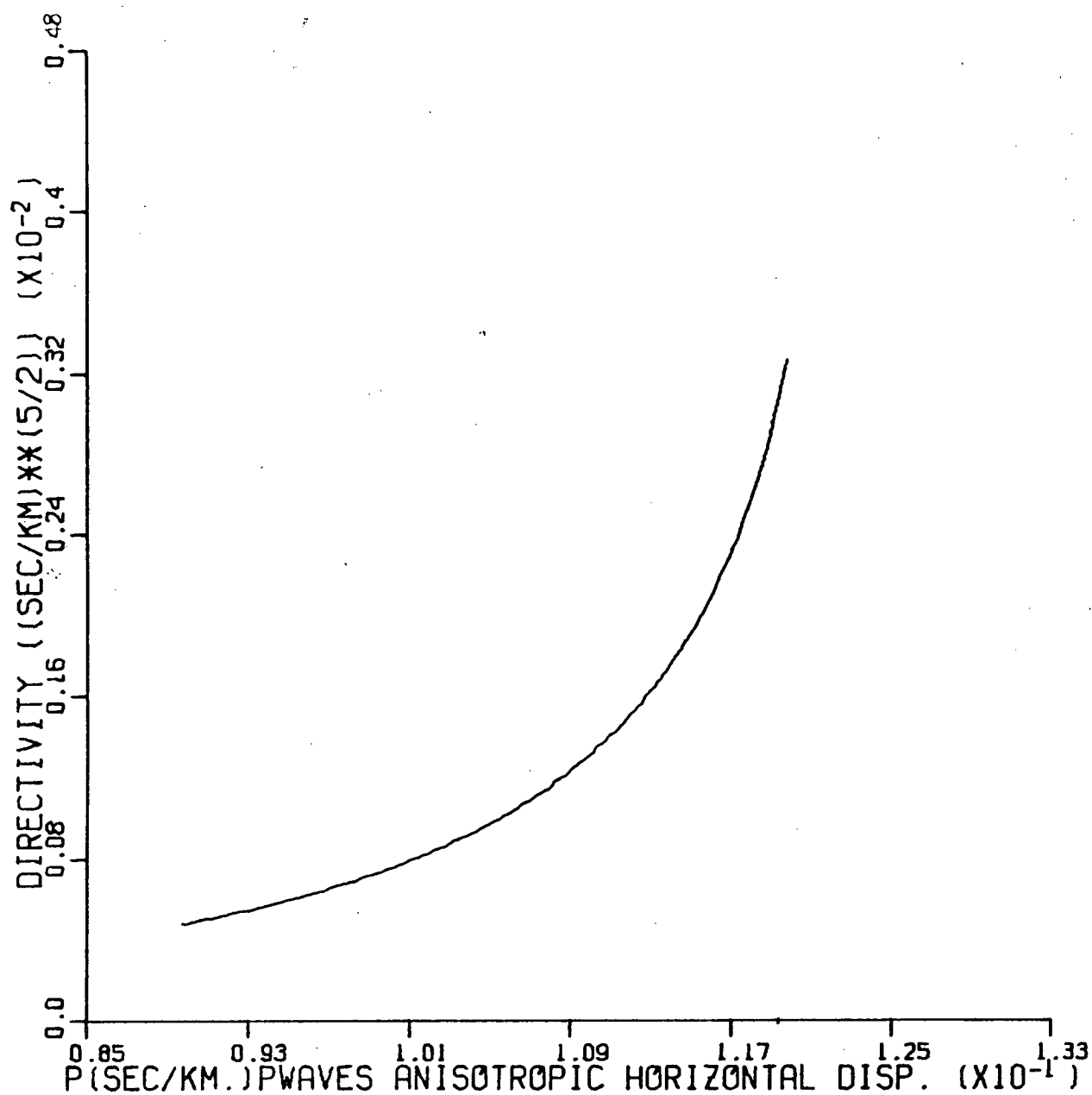


Figure 5.10 Directivity function (quasi-compressional waves)  
for horizontal displacement for anisotropic Model 3. 30%  
anisotropy



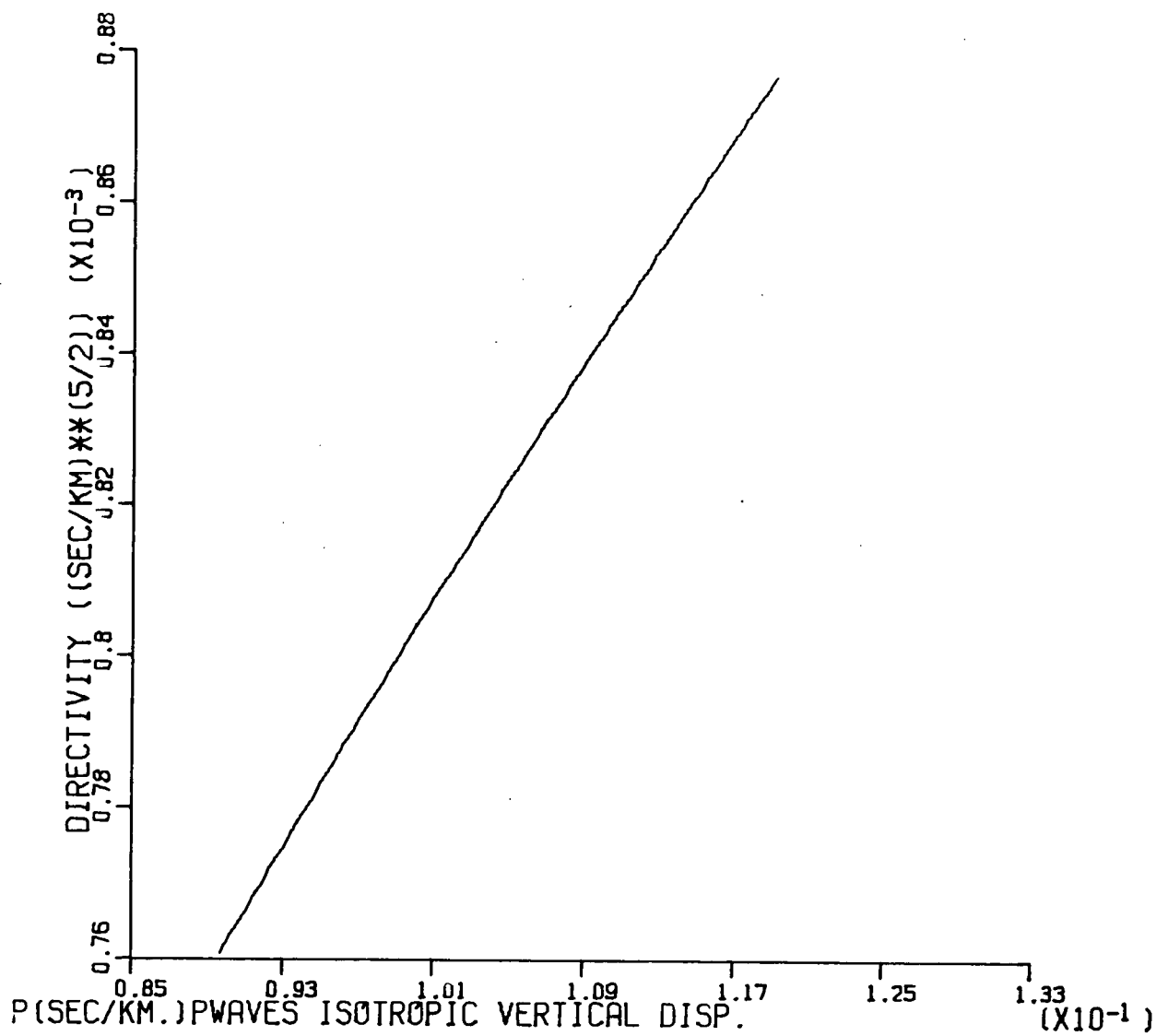


Figure 5.11 Directivity function (compressional waves) for vertical displacement for isotropic Model 1.

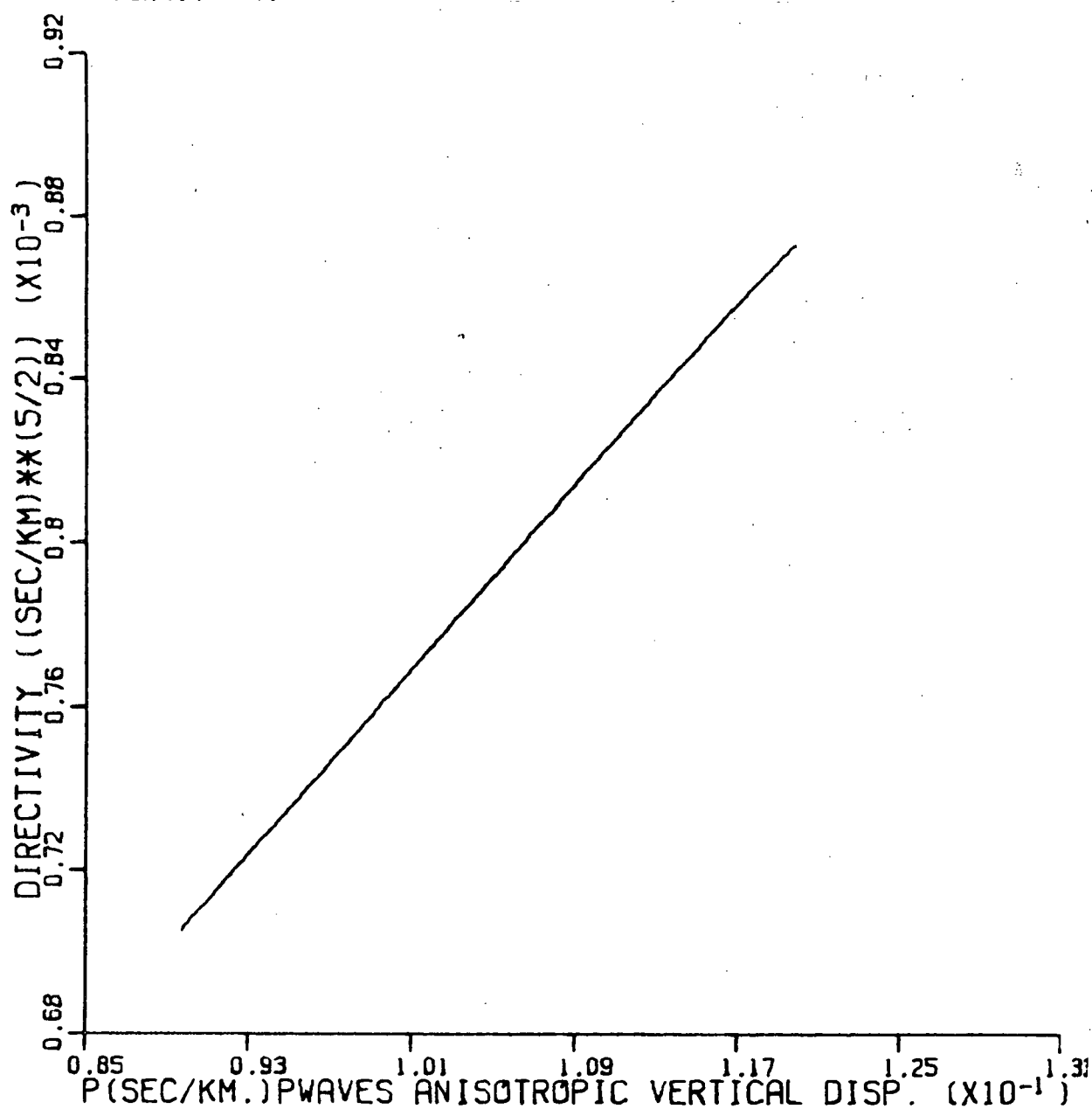


Figure 5.12 Directivity function (quasi-compressional waves)  
for vertical displacement for anisotropic Model 2. 10%  
anisotropy

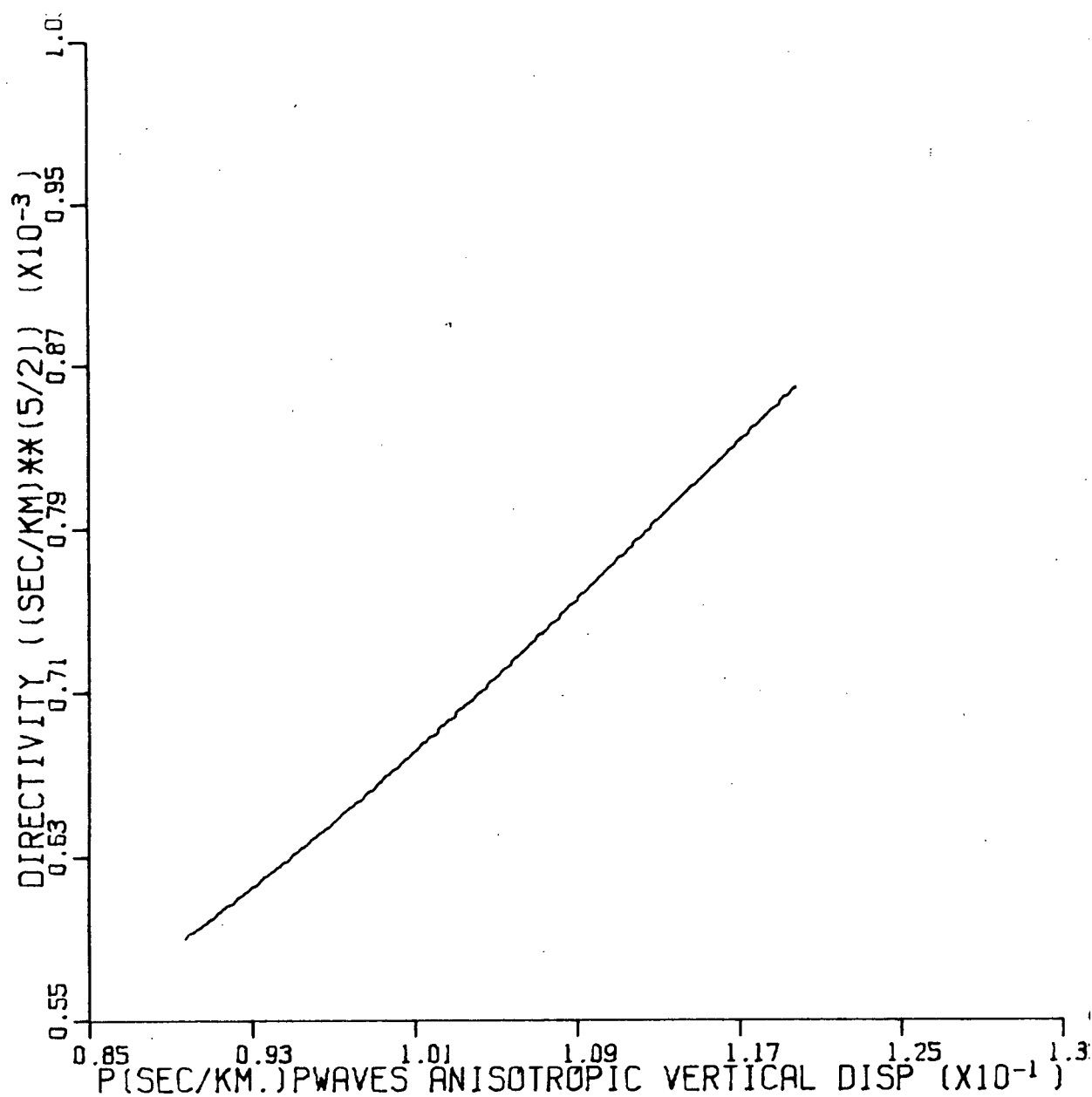


Figure 5.13 Directivity function (quasi-compressional waves)  
for vertical displacement for anisotropic Model 3. 30%  
anisotropy

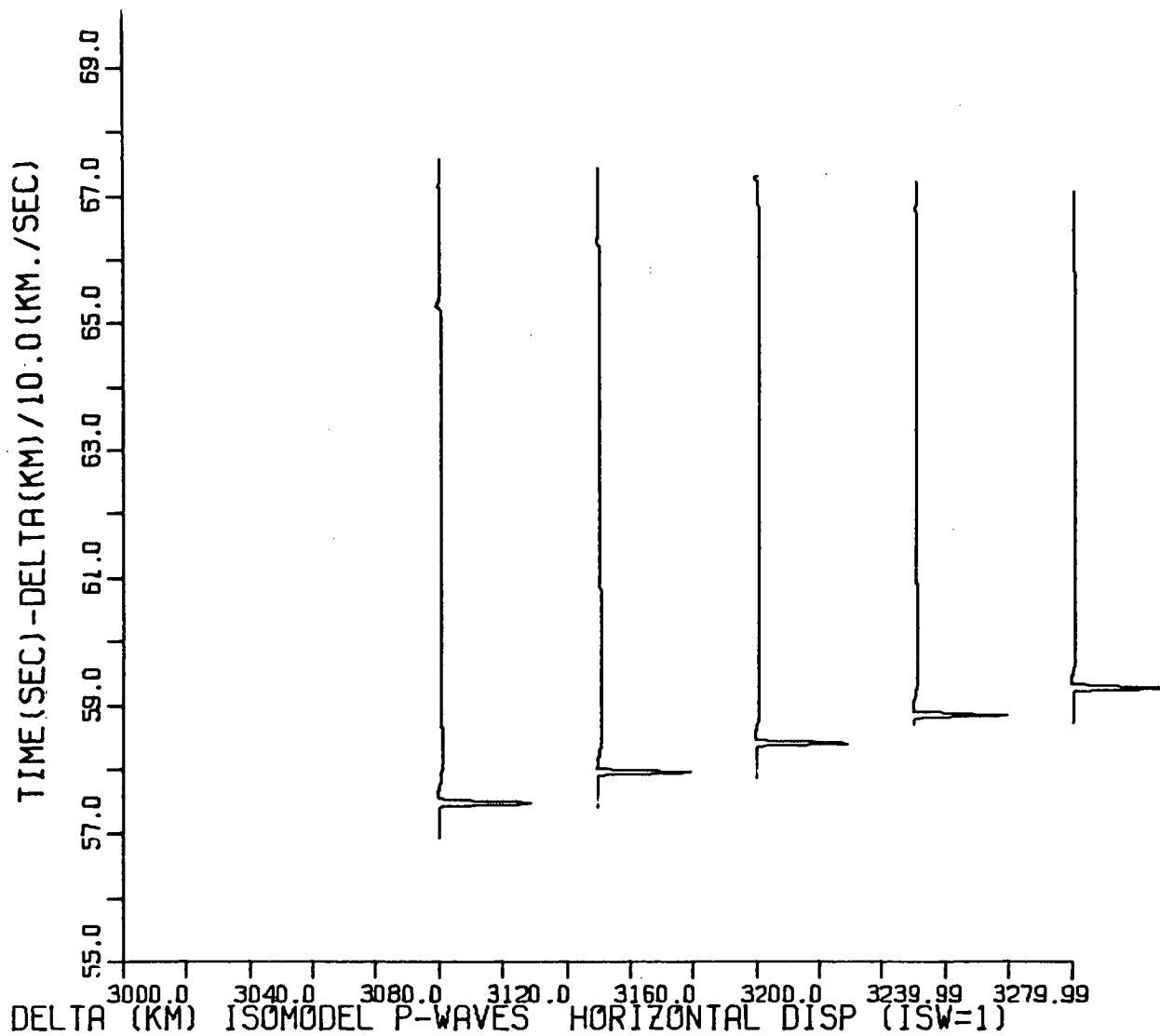


Figure 5.14 Synthetic seismogram of horizontal displacement for compressional waves calculated using p-delta curve shown in figure 5.5

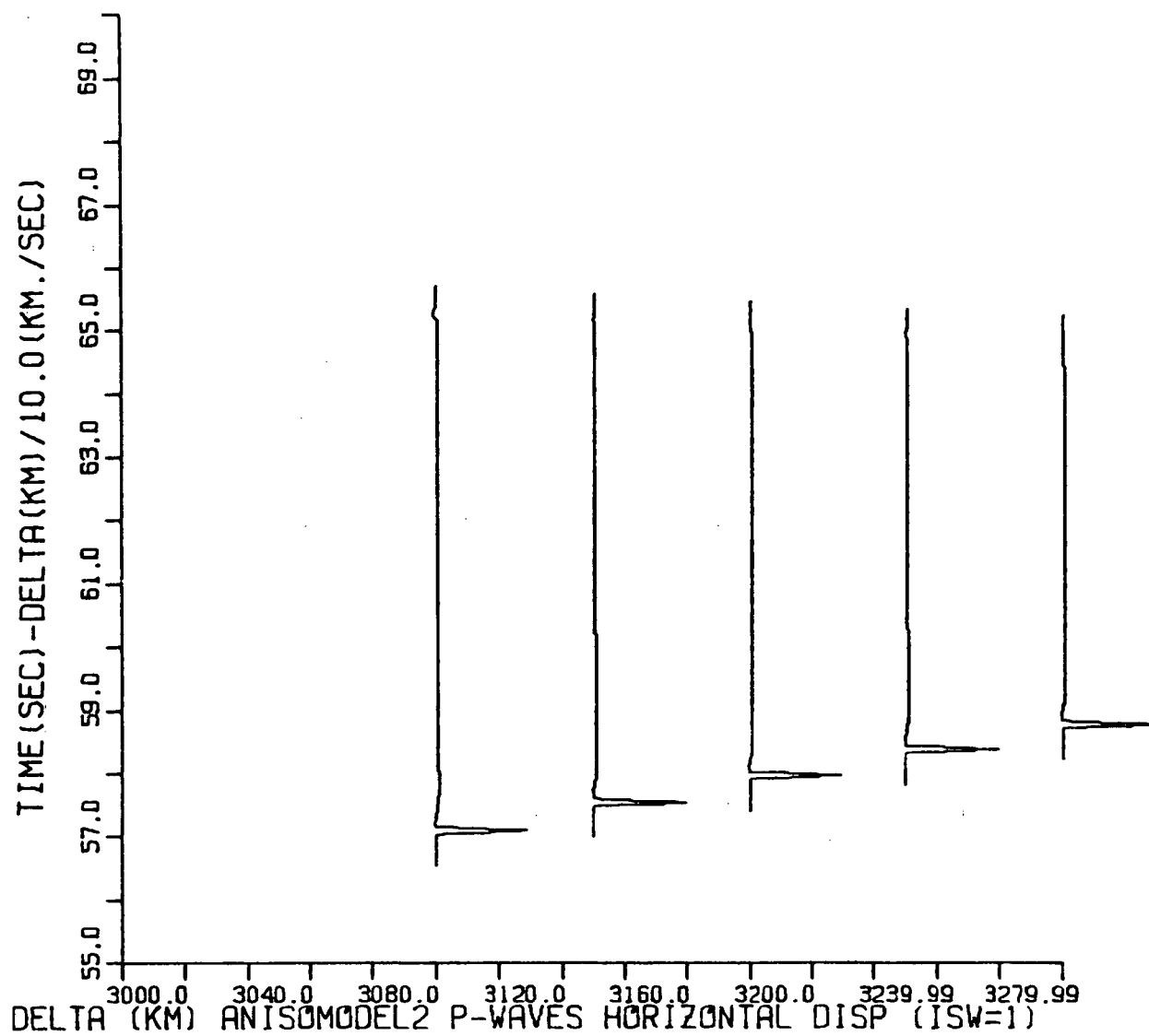


Figure 5.15 Synthetic seismogram of horizontal displacement for quasi-compressional waves calculated using p-delta curve shown in figure 5.6. 10% anisotropy

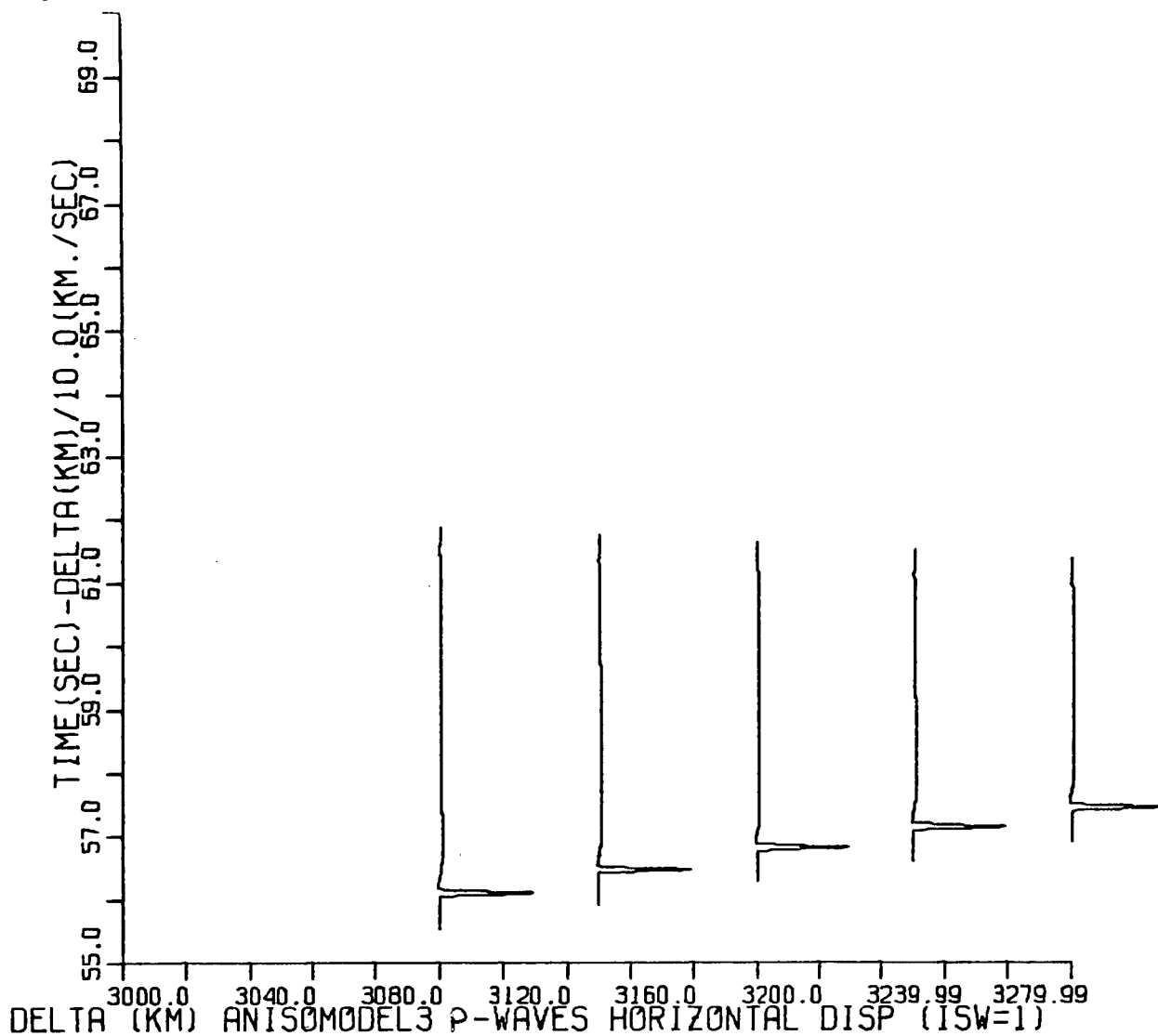


Figure 5.16 Synthetic seismogram of horizontal displacement for quasi-compressional waves calculated using p-delta curve shown in figure 5.7. 30% anisotropy

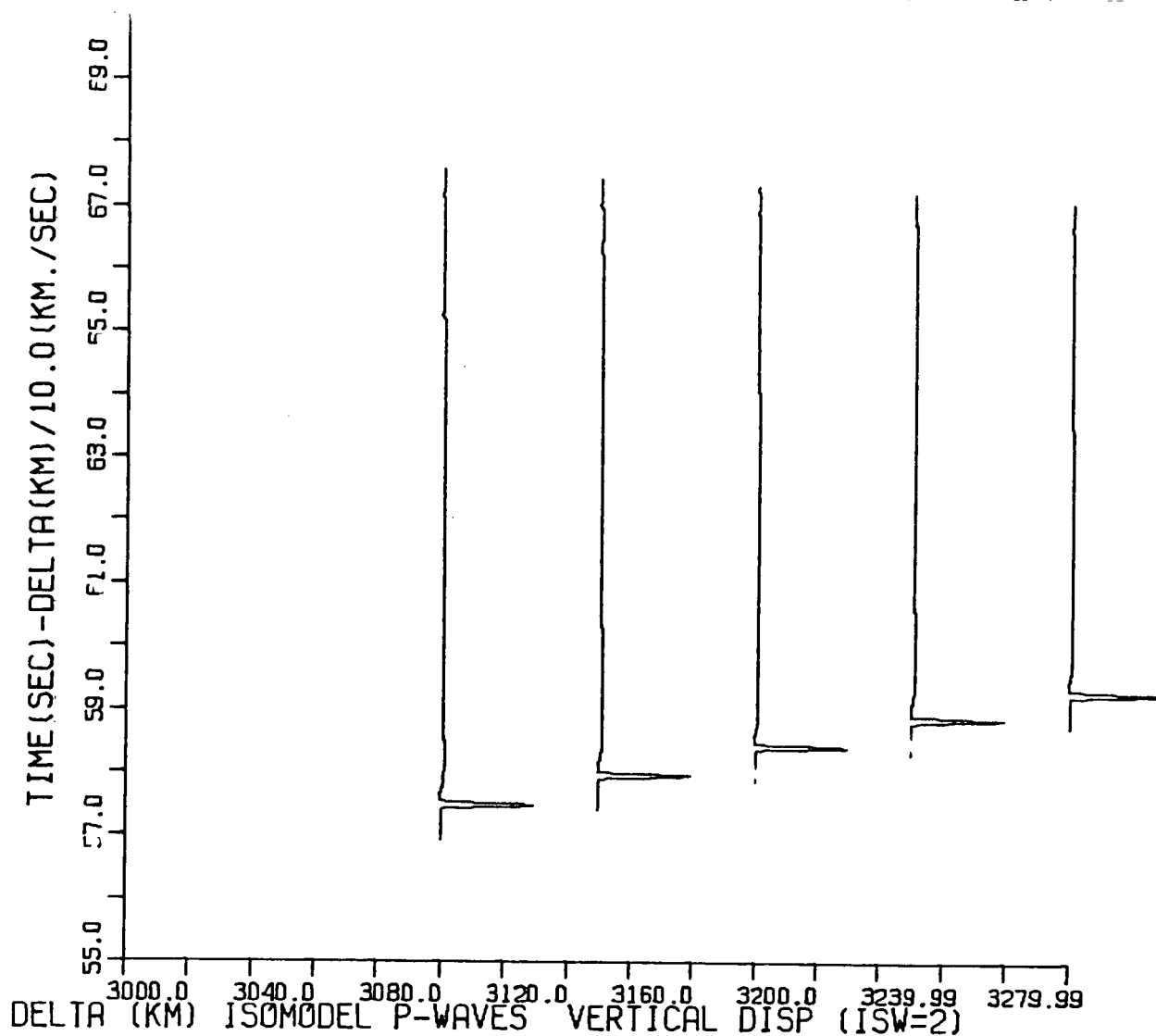


Figure 5.17 Synthetic seismogram of vertical displacement for compressional waves calculated using p-delta curve shown in figure 5.5

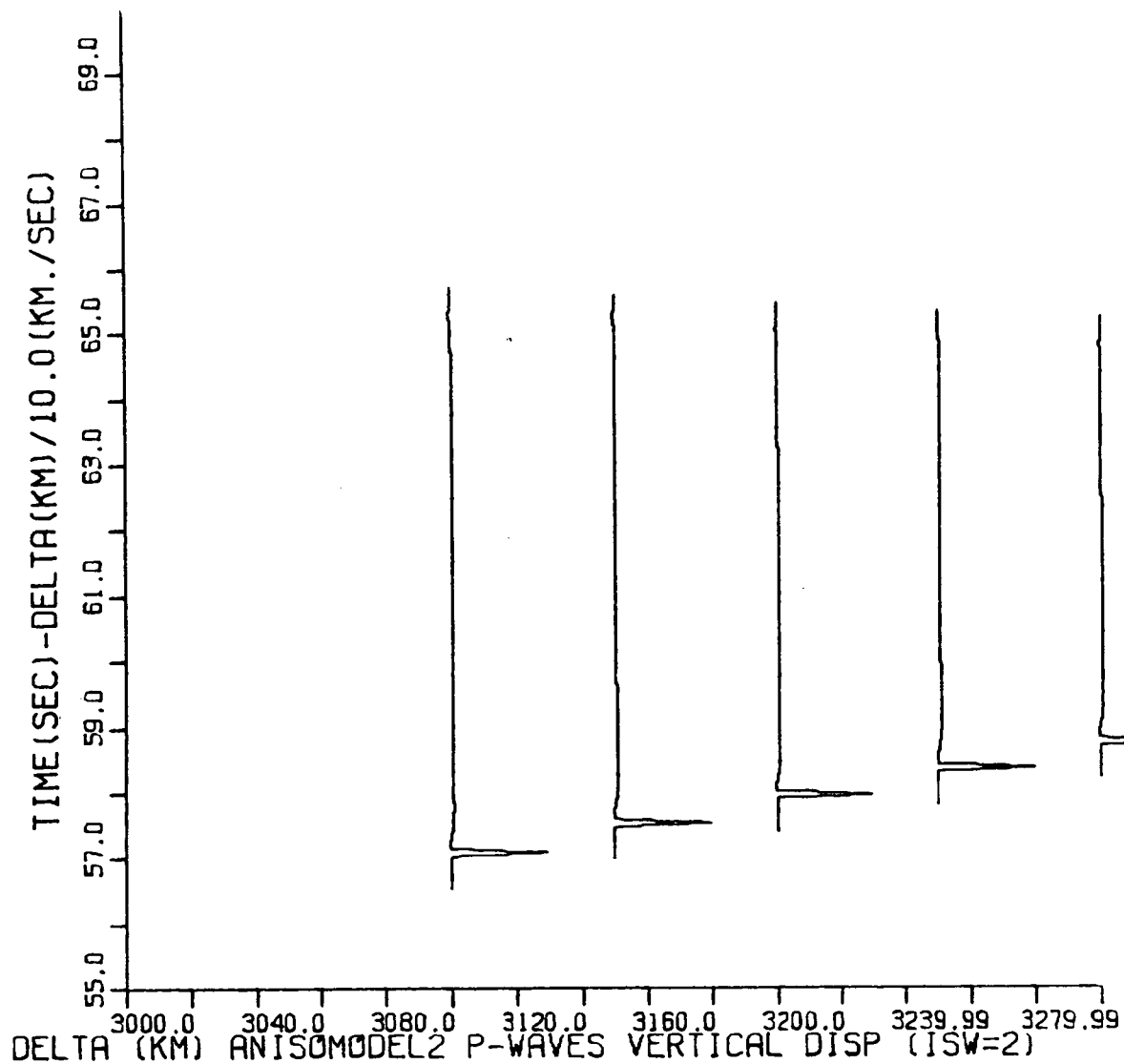


Figure 5.18 Synthetic seismogram of vertical displacement for quasi-compressional waves calculated using p-delta curve shown in figure 5.6 10% anisotropy.



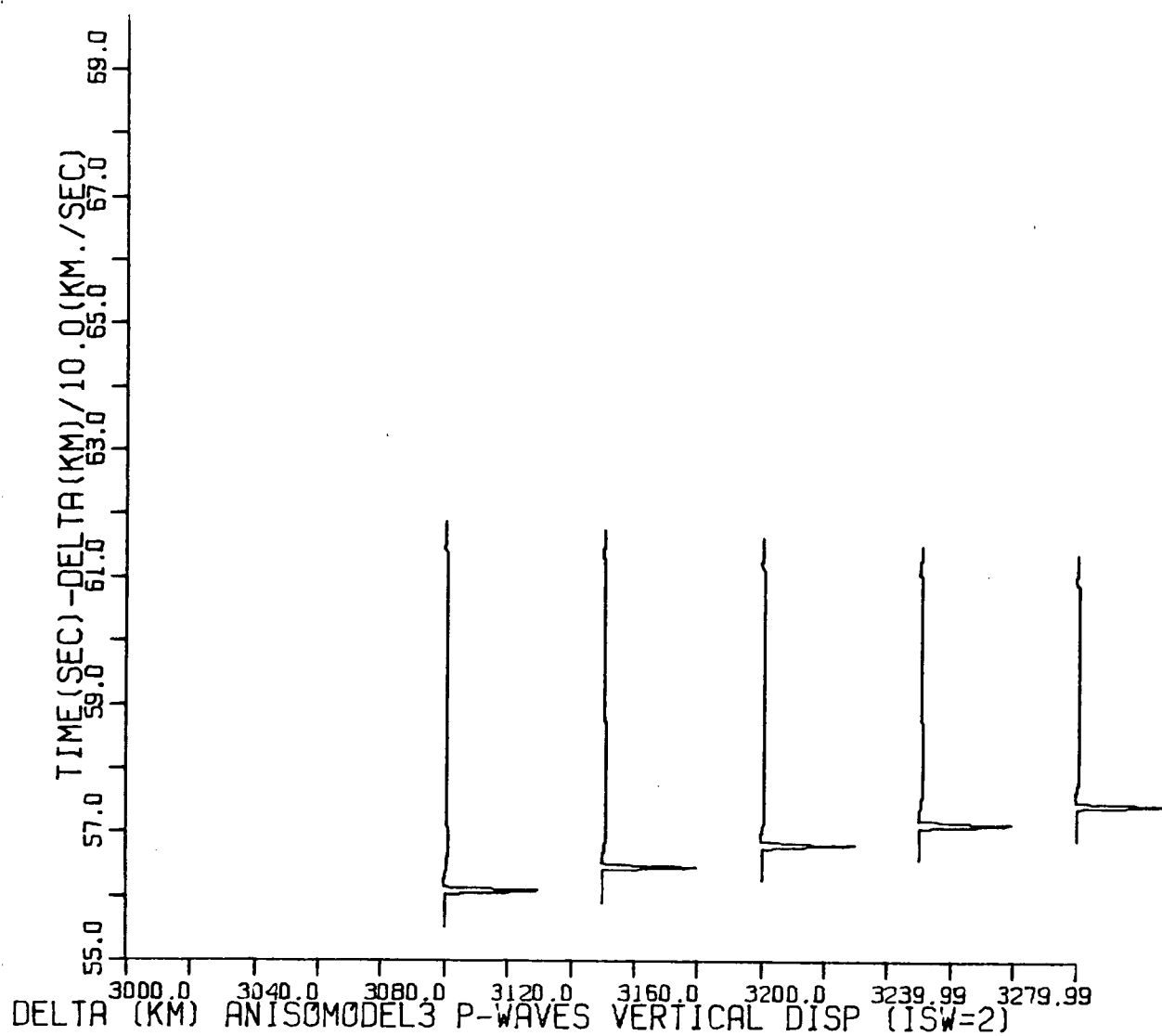


Figure 5.19 Synthetic seismogram of vertical displacement for quasi-compressional waves calculated using p-delta curve shown in figure 5.7. 30% anisotropy.

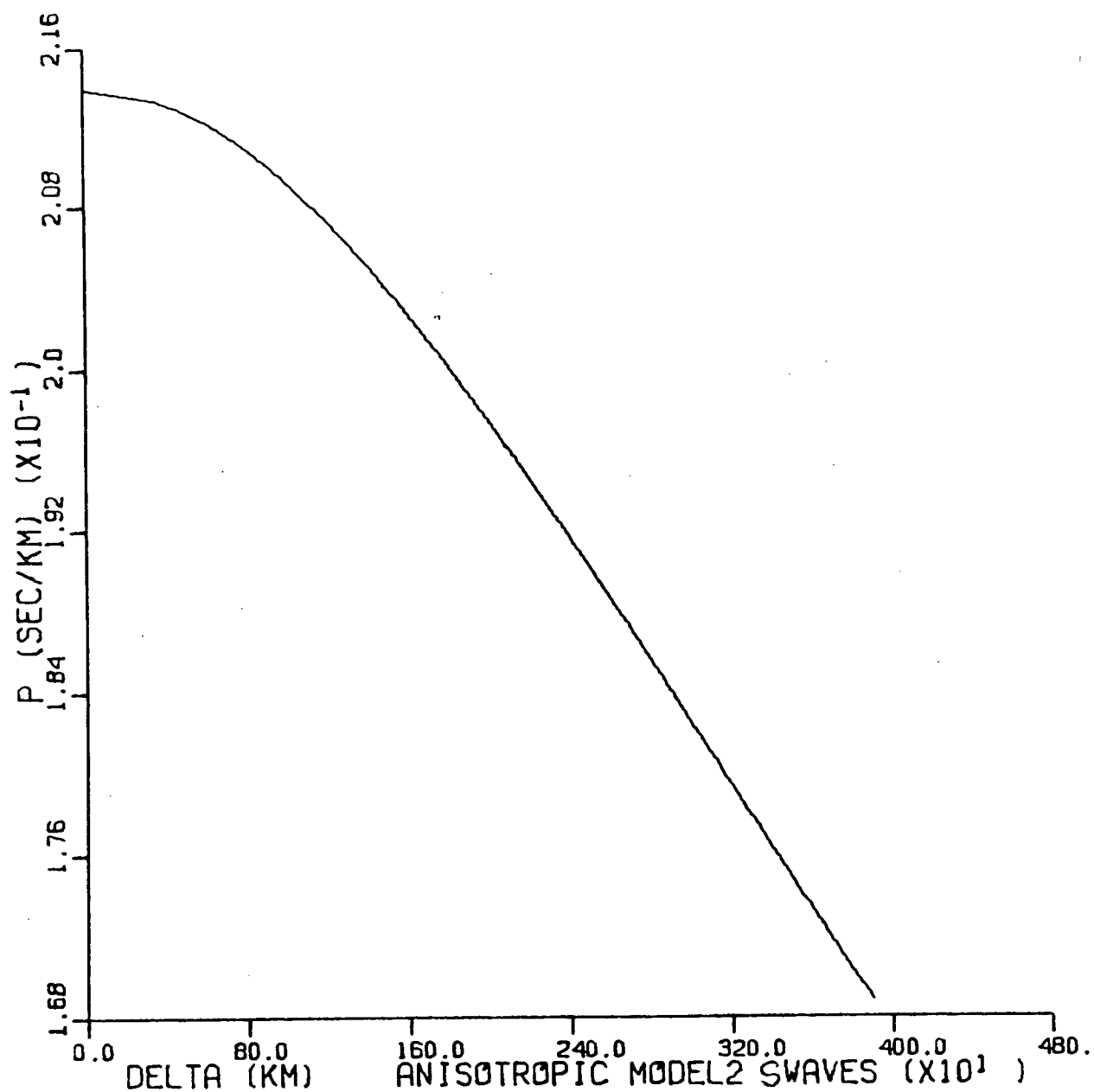


Figure 5.20 P-delta curve for anisotropic Model 2 for quasi-shear waves. Mantle model was used (velocity used for quasi-compressional waves divided by 1.732) 10% anisotropy.

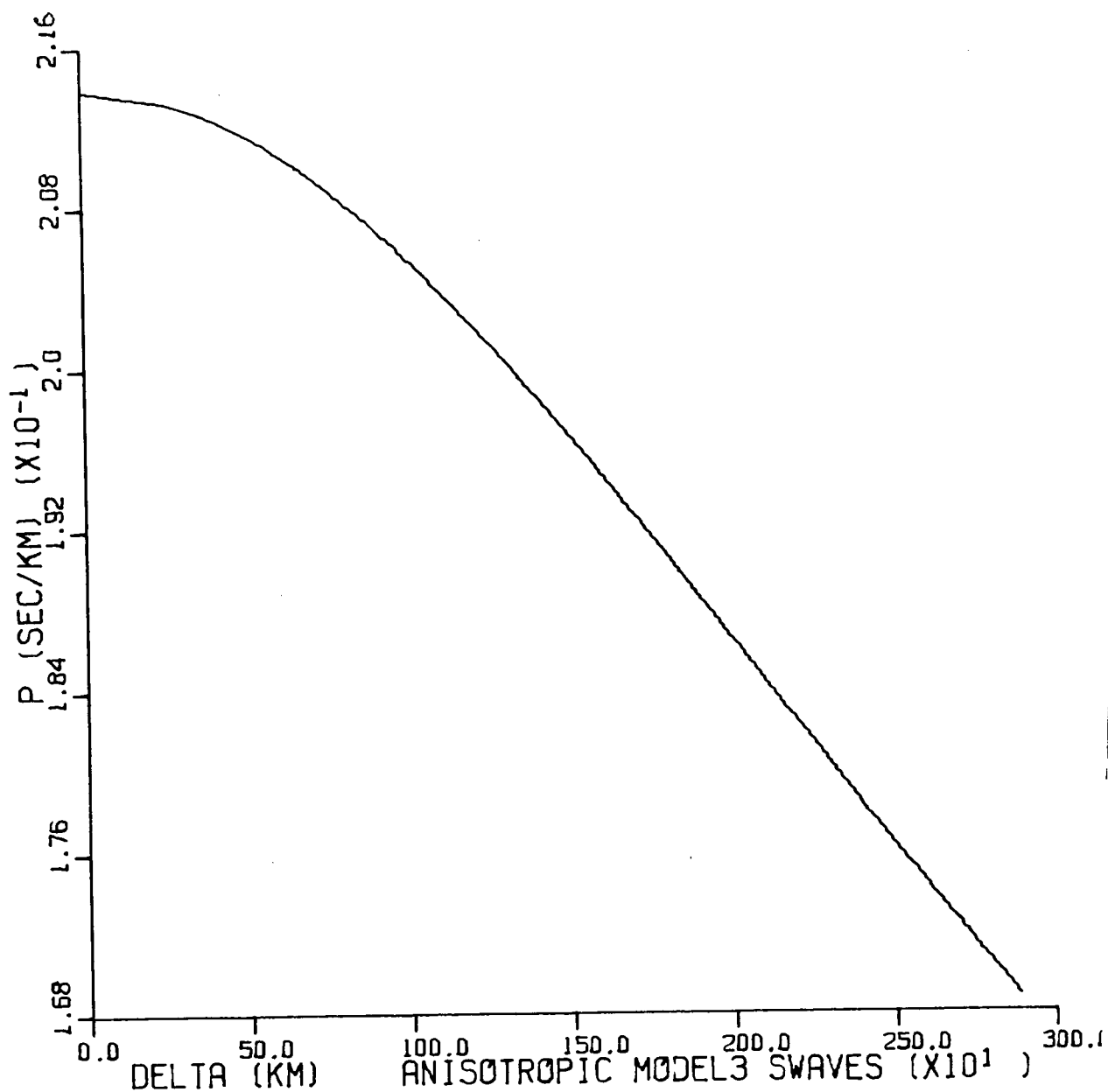


Figure 5.21 P-delta curve for anisotropic Model 3 for quasi-shear waves. Mantle model was used (velocity used for quasi-compressional waves divided by 1.732) 30% anisotropy.

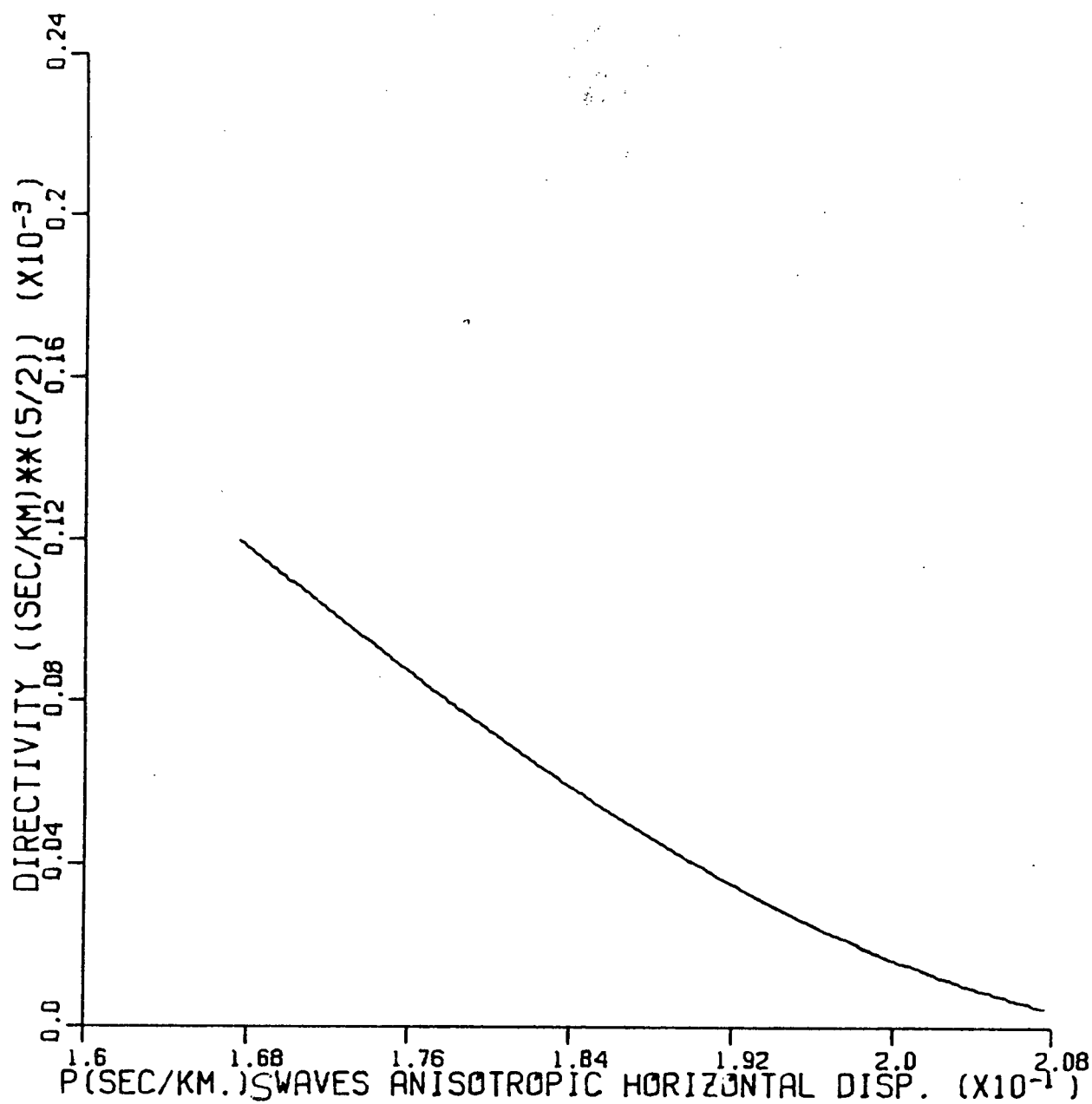


Figure 5.22 Directivity function (quasi-shear waves) for horizontal displacement using Model 2. 10% anisotropy

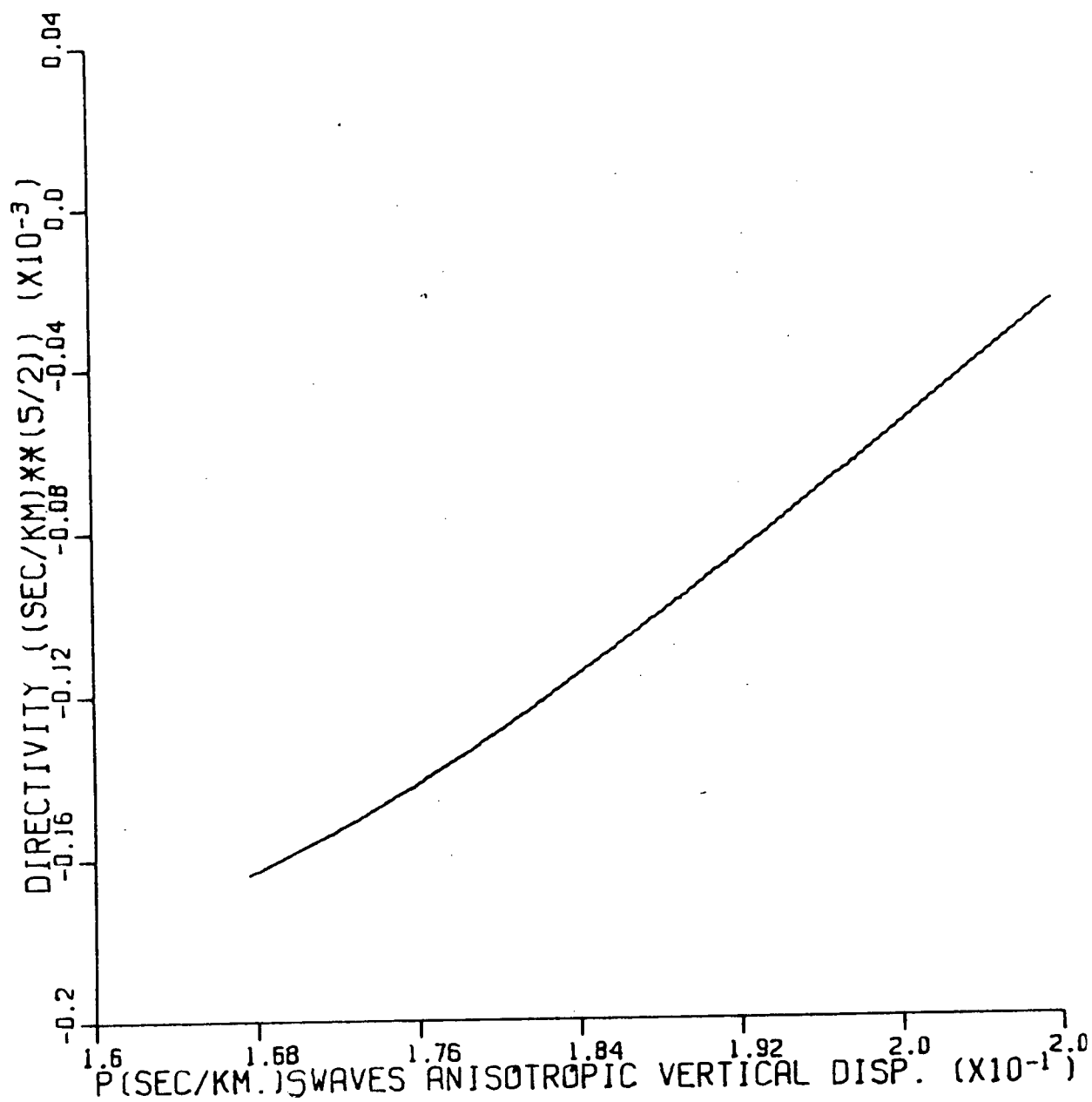


Figure 5.23 Directivity function (quasi-shear waves) for vertical displacement using Model 2. 10% anisotropy

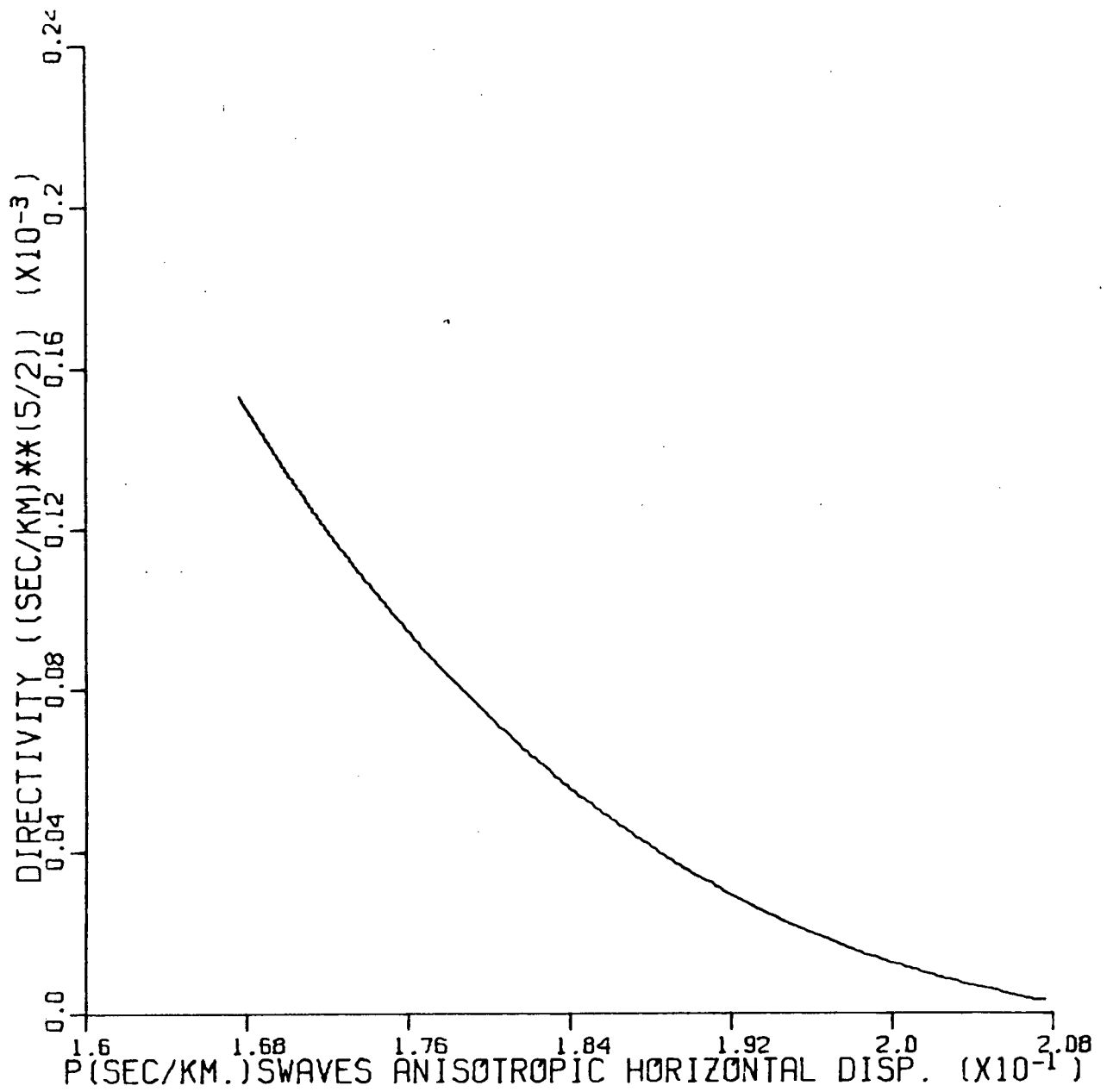


Figure 5.24 Directivity function (quasi-shear waves) for horizontal displacement using Model 3. 30% anisotropy

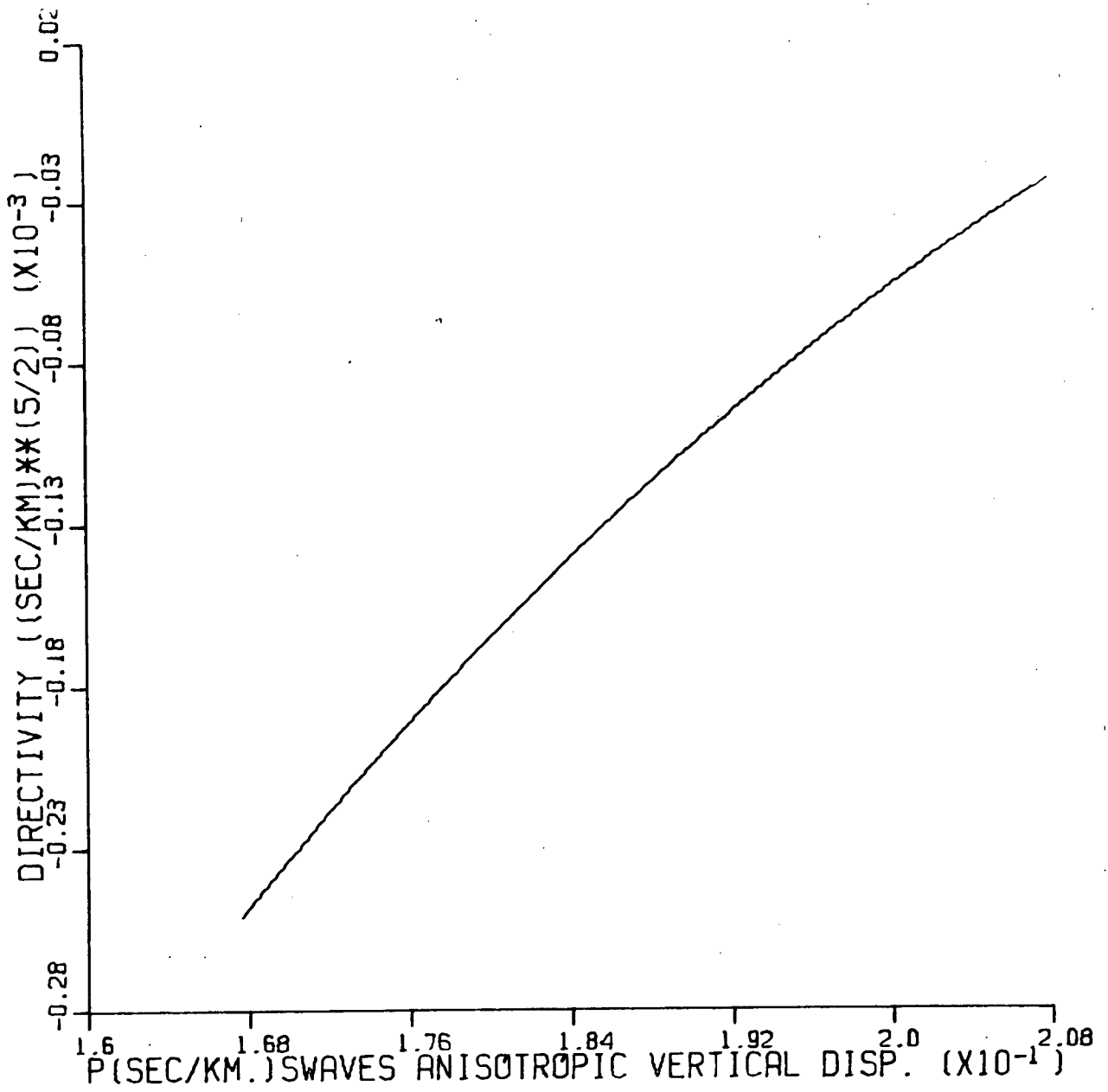


Figure 5.25 Directivity function (quasi-shear waves) for vertical displacement using Model 3. 30% anisotropy

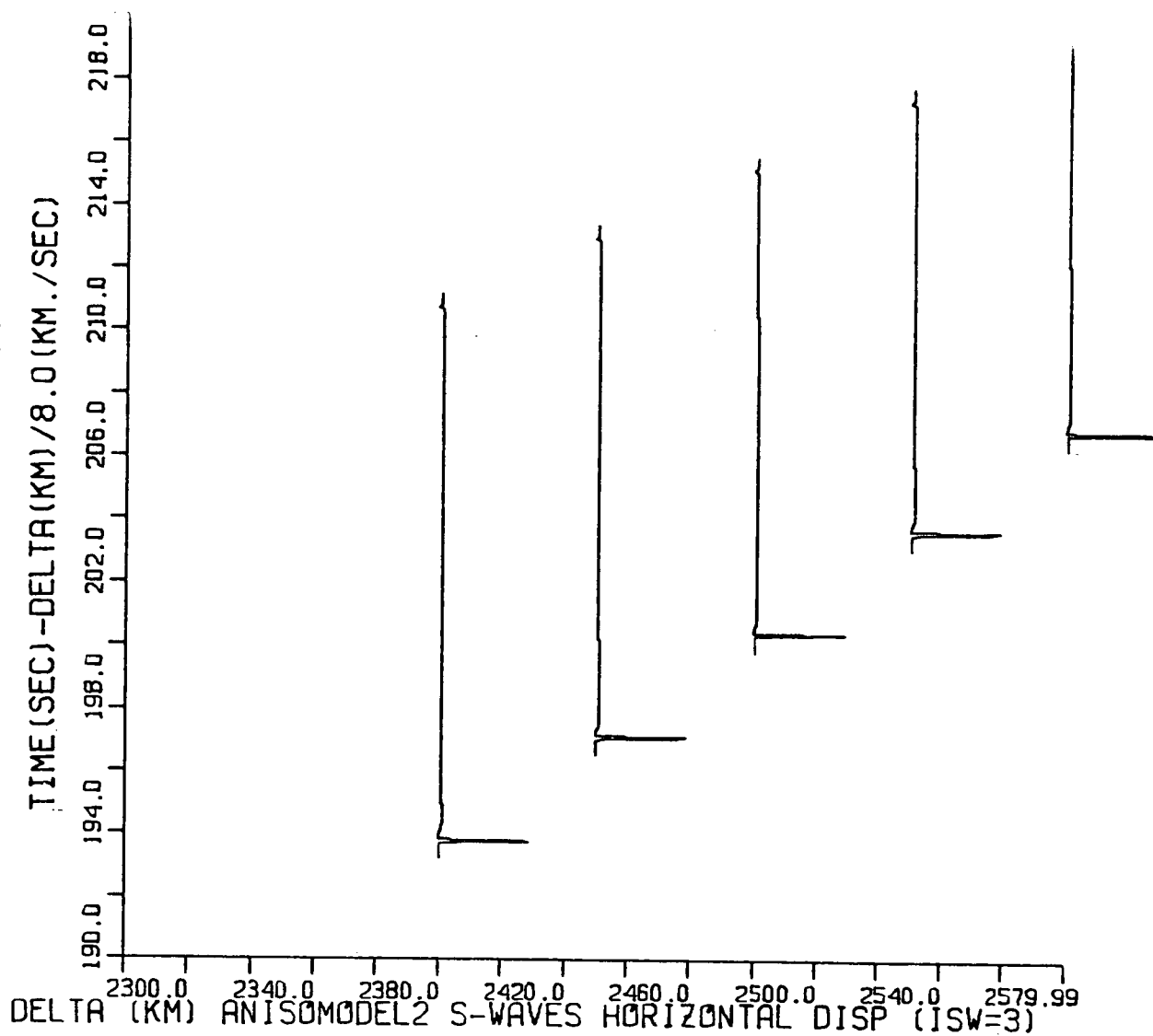


Figure 5.26 Synthetic seismogram of horizontal displacement for quasi-shear waves, calculated using p-delta curve shown in figure 5.20. 10% anisotropy.



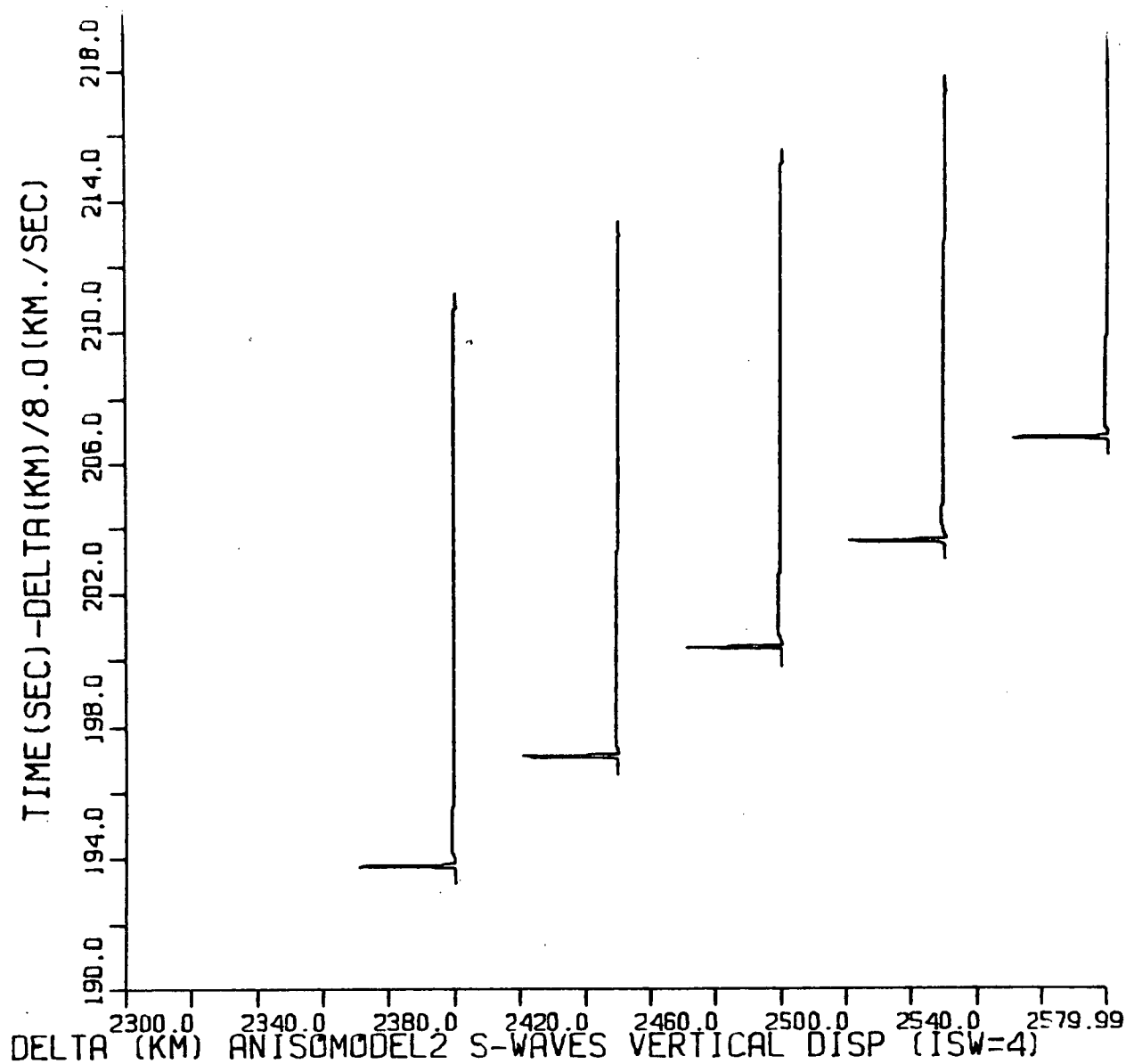


Figure 5.27 Synthetic seismogram of vertical displacement for quasi-shear waves, calculated using p-delta curve shown in figure 5.20. 10% anisotropy.

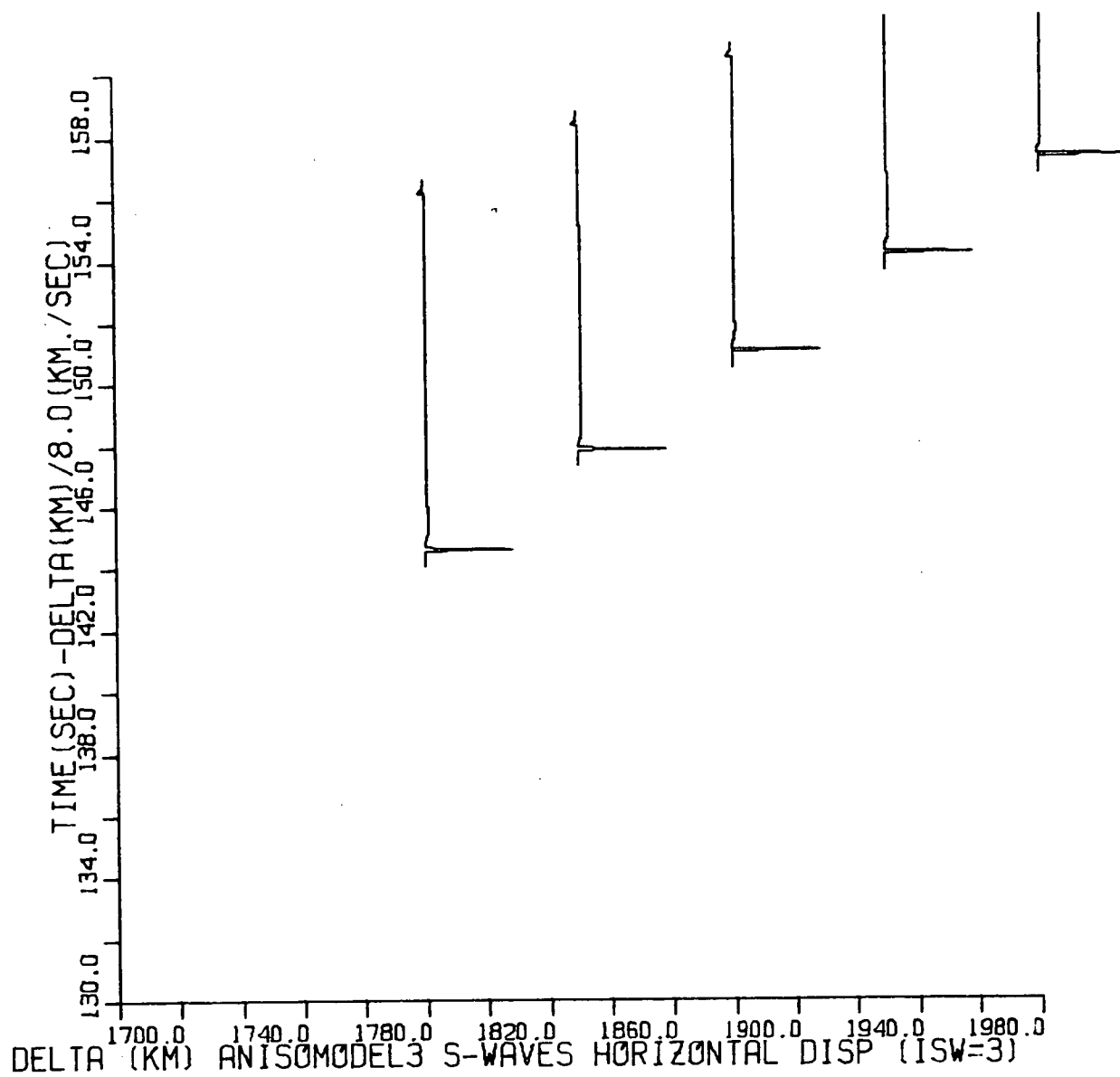


Figure 5.28 Synthetic seismogram of horizontal displacement for quasi-shear waves, calculated using p-delta curve shown in figure 5.21. 30% anisotropy.

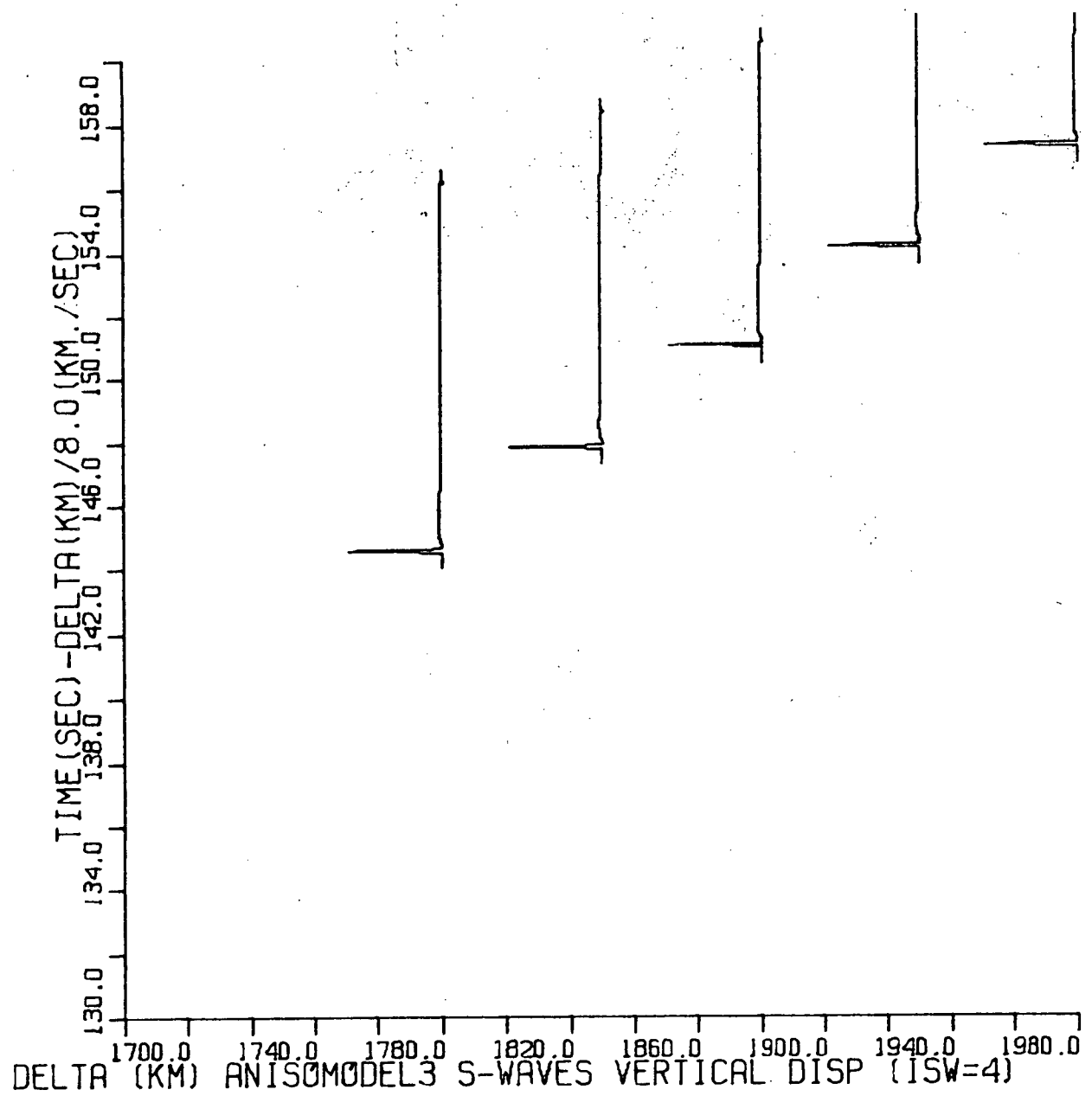


Figure 5.29 Synthetic seismogram of vertical displacement for quasi-shear waves, calculated using p-delta curve shown in figure 5.21. 30% anisotropy.

## Conclusions

For fast, cheap, and accurate synthetic seismogram calculations, in the geometrical optics limit, d.r.t. provides an important complement to existing methods. Since the geometrical optics limit is used, it is necessary to obtain the appropriate JWKB reflection coefficient. This has been achieved by using the Langer transformation and the radiation condition at infinity.

For the simple cases of anisotropy considered, the main effect seen on the seismograms is a kinematic one. The main arrivals for the anisotropic model were advanced in time, as compared with those for the isotropic model. As in the isotropic case, care must be taken in delimiting the range of ray parameters entering in the seismic calculation. In particular, since the d.r.t. algorithm operates in the far field, it is necessary that  $wpr \gg 1$ . This is a restriction on both the frequency content of the waves which are allowed to propagate and on the range of epicentral distances.

Further studies of the applications of d.r.t. to more general forms of anisotropy are profitable avenues of future research. This can be achieved by performing a third Fourier transform over angle and applying the necessary asymptotic methods to solve the initial value problem.

Currently, the author is investigating more complex transversely isotropic models, in which the wave surface for quasi-shear waves has a triplication. It is expected that focussing effects will appear in the seismogram (c.f. Chapter II) at appropriate epicentral distances.

The possible extensions of the methods used in this thesis show that indeed in the geometrical optics, far-field limit, d.r.t or the equal phase method is as powerful as Wiggins and Chapman have indicated.

# Bibliography

- Abramowitz, M., & Stegun, I. A., 1965. Handbook of mathematical functions, Dover Publicationsinc., New York,.
- Alekseyev, A. C., Babich, V. M., & Gelchinskiy, B. Y., 1961. Ray method for the computation of the intensity of wave fronts, Prblems of the Dynamic Theory of Propagation of Seismic Waves, Vol. 5, 3-24, Leningrad University Press, Leningrad (in Russian).
- Auld, B. A., 1973. Acoustic fields and waves in solids, Vol.1, John Wiley & Sons, New York.
- Ave Lallement, H. B., & Carter, N. L., 1970. Syntectonic recrystallization of olivine and modes of flow in the upper mantle, Bull. geol. Soc. Am., 81, 2203,2220.
- Babich, V. M., 1961. Ray method for the computation of the intensity of wave fronts in elastic inhomogeneous anisotropic medium, Problems of the Dynamic Theory of Propagation of Seismic Waves, Vol. 5 36-46, Leningrad University Press, Leningrad (in Russian).
- Backus, G. E., 1965. Possible forms of seismic anisotropy of the uppermost mantle under oceans, J. geophys. Res., 70, 3429-3439.
- Backus, G. E., 1962. Long-wave elastic anisotropy produced by horizontal layering, J. geophys. Res., 67, 4427-4440.
- Bamford, D., 1973. Refraction data in Western Germany-a time-term interpretation, Z. Geophys., 39, 907-927.
- Bamford, D., 1976. MOZAIC time-term analysis, Geophys. J. R. astr. Soc., 44, 433-446.

Bamford, D., 1977. Pn velocity anisotropy in a continental upper mantle, Geophys. J. R. astr. Soc., 49, 29-48.

Berry, M. F., & West, G. F., 1966. An interpretation of the first arrival data of the Lake Superior experiment by the rime-term method, Bull. seism. Soc. Am., 56, 141-170.

Biot, M. A., 1957. General theorems on the equivalence of group velocity and energy transport, Phys. Rev., 105, 1129-1137.

Birch, F., 1960. The velocity of compressional waves in rock to 10 kilobars: part 1, J. geophys. Res., 65, 1083-1102.

Bottinga, Y., & Allegre, C., 1976. Geophysical, petrological, and geochemical models of the oceanic lithosphere, Tectonophysics, 32, 9-59.

Briot, C. A. A., & Bouquet, J. C., 1896. Elements of analytical geometry of two dimensions, 14 ed. Trans. J. H. Boyd., Werner School Book Co., New York.

Bullen, K. E., 1965. An introduction to the theory of seismology, third edition Cambridge University Press.

Cerveny, V. & Psencik, I., 1972. Rays and travel time-curves in inhomogeneous anisotropic media, Z. Geophysik., 38, 565-577.

Cerveny, V., 1972. Seismic rays and ray intensities in inhomogeneous anisotropic media, Geophys. J. R. astr. Soc., 29, 1-14.

Chapman, C. H., 1971. On the computation of seismic rays, travel times, and amplitudes, Bull. seism. Soc. Am., 61, 1267-1274.

- Chapman, C. H., 1973. The earth flattening transformation in body wave theory, Geophys. J. R. astr. Soc., 35, 55-70.
- Chapman, C. H., 1974a. Generalized ray theory for an inhomogeneous medium, Geophys. J. R. astr. Soc., 36, 673-704.
- Chapman, C. H., 1974b. The turning point of elastodynamic waves, Geophys. J. R. astr. Soc., 39, 613-622.
- Chapman, C. H., 1976a. A first motion alternative to geometrical ray theory, Geophys. Res. Lett., 3, 153-156.
- Chapman, C. H., 1976b. Exact and approximate generalized ray theory in vertically inhomogeneous media, Geophys. J. R. astr. Soc., 46, 201-233.
- Chapman, C. H., 1977a. A new method for computing synthetic seismograms, Geophys. J. R. astr. Soc., to be published
- Chapman, C. H., 1977b. Review paper on calculation of synthetic seismograms, Bull. seism. Soc. Am., to be published
- Chopra, S. D., 1958. On the equivalence of saddle point approximations and ray theory in elastic wave problems, Geophys. J. R. astr. Soc., 8, 169-179.
- Christensen, N. I., 1971. Fabric, seismic anisotropy and tectonic history of the Twin Sisters dunite, Washington, Bull. geol. Soc. Am., 82, 1681-1694.
- Christensen, N. I., 1972. Seismic anisotropy in the lower oceanic crust, Nature, 237, 450-451.



- Christensen, N. J., & Crosson, R. S., 1968. Seismic anisotropy in the upper mantle, Tectonophysics, 6, 93-107.
- Clowes, R. M., & Malecek, S. J., 1976. Preliminary interpretation of a marine deep seismic sounding survey in the region of Explorer ridge, Can. J. Earth Sci., 13, 1545-1555.
- Courant, R. S., Hilbert, D., 1966. Methods of mathematical physics, Vol. 2, Interscience Publishers, John Wiley & Sons, Inc., New York.
- Crampin, S., 1966. Higher modes of seismic surface waves: propagation in Eurasia, Bull. seism. Soc. Am., 56, 1227-1239.
- Crampin, S., 1977. A review of the effects of anisotropic layering on the propagation of seismic waves, Geophys. J. R. astr. Soc., 49, 9-27.
- Crosson, R. S., & Christensen, N. I., 1969. Transverse isotropy of the upper mantle in the vicinity of the Pacific fracture zones, Bull. seism. Soc. Am., 59, 59-72.
- Daley, P. F., & Hron, F., 1977. Reflection and transmission coefficients for transversely isotropic media, Bull. seism. Soc. Am., 67, 661-675.
- Duff, G. F. D., 1975. Hyperbolic Differential Equations and Waves, NATO Advances Study Conference on hyperbolic differential equations.
- Durell, C. V., 1947. Modern geometry, Macmillan & Co., Limited, London.

- Feynman, R. P., Leighton, R. E., Sands, M., 1966. The Feynman lectures on physics, Vol. 2, Addison-Wesley Publishing Co. Inc., New York.
- Fowler, R. H., 1929. The elementary differential geometry of plane curves Cambridge University Press.
- Francis, T. J. G., 1969. Generation of seismic anisotropy in the upper mantle along the mid-oceanic ridges, Nature, 221, 162-165.
- Fuchs, K., & Muller, G., 1971. Computation of synthetic seismograms with the reflectivity method and comparison with observations, Geophys. J. R. astr. Soc., 23, 417-433.
- Fuchs, K., 1977. Seismic anisotropy of the subcrustal lithosphere as evidence for the dynamical processes in the upper mantle, Geophys. J. R. astr. Soc., 49, 167-179.
- Gilbert, F., & Backus, G. E., 1966. Propagator matrices in elastic wave and vibration problems, Geophysics, 31, 326-332.
- Goetz, A., 1968. Introduction to differential geometry, Addison-Wesley publishing Co. Inc., New York.
- Green, D. H., & Liebermann, R. C., 1976. Phase equilibria and elastic properties of a pyrolite model for the oceanic upper mantle, Tectonophysics 32, 61-92.
- Helmberger, D. V., 1968. The crust-mantle transition in the Bering sea, Bull. seism. Soc. Am., 58, 179-214.
- Hess, H., 1964. Seismic anisotropy of uppermost mantle under oceans, Nature, 2, 629-631.

- Jeffreys, Sir H., 1959. The earth, 5th ed. Cambridge University Press.
- Kantorovich, L. V., 1934. Sur le calcul approche de quelques types d'integrales definies, Mat.sbornik, 41, 235-245 (in Russian).
- Keen, C. E., & Barrett, D. E., 1971. A measurement of seismic anisotropy in the Northeast Pacific, Can J. Earth sci. 8, 1056-1066.
- Keen, C. E., & Tramontini, C., 1970. A seismic refraction survey on the mid-Atlantic ridge, Geophys. J. R. astr. Soc., 20, 473-491.
- Keith, C. M., & Crampin S., 1977. Seismic body waves in anisotropic media: synthetic seismograms, Geophys. J. R. astr. Soc., 49,
- Klein, F., 1939. Elementary mathematics from an advanced standpoint, Geometry, trans. E. R. Hedrick, Macmillan Co., New York.
- Kraut, E. A., 1963. Advances in the theory of anisotropic elastic wave propagation, Rev. Geophys. Space Phys., 1, 401-448.
- Krylov, V. I., 1962. Approximate calculation of integrals, trans. Stroud, a. H., Macmillan Co., New York
- Landau, L. D., & Lifshitz, E. M., 1959. Theory of elasticity, trans. J. B. Sykes & W.H. Reid, Pergamon Press, New York.
- Landau, L. D., & Lifshitz, E. M., 1960. Electrodynamics of continuous media, trans. J. B. Sykes & J. S. Bell, Pergamon Press, New York.

- Lighthill, M. J., 1960. Studies on magneto-hydrodynamic waves and other anisotropic wave motions, Phil. Trans. Roy. Soc. A., 252, 397-430.
- Love, A. E. H., 1945. The mathematical theory of elasticity, 4th rev.ed., Cambridge University Press.
- McMechan, G. A., 1976. Generalized P-Delta curves, Geophys. J. R. astr. Soc., 47, 9-18.
- Musgrave, M. J. P., 1970. Crystal acoustics, Holden-Day, San Francisco.
- Peselnick, L., Nicolas, A., & Stevenson, P. R., 1974. Velocity anisotropy in mantle peridotite from the Ivrea Zone: application to upper mantle anisotropy, J. geophys. Res., 79, 1175-1182.
- Poncelet, J. V. 1822. Traite des proprietes projectives des figures, 2nd ed. Paris.
- Potsma, G. W., 1955. Wave propagation in a stratified medium, Geophys., 20, 780-806.
- Raitt, R. W., Shor, G. G., Francis, T. J., & Morris, G. B., 1969. Anisotropy of the Pacific upper mantle, J. geophys. Res., 74, 3095-3109.
- Raitt, R. W., Shor, G. G., Morris, G. B. S., Kirk, H. K., 1971. Mantle anisotropy in the Pacific ocean, Tectonophysics, 12, 173-186.
- Raitt, R. W., 1963. Seismic refraction studies of the Mendocino fracture zone, MPL-U-23/63, Marine Physical Lab., Scripps Institute of Oceanography, University of California, San diego.

- Raleigh, C. B., 1967. Mechanisms of plastic deformation of olivine, J. geophys. Res., 73, 5391-5406.
- Richards, P. G., 1973. Calculations of body waves, for caustics, and tunnelling in core phases, Geophys. J. R. astr. Soc., 35, 243-264.
- Staudt, J. H., & Cook, B. D., 1967. Visualization of quasi-longitudinal and quasi-transverse elastic waves, J. acoust. Soc. Am., 41, 1547-1548.
- Takeuchi, H., & Saito, M., 1972. Seismic surface waves, in Methods of computational physics, Vol.11, ed. B. Bolt, Academic Press, New York.
- Thomson, W. T., 1950. Waves through a stratified solid medium, J. Appl. Phys., 21, 89-93.
- Uhrig, L. F., & Van Melle, G. A., 1955. Velocity anisotropy in stratified media, Geophys., 20, 774-779.
- Verma, R. K., 1960. Elasticity of some high density crystals, J. geophys. Res., 65, 757-766.
- Vlaar, N. J., 1968. Ray theory for an anisotropic inhomogeneous elastic medium, Bull. seism. Soc. Am., 58, 2053-2072.
- Wasow, W., 1965. Asymptotic expansions for ordinary differential equations, Vol.14, Pure and Applied Mathematics, Interscience Publishers, John Wiley & Sons, Inc. New York.
- Wiggins, R. A., & Helmberger, D. V., 1974. Synthetic seismogram computation by expansion in generalized rays, Geophys. J. R. astr. Soc., 37, 73-90.

- Wiggins, R. A., & Madrid, J. A., 1974. Body wave amplitude calculations, Geophys. J. R. astr. Soc., 37, 423-433.
- Wiggins, R. A., McMechan, G. A., & Toksoz, M. N., 1973. Range of earth structural nonuniqueness implied by body-wave observations, Rev. Geophys. Space Phys., 11, 87-113.
- Wiggins, R. A., 1976. Body wave amplitude calculations - ii, Geophys. J. R. astr. Soc., 46, 1-10.
- Witham, G. B., 1974. Linear and non-linear waves, John Wiley & Sons, New York.
- Woodhouse, J. H., 1978. Asymptotic propagator matrices, Geophys. J. R. astr. Soc., to be published
- Yeliseyevnin, V. A., 1964. Calculation of rays propagating in an inhomogeneous medium, akust. zh., 10, 284-288 (in Russian).